

# **Multidimensional Analytical Approach for the Characterization of Complex Ethylene-Propylene Copolymers**

By

**Mohau Justice Phiri**

*Dissertation presented in partial fulfilment of the requirements for the degree  
Doctor of Philosophy (PhD) in Polymer Science  
in the Faculty of Science at Stellenbosch University*



Promoter: Prof. Harald Pasch

March 2016

## **Declaration for the Dissertation**

By submitting this thesis electronically, I declare that the entirety of the work contained therein is my own, original work, that I am the authorship owner thereof (unless to the extent explicitly otherwise stated) and that I have not previously in its entirety or in part submitted it for obtaining any qualification.

Mohau Justice Phiri

December 2015

Copyright © 2016 Stellenbosch University

All rights reserved

## Declaration for the Publications

With regard to the three manuscripts in the dissertation, the nature and scope of my contribution were as follows:

Nature of Contribution	Extent of contribution (%)
Experimental work, Data Analysis, Discussion of Results, Write-up the manuscripts, Addressing the Comments of the Reviewers.	85

The following co-authors have contributed to the three manuscripts in the dissertation.

Name	e-mail address	Nature of contribution	Extent of contribution (%)
Sadiqali Cheruthazhekatt	Sadi21ct@gmail.com	Analytical instruments training	3
Anita Dimeska	adimeska@cbi.com	Synthesis of the copolymers	2
Harald Pasch	hпасч@sun.ac.za	Supervision and mentoring, revision and correction of the manuscript	10

Signature of candidate:.....

Date:.....

Declaration by co-authors:

1. the declaration above accurately reflects the nature and extent of the contributions of the candidate and co-authors to three manuscripts in the dissertation,
2. no other authors contributed to three manuscripts in the dissertation besides those specified above, and
3. potential conflicts of interest have been revealed to all interested parties and that the necessary arrangements have been made to use the material in the three manuscripts in the dissertation.

Signature	Institutional affiliation	Date
Declaration with signature in possession of candidate and supervisor	MES KVM College	30 Nov 2015
Declaration with signature in possession of candidate and supervisor	Novel Technology Company	30 Nov 2015
Declaration with signature in possession of candidate and supervisor	Stellenbosch University	30 Nov 2015

## Abstract

Impact polypropylene copolymers (IPC) are complex multiphase materials having ethylene-propylene rubber particles incorporated in a semi-crystalline isotactic polypropylene (iPP) matrix. The ethylene-propylene rubber (EPR) particles form the most critical part of IPC. They are continuously dispersed in the iPP matrix and are supposed to prevent crack propagation under mechanical stress. The EPR phase decreases the crystal size of the crystalline iPP phase, and as a result an improvement in the impact strength of IPC is usually observed. IPC materials have much improved impact resistance as compared to conventional iPP and, thus, they can be used in a wide temperature range.

IPCs usually have low melt flow rates (MFR) that limit their application in a number of moulding applications. One way to increase the MFR is the vis-breaking process that decreases the molar mass of the polymer. Details regarding the molecular structures of the vis-broken IPC and the molecular background of the vis-breaking process are not completely available up to date. Therefore, it was the main aim of the present study to investigate the compositional heterogeneities of EPR and vis-broken IPC materials using multidimensional analytical approaches.

A set of EPR copolymers prepared by Ziegler-Natta and metallocene catalyst systems were used in the present study as model systems to mimic the rubber phase in IPC. The EPR samples had high comonomer contents in the range of 30 – 70 mol %. For another part of the work, a set of vis-broken IPC samples with different MFR values were prepared by degradation with an organic peroxide. Bulk samples from the two sets of samples were analysed by SEC, DSC, FT-IR,  $^{13}\text{C}$  NMR, CRYSTAF and HT-HPLC. The bulk samples were fractionated by preparative TREF procedures to obtain fractions at different TREF elution temperatures which could be further analysed to obtain comprehensive information on the molecular compositions of the samples.

For the EPR copolymer samples, HT-SEC showed that the bulk samples and their TREF fractions have broader MMDs as compared to similar metallocene-based samples. The bulk sample analyses showed that the EPR samples consist mainly of random EP copolymers making about 65 % of the bulk samples. DSC and CRYSTAF were able to analyse only the semi- and highly crystalline TREF fractions. Both techniques did not fully characterise the 30 °C TREF fractions since these fractions contained random EP copolymers which were completely

amorphous.  $^{13}\text{C}$  NMR was used to determine the comonomer contents of the fractions as well as their monomer sequence distributions.

NMR analyses of comparable metallocene-based copolymer fractions showed that these had remarkably high chemical heterogeneities. The separation of the samples and their TREF fractions by HT-HPLC was found to be sensitive to the ethylene content of the samples. The exact chemical compositions of the fractions were determined by coupling HT-HPLC to FT-IR spectroscopy. This hyphenated technique provided information on the ethylene and propylene contents of the fractions as a function of the elution volume in HPLC separation. The late eluting TREF fractions were found to contain PE and iPP homopolymers in addition to the expected EP copolymers. These homopolymer fractions indicated that the EPR samples were not completely amorphous as it was suggested by previous studies.

Vis-broken IPC samples were analysed using a similar multidimensional analytical approach. HT-SEC showed that there was a decrease in molar masses of the bulk samples with the largest amount of the peroxide used in the degradation process. DSC and CRYSTAF showed that the 60 and 90 °C TREF fractions contain the segmented EP copolymers with complex molecular compositions. FT-IR was also useful in providing the chemical composition of the vis-broken IPC samples by detecting the presence of carbonyl groups in the degraded samples. The 30 °C TREF fractions were found to contain the highest concentration of carbonyl groups and the number of these groups increased with an increase of the amount of the peroxide. HPLC was able to analyse both amorphous and crystalline fractions since the HPLC separation depends mainly on the chemical composition of the samples and not the crystallizability. There was a significant shift to lower HPLC elution volumes of the samples with the most degraded sample showing the strongest shift of the elution volume peak maximum. This suggests that EP copolymers with longer ethylene sequences are affected most by action of an organic peroxide.

To summarize, the present study proved that a single technique approach is not sufficient to obtain comprehensive information on the molecular compositions of the vis-broken IPC and EPR copolymers. As a result, the present study established a number of multidimensional analytical approaches to fractionate and characterize these complex IPC polymer systems.

## Opsomming

Impak polipropileen ko-polimere (IPC) is komplekse multifase materiale met etileen-propileen rubber partikels, bevat in 'n semi-kristallyne isotaktiese polipropileen (iPP) matriks. Die etileen-propileen rubber (EPR) partikels vorm die mees kritieke deel van IPC. Hulle is dwarsdeur die IPP matriks versprei en is veronderstel om kraak verspreiding onder meganiese spanning te voorkom. Die EPR fase verminder die kristal grootte van die kristallyne IPP fase en as gevolg word 'n verbetering in die impak sterkte van IPC gewoonlik waargeneem. IPC materiale het baie beter impak weerstand in vergelyking met konvensionele IPP en dus kan hulle gebruik word oor 'n wye temperatuur reeks.

IPCs het gewoonlik 'n lae smelt vloeitempo (MFR) wat hul toepassing in 'n aantal giettoepassings beperk. Een manier om die MFR te verhoog is die vis-breking proses wat die molêre massa van die polimeer verlaag. Inligting oor die molekulêre strukture van die vis-gebreekte IPC en die molekulêre agtergrond van die vis-breking proses is tot op hede nog nie heeltemal beskikbaar nie. Daarom was dit die hoofdoel van die huidige studie om die komposisionele heterogeniteit van EPR en vis-gebreekte IPC materiale met behulp van multidimensionele analitiese benaderings te ondersoek.

'n Stel EPR ko-polimere, voorberei deur Ziegler-Natta en metalloseen katalisator sisteme, was gebruik in die huidige studie as model stelsels om die rubber fase in IPC na te boots. Die EPR monsters het hoë ko-monomeer inhoud in die reeks van 30-70 mol%. Vir 'n ander deel van die werk, was 'n stel vis-gebreekte IPC monsters met verskillende MFR waardes voorberei deur degradasie met 'n organiese peroksied. Ongefraksioneerde monsters van die twee stelle was ontleed deur SEC, DSC, FT-IR, <sup>13</sup>C KMR, CRYSTAF en HT-HPLC. Die monsters was gefraksioneer deur preparatiewe TREF prosedure om fraksies by verskillende TREF eluering temperature te verkry wat verder ontleed kon word om omvattende inligting oor die molekulêre samestelling van die monsters te bekom.

Vir die EPR ko-polimeer monsters, het HT-SEC getoon dat die ongefraksioneerde monsters en hul TREF fraksies breër MMDs in vergelyking met soortgelyke metalloseen-gebaseerde monsters het. Die ongefraksioneerde monster ontleding het getoon dat die EPR monsters hoofsaaklik uit ewekansige EP ko-polimere bestaan wat ongeveer 65% van die ongefraksioneerde monster opmaak. DSC en CRYSTAF was in staat om net die semi- en hoogs kristallyne TREF fraksies te ontleed. Beide tegnieke kon nie ten volle die 30 °C TREF fraksie karakteriseer nie aangesien hierdie fraksies ewekansige EP ko-polimere bevat wat heeltemal

amorfe was.  $^{13}\text{C}$  KMR was gebruik om die inhoud van die ko-monomeer in die fraksies, asook hul monomeer kombinasie verspreiding te bepaal.

KMR ontleding van vergelykbare metalloseen-gebaseerde ko-polimeer fraksies het getoon dat hul merkwaardig hoë chemiese heterogeniteit het. Die skeiding van die monsters en hul TREF fraksies deur HT-HPLC was gevind om sensitief teenoor die etileen inhoud van die monsters te wees. Die presiese chemiese samestelling van die fraksies was bepaal deur die koppeling van HT-HPLC en FT-IR spektroskopie. Hierdie gekoppelde tegniek het inligting oor die etileen en propileen inhoud van die fraksies verskaf as 'n funksie van die eluering volume in HPLC skeiding. Dit was gevind dat die TREF fraksies wat laat elueer, PE en iPP homopolimere bevat tesame met die verwagte EP ko-polimere. Hierdie homopolimeer fraksies het aangedui dat die EPR monsters nie heeltemal amorfe was, soos voorgestel deur vorige studies nie.

Vis-gebreekte IPC monsters was ontleed met behulp van 'n soortgelyke multidimensionele analitiese benadering. HT-SEC het getoon dat daar 'n afname in molêre massas van die ongefraksioneerde monsters was waar die grootste hoeveelheid van die peroksied gebruik was in die degradasie proses. DSC en CRYSTAF het getoon dat die 60 en 90 °C TREF fraksies, die gesegmenteerde EP ko-polimere met komplekse molekulêre komposisies bevat. FT-IR was ook nuttig in die verskaffing van die chemiese samestelling van die vis-gebreekte IPC monsters deur die opsporing van die teenwoordigheid van karbonielgroepe in die gedegradeerde monsters. Dit was gevind dat die 30 °C TREF fraksies die hoogste konsentrasie karbonielgroepe bevat en die aantal van hierdie groepe het toegeneem met 'n toename in die hoeveelheid peroksied. HPLC was in staat om beide amorfe en kristallyne fraksies te analiseer aangesien die HPLC skeiding hoofsaaklik afhang van die chemiese samestelling van die monsters en nie die kristalliseerbaarheid nie. Daar was 'n beduidende verskuiwing na laer HPLC eluering volumes van die monsters met die mees gedegradeerde monster wat die sterkste verskuiwing van die eluering volume piek maksimum gewys het. Dit dui daarop dat EP ko-polimere met langer etileen reekse, die meeste geaffekteer word deur die aksie van 'n organiese peroksied.

Om op te som, die huidige studie het bewys dat 'n enkel tegniek benadering nie voldoende is om omvattende inligting oor die molekulêre samestelling van die vis-gebreekte IPC en EPR ko-polimere te bekom nie. As gevolg hiervan het die huidige studie 'n aantal multidimensionele analitiese benaderings gevestig om hierdie komplekse IPC polimeer sisteme te fraksioneer en karakteriseer.

## Acknowledgements

I will like to thank the following people and institutions for their support in the completion of the present research study.

Prof. Harald Pasch, for the opportunity to allow me to work in his excellent research group. Most importantly, his outstanding supervision and financial support are highly appreciated.

Dr. Sadiqali Cheruthazhakatt, for his mentoring capacity for a part of the study. His training sessions on the analytical instruments and polyolefin characterization in general I will always remember.

Novolen Technology and SASOL companies, for the financial support to complete the present study. The samples provided by Novolen Technology company are gratefully acknowledged.

Dr. Anita Dimeska, for the valuable discussion on the  $^{13}\text{C}$  NMR analyses of the samples and for giving more insight about the synthesis part of the samples used in the study. Dr. Jaco Brand and Mrs Elsa Malherbe for the assistance in running the  $^{13}\text{C}$  NMR experiments.

Mpho Phiri, for the unconditional love and emotional support during the course of the study. Her ability to act as both wife and mentor has been influential to push myself beyond the limits to complete the present study.

Family, my sisters and brother, for the encouragement and support they have given me. My son, Poloko Phiri, for being my great motivation towards successful completion of the current study.

Friends and colleagues, for their ongoing support which aided to the completion of the study. The extended support from Dr. Lebohang Hlalele, Thato Ralebakeng and Anthony Ndiripo is much appreciated.

Members of Prof. Pasch's research group, for the discussions and great moments we shared together. Their suggestions and comments during the course of the study were very welcome.



Prof. Albert van Reenen and members of his research group, for the warm welcome in their lab. The assistance and support on the DSC and CRYSTAF instruments provided by Dr. Divaan Robertson and Dr. Maggie Brand.

Mr. Deon Koen, Mrs. Erinda Cooper, Mrs. Aneli Fourie, Mr. Jim Motsweni and Mr. Calvin Maart, for the technical and administrative support provided during my study; ensuring that the chemicals and equipments were always available for use.

I give the greatest gratitude to Almighty God, Jesus Christ, for the strength and wisdom to face all the challenges encountered during my PhD work. His guidance along the present research work will be forever appreciated.

## **Dedication**

*To my wife, Mpho Phiri; my son, Poloko Phiri and my daughter, Phomolo Phiri*

## Research outputs

### Journal Articles

1. Phiri, M.J.; Cheruthazhekatt, S.; Dimeska, A.; Pasch, H., **Molecular Heterogeneity of Ethylene-Propylene Rubbers: New Insights through Advanced Crystallization-based and Chromatographic Techniques.** *Journal of Polymer Science Part A: Polymer Chemistry* 53 (2015) 863-874, DOI: 10.1002/pola.27512.
2. Phiri, M.J.; Dimeska, A.; Pasch, H., **On the Homogeneity of Metallocene Ethylene-Propylene Copolymers as Investigated by Multiple Fractionation Techniques,** *Macromolecular Chemistry and Physics* 216 (2015) 1619-1628, DOI: 10.1002/macp.201500135.
3. Phiri, M.J.; Pasch, H., **Exploring the Compositional Heterogeneity of Vis-broken Impact Polypropylene Copolymers by Advanced Fractionation Methods,** *submitted to Macromolecular Chemistry and Physics on 3 Nov 2015.*

### Presentations

1. Phiri, M, Cheruthazhekatt, S and Pasch, H.: **Studies on compositional heterogeneity in ethylene-propylene copolymers;** *Student Symposium in Analytical Sciences,* Stellenbosch, 27 March 2014. (Poster Presentation)
2. Phiri, M, Cheruthazhekatt, S and Pasch, H.: **Studies on Compositional Heterogeneity in Ethylene-Propylene copolymers using Fractionation Methods:** *Polychar 22: World Forum on Advanced Materials,* Stellenbosch, 8 – 11 April 2014. (Oral Presentation)
3. Phiri, M, Cheruthazhekatt, S and Pasch, H.: **Characterization of Ethylene-Propylene Rubbers using DSC, CRYSTAF and HT-HPLC;** *5<sup>th</sup> International Conference on Polyolefin Characterization (ICPC),* Valencia, Spain, 19-22 September 2014 (Poster Presentation)
4. Phiri, M and Pasch, H: **Thermal and Molecular Properties of the Vis-broken Impact Polypropylene Copolymers;** *SACI Young Chemists' Symposium,* University of Western Cape, Bellville, 10 November 2015. (Oral Presentation).

**CONTENTS**

Declaration for the Dissertation .....	i
Declaration for the Publications .....	ii
Abstract .....	iii
Opsomming .....	v
Acknowledgements .....	vii
Dedication .....	ix
Research outputs .....	x
Journal Articles .....	x
Presentations.....	x
List of Figures .....	xiv
List of Scheme.....	xv
List of Abbreviations.....	xvi
1 INTRODUCTION.....	1
1.1 Polyolefins: Background .....	1
1.2 Motivation of the Research.....	3
1.3 Objectives of the Research .....	3
1.4 Hypothesis and Research Questions.....	4
1.5 Significance of the Research .....	4
1.6 Scope of the Research.....	4
1.7 Layout of the Research .....	5
1.8 References .....	6
2 LITERATURE REVIEW.....	8
2.1 Overview on Ethylene-Propylene Copolymers .....	8
2.2 Separation and Characterisation Techniques.....	9
2.2.1 Molar Mass Analysis Techniques .....	9
2.2.2 Average Chemical Composition Analysis Techniques.....	11

2.2.3	Crystallization-Based Techniques.....	12
2.2.4	Interactive Chromatographic Techniques .....	17
2.3	References .....	19
3	Experimental Procedures: Analytical Techniques .....	24
3.1	Temperature Rising Elution Fractionation (TREF).....	24
3.2	Differential Scanning Calorimetry (DSC).....	24
3.3	Crystallization Analysis Fractionation (CRYSTAF).....	24
3.4	High Temperature Size Exclusion Chromatography (HT-SEC).....	25
3.5	High Temperature High Performance Liquid Chromatography (HT-HPLC).....	25
3.5.1	Collection of HPLC fractions by the LC Transform Interface.....	26
3.5.2	FTIR analyses of the deposited fractions .....	27
3.6	Fourier Transform Infrared Spectroscopy (FTIR).....	27
3.7	High Temperature <sup>13</sup> C NMR Spectroscopy.....	27
3.8	References .....	27
4	Molecular Heterogeneity of Ethylene-Propylene Rubbers: New Insights through Advanced Crystallisation-based and Chromatographic Techniques.....	29
4.1	Summary of the Research Study .....	29
4.2	References .....	33
5	On the Homogeneity of Metallocene Ethylene-Propylene Copolymers as Investigated by Multiple Fractionation Techniques .....	46
5.1	Summary of the Research Study .....	46
5.2	References .....	50
6	Exploring the Compositional Heterogeneity of Vis-broken Impact Polypropylene Copolymers using Advanced Fractionation Methods .....	61
6.1	Summary of the Research Study .....	61
6.2	References .....	65
7	CONCLUSIONS AND RECOMMENDATIONS.....	74

7.1	Conclusions .....	74
7.2	Future work.....	76

## List of Figures

Figure 1.1: Schematic diagram illustrating the production of IPC materials using two-stage polymerisation processes.....	2
Figure 2.1: Schematic diagram of the preparative TREF set-up used for fractionation of the vis-broken IPC and EPR copolymers.....	15
Figure 3.1: Linear gradient profile for the mobile composition in HPLC separations. ....	26
Figure 4.1: prep-TREF fractionation results of EPR copolymers (A) and analyses of the 90 °C TREF fraction using SEC (B), HT-HPLC (C), DSC (D) and CRYSTAF (E).....	31
Figure 5.1: HT-HPLC chromatograms for the bulk EPR samples (A), and the 30 (B) and 130 °C (C) TREF fractions, solvent gradient elution (1-decanol to TCB) after an initial isocratic step. ....	48
Figure 6.1: prep-TREF fractionation (A) results of vis-broken IPC samples and analyses of the TREF fractions using DSC (B), FT-IR (C) and HT-HPLC (D).....	63

## List of Scheme

Scheme 1: Vis-breaking of polypropylene sequence by an organic peroxide.....	62
--	----



## List of Abbreviations

$^{13}\text{C}$ NMR	Carbon-13 nuclear magnetic resonance
CCD	Chemical composition distribution
CEF	Crystallization elution fractionation
CRYSTAF	Crystallization analysis fractionation
DSC	Differential scanning calorimetry
EP	Ethylene-propylene
EPC	Ethylene-propylene copolymer
EPR	Ethylene-propylene rubber
FT-IR	Fourier transform infrared
HPLC	High performance liquid chromatography
HT-HPLC	High temperature high performance liquid chromatography
HT-SEC	High temperature size exclusion chromatography
IPC	Impact polypropylene copolymer
iPP	isotactic polypropylene
MMD	Molar mass distribution
NMR	Nuclear magnetic resonance
PE	Polyethylene
PP	Polypropylene
Prep TREF	preparative temperature rising elution fractionation
SEC	Size exclusion chromatography
TCB	1,2,4-trichlorobenzene

TREF

Temperature rising elution fractionation

## CHAPTER 1:

## INTRODUCTION

---

### 1 INTRODUCTION

*This chapter gives a brief outline of two different types of ethylene-propylene copolymers, namely EPR and vis-broken IPC materials. It details properties, applications and the production process of these complex materials, highlighting differences between them. From the gap identified in literature, motivation, aims and objectives of the research work are formulated. The importance of this study is pointed out together with the scope to be covered. Finally, the layout of the whole dissertation is presented to give the reader an overview what to expect throughout the whole document.*

#### 1.1 Polyolefins: Background

Polyolefins are the largest group of thermoplastics in the global plastics market. They are found in numerous applications ranging from packaging films, bottles, artificial turf to car body parts<sup>1-3</sup>. These synthetic polymer commodities include polyethylene (PE), polypropylene (PP) and copolymers of both ethylene and propylene. The increased use of polyolefins in daily life resulted from the simple production process which requires only cheap and readily available monomers. The annual production of polyolefins exceeds 100 million metric tons per year and continues to grow exponentially<sup>4,5</sup>. The most common class of polyolefins is PP due to its widespread application in reusable plastic containers, automotive parts and electrical industries. In addition, PP materials exhibit high performance in terms of heat resistance and tensile strength, however, PP has a low impact resistance hence it cannot be used at low temperatures<sup>1,6-10</sup>.

In order to improve the impact properties of PP, several approaches including the nucleation process<sup>11</sup>, blending with elastomers<sup>12-14</sup> and copolymerization with  $\alpha$ -olefins<sup>15-17</sup>, have been used in both academia and industry. Among these approaches, copolymerization of propylene with ethylene using two-stage, two-reactor polymerisation processes have been found to be the most effective to obtaining high impact resistant PP<sup>2,18</sup>. A schematic diagram of the process is shown in Figure 1. This process produces microphase-separated materials with a continuous iPP phase and a dispersed EP rubber phase. The random rubber plays a major role as a component for toughness improvement in the PP matrix. During the polymerisation process, the amount of ethylene added determines the percentage of rubber in the final copolymers. Impact polypropylene copolymers (IPC) are formed with ethylene contents up to ~20 mol %.

IPC materials consist of iPP homopolymer as the major crystalline phase with a small amount of rubber phase and segmented ethylene-propylene (EP) copolymers. Vis-broken IPC is the treated IPC material with peroxide to decrease its molar mass<sup>19,20</sup>. As such the melt flow index of vis-broken IPC material is increased to improve the processability of the polymer<sup>21</sup>. However, there is also an increase in the chemical composition complexity due to carbonyl products that are formed upon the degradation with peroxide<sup>20</sup>. EPR materials consist mainly of an amorphous or rubbery phase and small amounts of segmented EP copolymers, PP and PE homopolymers.

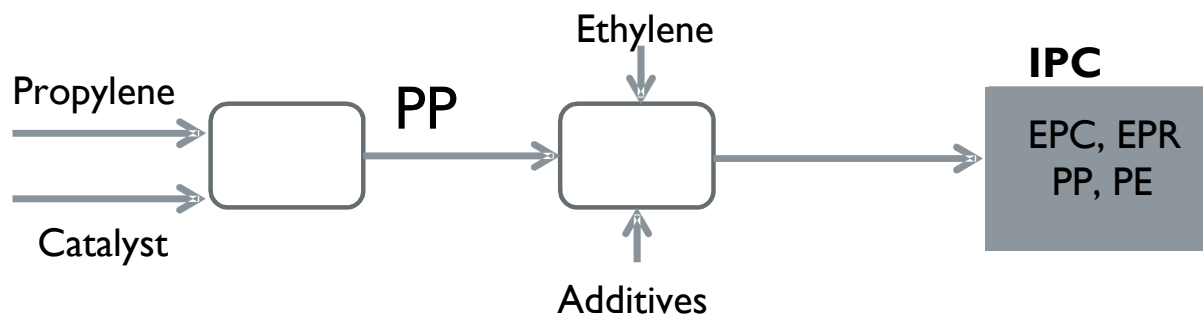


Figure 1.1: Schematic diagram illustrating the production of IPC materials using two-stage polymerisation processes.

According to Figure 1.1, the final IPC material has a very complex composition. In addition to the chemical composition distribution (CCD), the molar mass distribution (MMD) also contributes to the complex nature of the IPC. The complexity in this type of IPC materials is also brought about by the nature of the catalyst system being used. For instance, Ziegler-Natta catalyst systems result in broad compositional distributions due to their multiple active sites to produce different chain structures<sup>22,23</sup>. On the other hand, metallocene catalysts with their single active sites produce polymer materials with narrow compositional distributions<sup>5,22,24,25</sup>. For a polymer chemist, the need to relate the molecular composition of the polymer to its final applicability is always a major challenge since the compositional heterogeneity and sequence distribution of comonomer units along the polymer chains influence the microstructure of the final copolymer. As such a comprehensive analytical approach must be developed to achieve proper understanding of the complex polymer distributions.

## 1.2 Motivation of the Research

EPRs with high comonomer contents and vis-broken IPC samples have complex distributions in terms of molar mass and chemical composition as depicted in Figure 1.1. The rubber phase plays a critical role for the impact resistance of IPC materials and its molecular structure has not been largely investigated in previous work since it is regarded as completely amorphous material<sup>26</sup>. In addition, the molecular structure of vis-broken IPC materials have not been studied extensively in previous work<sup>21,27</sup>. The determination of the relationship between molecular structures of bulk samples and the individual components of the EPR copolymers and vis-broken IPC is a major challenge for polymer analysis. As such a single analytical technique approach cannot be used to fully characterise these types of complex polymer materials since minor components might not be detected and analysed due to their low concentrations. Hence, a comprehensive approach which combines various advanced analytical techniques must be developed to fully separate and characterise all components of these complex materials. This approach will be used in the present research project.

## 1.3 Objectives of the Research

From the literature review done, it can be deduced that vis-broken IPC and EPR copolymers are complex materials in terms of microstructural properties. Hence, the main aim of this study is to modify known analytical methods, to combine these methods and to develop a multidimensional analytical approach to obtain comprehensive information regarding the molar mass distribution (MMD) and chemical composition distribution (CCD) present in these complex polymeric systems.

The specific objectives for this research work include the following:

1. To determine MMD and CCD for bulk samples of both EPR and vis-broken IPC using various analytical techniques including SEC, DSC, CRYSTAF, FT-IR, <sup>13</sup>C NMR, HT-HPLC and HPLC-FT-IR.
2. To perform fractionations on bulk samples of both EPR and vis-broken IPC using the preparative TREF technique.
3. To determine the molecular heterogeneities of all TREF fractions using the previously mentioned analytical techniques for bulk sample analyses.

## **1.4 Hypothesis and Research Questions**

The aims and objectives of this study will answer the following key questions to fully understand the complexity of these two polymer systems by looking at the following three hypotheses:

In the first part of the study, the EPR copolymers prepared by Ziegler-Natta catalyst are studied using various analytical techniques. The aim in the current study is to test the hypothesis if EPR samples with high comonomer contents are completely amorphous or if the samples contain semi-crystalline components.

The second part of the study deals with the molecular characterization of the EPR copolymers synthesized by the metallocene catalyst. The present study will determine if the metallocene-based EPR samples are homogeneous regarding their chemical composition.

The last part of the study deals with the effect of an organic peroxide on the molecular structures of the IPC materials. From the present study, the key question to be answered is which components of IPC material are largely affected by thermo-oxidative degradation which is part of the vis-breaking process.

## **1.5 Significance of the Research**

Through a detailed literature survey it was found that there is little known in terms of the microstructures in EPR with high comonomer contents and vis-broken IPC samples. Thus, for the first time and based on knowledge of the current research, detailed and comprehensive microstructural analyses of EPR copolymers and vis-broken IPC materials will be done to achieve the following goals. Firstly, the characterization and separation of the individual components in the bulk samples will be achieved through various fractionation techniques. Secondly, the changes in both chemical composition and molar mass of the IPC as a result of vis-breaking will be monitored. Lastly, a better understanding of these two complex polymer systems will be attained after completion of this study.

## **1.6 Scope of the Research**

This study will focus only on two types of EP copolymers namely EPR and vis-broken IPC samples. The scope of this research work was based on the following observations or gaps seen in previous work. Firstly, separation and characterization was only done on bulk samples of EPR with high comonomer contents, where these copolymers were considered to be

amorphous<sup>26</sup>. The present study will extend the analyses to preparative fractionation procedures using TREF. The analyses of the TREF fractions will provide the detailed molecular heterogeneities of the EPR samples. Another part of this study will focus on degraded IPC materials. The previous work done on vis-broken IPC material had only covered the thermal and average chemical composition analyses<sup>19,21</sup>. The current study will deal with the comprehensive microstructural analyses of the vis-broken IPC using advanced fractionation techniques.

The non-degraded IPC materials have been dealt with extensively in the literature. Several authors<sup>21,26,28,29</sup> reported some research work on the physical, chemical and mechanical properties of the bulk samples of IPC. Cheruthazhekatt *et al.*<sup>30</sup> separated and characterized the IPC bulk samples using advanced analytical techniques. In their work, they did analyses on TREF fractions to explore the microstructure of these complex polymeric materials. Therefore, comprehensive work on the non-degraded IPC materials will not be part of the current work. The mechanical and morphological properties of both EPR and vis-broken IPC materials will also not be covered in the present study.

## 1.7 Layout of the Research

The work of this research is presented in four different chapters as outlined below.

- Chapter 1 gives the reader some historical background on both EPR and vis-broken IPC materials highlighting major findings in their separation and characterization. The motivation, aims and objectives of the study are given based on the gaps observed in previous work. Finally, the significance and scope of the study are illustrated to guide the reader for what to expect in this current research work.
  
- Chapter 2 gives the reader some insight into properties and applications of EPR and vis-broken IPC materials. Based on the complex nature of these materials, various analytical techniques are needed and thus extensive literature review is done to cover most of the separation and characterization techniques. Through the literature, attention is given to recent developments in polyolefin analysis so that the strengths and limitations of the techniques can be identified.

- In Chapters 3, 4 and 5, the results and discussions of three different studies done under this research work are summarized. The major findings are highlighted and presented in these chapters. For detailed information, the reader is referred to peer-reviewed articles attached to this dissertation.
  
- Chapter 6 gives conclusions on the results of the three studies that were conducted. Once more the reader is referred to full articles at the appendix since only major points are presented in this chapter. Recommendations for future work are also given here so that additional information about these complex materials can be obtained.

## 1.8 References

1. M. Gahleitner, C. Tranninger, P. Doshev. *Journal of Applied Polymer Science* **2013**, *130*, 3028-3037.
2. C. Kock, N. Aust, C. Grein, M. Gahleitner. *Journal of Applied Polymer Science* **2013**, *130*, 287-296.
3. S. Cheruthazhekatt, H. Pasch. *Analytical and Bioanalytical Chemistry* **2013**, *405*, 8607-8614.
4. T. Macko, R. Brüll, Y. Zhu, Y. Wang. *Journal of Separation Science* **2010**, *33*, 3446-3454.
5. W. Kaminsky. *Macromolecular Chemistry and Physics* **2008**, *209*, 459-466.
6. V. Agarwal, T. B. Van Erp, L. Balzano, M. Gahleitner, M. Parkinson, L. E. Govaert, V. Litvinov, A. P. M. Kentgens. *Polymer* **2014**, *55*, 896-905.
7. C. Grein, M. Gahleitner, K. Bernreitner. *Express Polymer Letters* **2012**, *6*, 688-696.
8. F. M. Mirabella Jr. *Polymer* **1993**, *34*, 1729-1735.
9. R. Zacur, G. Goizueta, N. Capiati. *Polymer Engineering and Science* **2000**, *40*, 1921-1930.
10. R. Zacur, G. Goizueta, N. Capiati. *Polymer Engineering and Science* **1999**, *39*, 921-929.
11. M. Sun, D. Gao, H. Zhang, H. Zou, M. Xu, S. Zhang, J. Li, J. Liu. *Journal of Applied Polymer Science* **2014**, *131*, 8705-8713.
12. Z. Q. Fan, Y. Q. Zhang, J. T. Xu, H. T. Wang, L. X. Feng. *Polymer* **2001**, *42*, 5559-5566.
13. Z. Fu, J. Xu, Y. Zhang, Z. Fan. *Journal of Applied Polymer Science* **2005**, *97*, 640-647.
14. M. H. Ha, B. K. Kim. *Polymer Engineering and Science* **2004**, *44*, 1858-1865.
15. L. Botha, P. Sinha, S. Joubert, H. Duveskog, A. J. van Reenen. *European Polymer Journal* **2014**, *59*, 94-104.
16. L. Botha, A. J. van Reenen. *European Polymer Journal* **2013**, *49*, 2202-2213.
17. S. Mncwabe, N. Luruli, E. Marantos, P. Nhlapo, L. Botha. *Macromolecular Symposia* **2012**, *313-314*, 33-42.



18. C. Kock, M. Gahleitner, A. Schausberger, E. Ingolic. *Journal of Applied Polymer Science* **2012**, *128*, 1484-1496.
19. E. de Goede, P. E. Mallon, K. Rode, H. Pasch. *Macromolecular Materials and Engineering* **2011**, *296*, 1018-1027.
20. H. Pasch, E. de Goede, P. Mallon. *Macromolecular Symposia* **2012**, *312*, 174-190.
21. M. Swart, A. J. van Reenen. *Journal of Applied Polymer Science* **2015**, *132*, 41783.
22. A. Shamiri, M. H. Chakrabarti, S. Jahan, M. A. Hussain, W. Kaminsky, P. V. Aravind, W. A. Yehye. *Materials* **2014**, *7*, 5069-5108.
23. E. de Goede, P. Mallon, H. Pasch. *Macromolecular Materials and Engineering* **2010**, *295*, 366-373.
24. C. Piel, F. G. Karssenber, W. Kaminsky, V. B. F. Mathot. *Macromolecules* **2005**, *38*, 6789-6795.
25. K. Jeon, Y. L. Chiari, R. G. Alamo. *Macromolecules* **2008**, *41*, 95-108.
26. T. Macko, A. Ginzburg, K. Remerie, R. Brüll. *Macromolecular Chemistry and Physics* **2012**, *213*, 937-944.
27. E. de Goede, P. E. Mallon, H. Pasch. *Macromolecular Materials and Engineering* **2012**, *297*, 26-38.
28. J. Tocháček, J. Jančář, J. Kalfus, P. Zbořilová, Z. Buráň. *Polymer Degradation and Stability* **2008**, *93*, 770-775.
29. S. Cheruthazhekatt, H. Pasch. *Macromolecular Symposia* **2014**, *337*, 51-57.
30. S. Cheruthazhekatt, G. W. Harding, H. Pasch. *Journal of Chromatography A* **2013**, *1286*, 69-82.

## CHAPTER 2: LITERATURE REVIEW

---

### 2 LITERATURE REVIEW

*In this chapter, an overview of ethylene – propylene copolymers (EPC) is given, illustrating the properties and final applicability of these materials. Also, on the basis of the polymerization conditions, the compositional complexities for two types of EPC materials namely vis-broken IPC and EPR copolymers are highlighted. A comprehensive survey on various analytical techniques used for separation and characterisation of EPC materials is also presented. The strengths and weaknesses of each technique are pointed out.*

#### 2.1 Overview on Ethylene-Propylene Copolymers

Isotactic polypropylene (iPP) has a number of valuable properties such as excellent heat resistance and high tensile strength, however, it exhibits poor low-temperature impact resistance<sup>1-4</sup>. The incorporation of a rubber material as a toughening agent has been proven to be an effective way to improve the low impact resistance of iPP<sup>5</sup>. Materials with high impact resistance have found widespread applications in automotive, packaging and industrial sewage pipelines<sup>6-8</sup>. Several approaches to improve the impact resistance of iPP have been reported in literature, for example reducing crystal size of iPP by influencing the nucleation process<sup>4</sup>, blending with elastomers<sup>6,9-14</sup> and copolymerization with ethylene species<sup>6-8,15-18</sup>. The binary and ternary blends prepared by mechanical blending have been used extensively to determine the influence of various components in the matrix of the iPP homopolymer<sup>12,19</sup>. The materials produced by copolymerization have been proved to be superior both in mechanical and chemical properties<sup>9,15-17,20</sup>.

Several types of ethylene-propylene copolymers (EPC) including impact polypropylene copolymers have been produced on industrial scale. The production process is carried out as a two-stage polymerization reaction. In the first reactor, the iPP matrix is produced and transferred to the second reactor where ethylene is introduced together with propylene to produce different types of EPC materials. The percentage of ethylene in the second reactor determines the final product composition since higher percentage values between 20 – 80 mol %, have resulted in the formation of ethylene-propylene rubber (EPR) copolymers with high comonomer contents<sup>21</sup>. The inclusion of the rubbery material in the iPP matrix results in impact polypropylene copolymers (IPC)<sup>22</sup>. In addition, other segmented copolymers with different ethylene or propylene sequences are produced to form semi-crystalline structures<sup>23</sup>.

The addition of organic peroxides to IPC produces vis-broken or degraded IPC materials. Several authors have shown that the process of vis-breaking can be done by adding the organic peroxide as additive either during copolymerization<sup>24-26</sup> or during the post-modification process using extruders<sup>7</sup>. A decrease in molar mass is always observed after the vis-breaking process indicating that the complex nature of vis-broken IPC materials is much increased as compared to non-degraded materials. The determination of the relationship between bulk molecular structures and the individual components of the vis-broken IPC and EPR copolymers is a challenge for polymer analysis. Complex analytical approaches to separate and characterize all components in these copolymer systems are needed to obtain comprehensive information on the EPC materials.

## 2.2 Separation and Characterisation Techniques

The complex nature of the EPC materials requires comprehensive analysis in terms of molar mass distribution (MMD) and chemical composition distribution (CCD), therefore, full separation and characterisation of all fractions of the materials must be achieved. As typical semi-crystalline polyolefins, both IPC and EPR copolymers cannot be fractionated at room temperature since they are soluble only above their crystallization temperatures which are above 120 °C. There are numerous techniques available for analysis of EPC materials. However, the techniques to be presented here will focus mainly on those used to carry out the current research work. Other analytical techniques not relevant to the study will only be highlighted where necessary.

### 2.2.1 Molar Mass Analysis Techniques

Molar mass averages, molar mass distributions (MMD) and dispersity ( $\mathcal{D}$ ) values of EPC materials are typically determined by high temperature size exclusion chromatography (HT-SEC)<sup>2,27-35</sup>. The dispersity values are a unique characteristic which can be used to differentiate EPR copolymers prepared by different catalyst systems. Metallocene-catalysed EPR copolymers have lower values of  $\mathcal{D}$ <sup>36,37</sup> due to the homogenous nature of the active sites of the catalyst while Ziegler-Natta-catalysed copolymers have higher values<sup>15,16</sup> which are the result of the high heterogeneity of the catalyst. Botha *et al*<sup>16</sup> studied EPR copolymers with different ethylene contents and they found that copolymers with the highest ethylene contents have higher molar masses. In the same study, when they coupled SEC to FT-IR spectroscopy, they observed that the ethylene content increased with increasing molar mass whereas the propylene

content decreased. Several studies<sup>26,38-41</sup> have shown that vis-broken IPC materials have decreased molar masses since the peroxide breaks long ethylene or propylene sequences to shorter chain sequences. Swart and van Reenen<sup>24</sup> showed that the amount of peroxide had a significant influence in lowering the molar masses of EP copolymers having similar ethylene contents. Pasch *et al.*<sup>26,39,40</sup> showed that the low molar mass region of degraded IPC copolymers contain more carbonyl products and this was an indication of increased chain scission upon degradation.

HT-SEC analyses of EP copolymer fractions from temperature rising elution fractionation (TREF) have been largely explored by Cheruthazhekatt and co-workers<sup>35,42,43</sup>. In their work, they have shown that bulk samples and their TREF fractions have different MMDs. The fractions show clear multimodality in MMD which indicates compositional heterogeneity especially for the mid-elution TREF fractions (elution temperatures between 60 and 100 °C). This observation was further supported by other studies in which it was reported that fractions collected at 60 – 100 °C show multiple MMDs since semi-crystalline parts of the copolymer and PP homopolymer co-elute due to the isotacticity and molar mass distribution found in PP<sup>44</sup>. However, higher eluting TREF fractions were observed to exhibit monomodal MMDs. Pasch and co-workers<sup>26,39,44</sup> have extensively studied the TREF fractions obtained from vis-broken IPC materials and they have observed that early and late eluting fractions have a definite shift towards lower molar masses upon degradation. Swart and van Reenen<sup>24</sup> further indicated that the organic peroxide had a significant effect on the 30 °C TREF fraction which is composed of soluble EP rubber. Furthermore, both studies have confirmed that the mid-elution TREF fractions show more complicated changes in MMD since lower and higher molar masses are affected differently by the degradation.

High temperature SEC has been applied successfully for the analyses of EP copolymers, however, the analysis of MMD was not sufficient to fully characterise these copolymer materials. In most applications, SEC was coupled to other detection techniques like FT-IR<sup>44-47</sup> and DSC<sup>42,43,48</sup> to enrich the information obtained from this technique. In general, this review on SEC techniques shows that SEC analyses alone cannot provide comprehensive separation and characterisation of these complex polyolefin materials, hence chemical composition techniques are always needed to enhance the information to be gathered during the analysis. The next section will deal with chemical composition analysis techniques which are both relevant to the present research project and have been previously used in the analyses of EPC materials.

## 2.2.2 Average Chemical Composition Analysis Techniques

In most studies dealing with the determination of the average chemical composition of EPC materials, Fourier transform-infrared (FT-IR)<sup>49</sup> and carbon-13 nuclear magnetic resonance (<sup>13</sup>C NMR)<sup>49-51</sup> spectroscopy have been employed to determine the comonomer content of such materials. In most industrial and academic research applications, FT-IR is used not only to identify the functional groups (i.e. -CH<sub>2</sub>- and -CH<sub>3</sub>) in EPC materials but also to determine the crystallinity of the materials. Cheruthazhekatt *et al.*<sup>43,48,51</sup> studied two IPC bulk samples with different ethylene contents, (10.4 and 11.8 mol %) and they could not differentiate between the two samples using the FT-IR spectroscopy technique alone. However, after TREF fractionation of the samples, the individual fractions were able to be differentiated using the ethylene crystallinity which is characterised by FT-IR absorption bands at 720 – 730 cm<sup>-1</sup>. The split of the peaks was found to increase with increasing TREF elution temperature, but the 130 °C fraction showed no split in the same spectral range due to the presence of predominantly long propylene units.

In a different study<sup>49</sup>, two EPR copolymers with higher ethylene contents, 71 and 80 mol %, were characterised and differentiated using the FT-IR technique on the basis of the relative intensities of the doublet at 720 – 730 cm<sup>-1</sup>. The appearance of this doublet indicated that some of the ethylene units were long enough to form crystalline lamellae. Propylene units were also observed to be present based on specific IR bands of these copolymers. The presence of carbonyl-containing degradation products was observed in vis-broken IPC materials based on the study done by de Goede *et al.*<sup>39</sup>. In their study, they used wavenumbers in the range of 1600 – 1750 cm<sup>-1</sup> to quantify the carbonyl-containing species and they showed that IPC materials with higher ethylene contents degrade at a slower rate due to their lower tertiary carbon contents. In other studies, the FT-IR spectroscopy technique has been applied as a very useful supplementary tool when it was coupled to other techniques such as SEC<sup>44</sup> and HPLC<sup>45,52</sup> since the propylene and ethylene contents of the copolymers could be determined as a function of elution volume.

High temperature <sup>13</sup>C NMR spectroscopy has been applied successfully to differentiate IPC and EPR copolymers based on their comonomer contents. The technique can be further utilised to determine the monomer composition and sequence distributions in EPC materials<sup>53-55</sup>. The research works done by both Randall<sup>56</sup> and Ray *et al.*<sup>57</sup> form the basis for microstructural

analysis of monomer sequences in polyolefin materials since they have developed relationships for quantifying dyads and triads in EPC materials. Ray *et al.*<sup>57</sup> further showed that EPR copolymers have complicated NMR spectra because of additional peaks which result from different tactic units of propylene. The complex nature of the NMR spectra for EPR copolymers was also confirmed by Tynys *et al.*<sup>58</sup>. In their work, they studied EPC materials prepared with metallocene catalyst systems and they were able to deduce mechanisms of chain initiation and termination for the polymerization reaction.

Fu *et al.*<sup>49</sup> fractionated two EPR copolymers using a thermal-gradient extraction fractionation technique and analysed the resulting fractions using <sup>13</sup>C NMR spectroscopy. The NMR spectra obtained for soluble fractions were found to be quite complex due to presence of random ethylene-propylene rubber components. The mid-elution fractions were observed to have different ethylene and propylene segments ranging from shorter to longer sequences<sup>15,24</sup>. In addition, these fractions indicated the presence of EP junctions in the polymer chain. The late eluting fractions at 120 and >120 °C had NMR characteristics similar to those of PE and iPP homopolymers, respectively. However, trace amounts of PE-b-PP block copolymers were also observed in these fractions further proving the complex nature of the EPR copolymers<sup>49</sup>. Swart and van Reenen<sup>24</sup> also used <sup>13</sup>C NMR spectroscopy to track the changes in both dyad and triad sequences along the TREF fractions. They showed that vis-breaking affects the segmented ethylene-propylene copolymers with long ethylene sequences. NMR spectroscopy can be further coupled to HPLC<sup>32,59-61</sup> to provide additional information on the chemical composition of the copolymers. Therefore, it remains a critical tool for microstructural analysis in polyolefin characterisation irrespective of the complex nature of the NMR spectra of EPC materials.

FT-IR and NMR can only give average chemical composition information about the EPC copolymer being analysed. This means that these techniques are not sufficient to determine the compositional heterogeneity of the EPC materials. In order to obtain comprehensive information on the chemical composition for the EPC materials, various fractionation techniques are available to separate polyolefins according to their chain structure. These techniques are either based on crystallization or interaction chromatographic principles.

### 2.2.3 Crystallization-Based Techniques

Thermal analysis is an effective way to obtain a wealth of information regarding the chemical composition of polyolefin materials. Differential scanning calorimetry (DSC) has been used

extensively in both industrial and academic applications to determine the crystallization and melting behaviour of EPC materials<sup>5,20,35,62-68</sup>. The technique is fast and reliable for routine analysis since there is little or no sample preparation required. Bulk IPC materials were analysed with DSC and single distinct peak maxima for melting were detected at ~ 155 °C. This peak was related to the melting behaviour of the iPP matrix<sup>37,42,43</sup>. The melting and crystallization temperatures of other minor IPC components (random EPR, segmented EPC and PE homopolymer) were not detected, they were assumed to be masked by the major component of the material. Stephens *et al.*<sup>69</sup> used the DSC technique to study the thermal behaviour of metallocene-catalysed copolymers with varying ethylene contents. They found that increasing comonomer contents resulted in a decrease of the peak melting temperature. In another study<sup>26</sup>, the IPC material was studied through stages of degradation using DSC and it was observed that the melt endotherm broadens and splits into two peaks with increasing degradation time. The second peak was assumed to be caused by carbonyl-containing species formed in the degradation process.

DSC analysis of TREF fractions has been done successively on both IPC and EPR copolymers. Pires *et al.*<sup>9</sup> fractionated reactor blends of different compositions containing segmented EP copolymers which were prepared by a Ziegler-Natta catalyst system. The TREF fractions collected at the same temperature, 50 °C, showed different melting endotherms indicating different chemical compositions among the copolymers. Several studies have shown that 30 °C TREF fractions show no observable melting and crystallization since these fractions contain amorphous random EP rubbers. On the other hand, the late eluting TREF fractions have melting and crystallization characteristics similar to those of PE and iPP homopolymers. de Goede *et al.*<sup>44</sup> further showed that the mid-eluting TREF fractions at 60 – 100 °C exhibit multiple melt endotherms which indicate the presence of various crystallisable components. The same observation was also made by Liberman *et al.*<sup>70</sup> where it was demonstrated that the mid-eluting fractions have compositional heterogeneities due to different crystalline structures. Moreover, their DSC results were consistent with their <sup>13</sup>C NMR analyses.

Despite the successful application of DSC for the analysis of EPC materials, the technique has a major drawback of co-crystallization experienced during the analysis of materials having different crystallisable components<sup>20,71-73</sup>. This effect in DSC analysis is caused by the fact that macromolecules containing propylene sequences have reduced mobility during the crystallization step and as such they form crystals at lower temperatures<sup>74,75</sup>. Another limiting factor in DSC analysis is that the quantitative determination of the crystallizing material is

depended on the thermal history and also the crystallization behaviour of the components are strongly influenced by their molecular environment<sup>71</sup>.

Solution crystallization-based fractionation techniques have been developed to overcome the difficulties encountered in DSC analysis. These techniques have the advantage that crystallization takes place in a thermodynamically good solvent, hence the effects of co-crystallization are minimised. There are numerous methods that exist for fractionation of polyolefins in solution, but the focus of this discussion will be only on two techniques namely, temperature rising elution fractionation (TREF) and crystallization analysis fractionation (CRYSTAF).

The TREF technique has been widely applied for polyolefin analysis after its development done by Wild<sup>76,77</sup>. The technique has been used for the determination of chemical composition distributions of EPC and other polyolefins as either analytical<sup>70,78-81</sup> or preparative TREF<sup>17,35,48,73</sup>. Aust *et al.*<sup>82</sup> performed a comprehensive study to optimise the experimental run parameters of TREF using heterophasic EPC materials. In their work, they used factorial design experiments to improve the resolution of TREF curves for EP copolymers and they found that increasing the start temperature of crystallization has a significant impact on the separation of the copolymer components. Monrabal and del Hiero<sup>81</sup> used analytical TREF to fractionate and characterise blends of PE, iPP and EPC and found that the technique provides poor resolution for combinations of PE and EPC materials but better separation was obtained for blends of highly regular iPP and PE homopolymers.



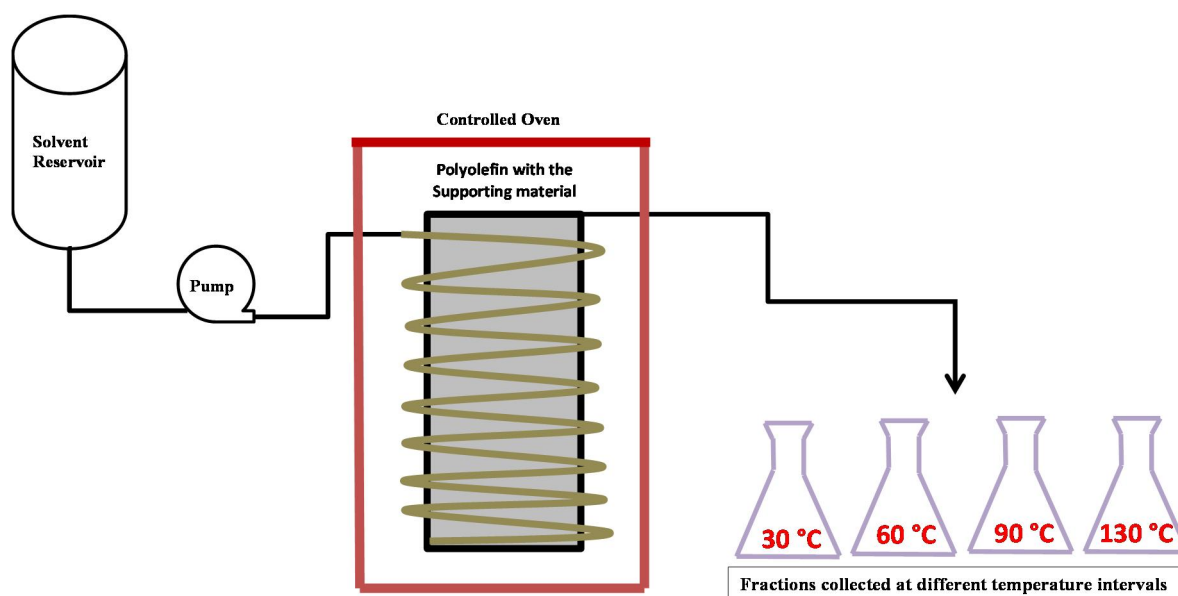


Figure 2.1: Schematic diagram of the preparative TREF set-up used for fractionation of the visbroken IPC and EPR copolymers.

Figure 2.1 shows the schematic diagram of the preparative set-up used for the fractionation experiments in the present study. Polyolefin material is usually dissolved in the xylene at 130 °C. The reactor with polyolefin solution is filled with purified sand which acts as the crystallization support. The controlled crystallization of the mixture is achieved by the oil bath which is cooled at a controlled rate of 1 °C/hour. The polyolefin together with the support material (purified sand) are heated in the oven at a specified heat rate as shown in Fig.2.1. At the same time, xylene solvent is passed through the mixture of the polyolefin to collect different fractions of the bulk material at the predetermined temperature intervals. de Goede *et al.*<sup>44</sup> did preparative TREF experiments of the IPC materials and they showed that the early eluting fractions at 30 °C consist mainly of random EP copolymers which are completely amorphous. Several authors<sup>17,48,52,83</sup> found that the mid-elution fractions collected in the temperature range of 60 – 100 °C consist of segmented EP copolymers. Cheruthazhekatt *et al.*<sup>42,43</sup> suggested that the mid-elution fractions form the interphase between the rubber and homopolymer phases since they have broad molecular compositions in terms of the MMD and CCD. PE and iPP homopolymers are usually found in the late eluting fractions above temperatures of 120 °C.

Despite the fact that preparative TREF is a very tedious and time consuming technique, it is considered as suitable method for the separation, isolation and analysis of the individual components in the copolymer matrix. Most importantly, it has been used as the concentrating step for minor components in the bulk copolymers. Pasch *et al.*<sup>26</sup> emphasised the need for preparative TREF when characterising degraded IPC materials since there was significant

heterogeneity in chemical composition due to the degradation process. In most studies, the collected individual fractions are analysed using different offline techniques like SEC, FT-IR and DSC. Kock *et al.*<sup>1,8</sup> used both analytical and preparative TREF techniques separately to fractionate IPC materials which have different PE modifiers. The combination of the two techniques has allowed for the fractionation and characterisation of both the amorphous and crystalline components of the copolymers. However, they found that the separation of random EPC and high density PE was quite difficult to achieve and this was also supported by the work done by Monrabal *et al.*<sup>71,80,81</sup>.

Monrabal and co-workers<sup>84-87</sup> developed CRYSTAF as an alternative technique to overcome the limitations of TREF for the separation and characterisation of EPC and other polyolefins. Since its introduction into polyolefin analysis, CRYSTAF has been established as an indispensable tool due to its short analysis time<sup>80,87-92</sup>. Macko *et al.*<sup>37</sup> used CRYSTAF to study EPR copolymers having different ethylene contents ranging from 14 – 56 mol %. The copolymers were found to be completely amorphous and could not be separated according to their chemical composition. However, for lower comonomer contents of 2 – 9 mol %, Chitta *et al.*<sup>28</sup> showed that separation is possible with the CRYSTAF technique since all peak maximum crystallization temperatures can be resolved and identified. The degradation process of IPC bulk materials was examined by the CRYSTAF technique and a decrease in the peak maximum of the crystallization curves was observed for layers close to the surface of the material<sup>26,40</sup>. Similar to TREF results presented elsewhere<sup>24</sup>, a significant increase in the soluble fraction was also noticed.

Bulk IPC materials have been studied extensively using the CRYSTAF technique to determine their CCDs. Several authors<sup>37,51,93</sup> have shown that bulk IPC samples have peak maximum crystallization temperatures similar to those of the iPP homopolymer. However, IPC materials show much higher soluble material than iPP due the amount of ethylene units incorporated into the copolymer. From CRYSTAF analysis, the early eluting TREF fractions have been shown to have no observable amount of crystallisable material, rendering them to be completely amorphous. Cheruthazhekatt *et al.*<sup>93</sup> analysed mid-eluting fractions using the CRYSTAF technique. In their research work, they reported broad CCDs for the fractions and they assumed that these fractions are the important components of the IPC material. Numerous studies have shown that it is difficult to separate PE and iPP homopolymers using the CRYSTAF technique since their peak maxima crystallization temperatures are close to each other<sup>71,81</sup>. The

crystallization temperature of the iPP homopolymer appears below that of PE due to the super-cooling effects experienced by iPP when in solution.

Regardless of the success in the applications of both TREF and CRYSTAF techniques for polyolefin analyses, these two techniques suffer from co-crystallization effects for components with different CCDs but having similar crystallization temperatures. Furthermore, these techniques are less useful in the analyses of amorphous materials, making them only applicable to semi- or highly crystalline materials. Lastly, the large amounts of solvent being used are a major concern for their application in the polyolefin industry.

#### **2.2.4 Interactive Chromatographic Techniques**

A comprehensive solvent-gradient chromatographic technique which allows the separation and characterization to occur above the melting and crystallization temperatures of EPC materials has been used to avoid the problems of co-crystallization effects that take place in DSC, TREF and CRYSTAF<sup>2,30,32,38,94-99</sup>. High temperature high performance liquid chromatography (HT-HPLC) permits the analysis of both amorphous and crystalline materials since the separation of the macromolecules depends on their interaction with the stationary phase (according chemical composition) in the presence of a binary mobile phase<sup>2,100-102</sup>.

Macko *et al.*<sup>98,99</sup> have selectively separated PE and PP from their blends using two types of zeolite materials as the stationary phases. They showed that PE or PP macromolecules are either fully eluted or retained depending on the zeolite type and solvents. They further observed that the retained material is quite difficult or sometimes impossible to desorb from the stationary phase. The limitation of the zeolite materials was overcome by the use silica gel as stationary phase and several authors<sup>38,103,104</sup> have reported that EP copolymers are effectively separated and eluted from the column with use of binary mobile phases. However, poor resolution and selectivity towards certain polyolefin systems like vinyl acetate was observed with silica gel materials as stationary phase<sup>38,103,105</sup>. A major breakthrough in interactive chromatographic analysis came from the work done by Macko and Pasch<sup>97</sup> where a HT-HPLC method that utilises a porous carbon-based material as stationary phase was developed. Their method has shown superior capabilities by separating polypropylene according to its three different tacticities (isotactic, atactic and syndiotactic) as well as from other polyolefins.

The same chromatographic system has been improved in recent years to separate different polyolefin materials according to their chemical composition<sup>104,106-109</sup>. In HPLC analysis of EPC materials, the elution volumes increase with the ethylene contents of the copolymers<sup>28,36</sup>. This behaviour results from a stronger adsorption of PE on the planar surface of graphite as compared to other species of PP or segmented EP macromolecules. Chitta *et al.*<sup>36,106</sup> studied metallocene-catalysed EPR copolymers with high comonomer contents of between 18 – 80 mol % using HT-HPLC. They found that the molar mass had no effect on the separation behaviour of the EPR copolymers but the ethylene content had an influence on separation using the Hypercarb column. Pasch and co-workers<sup>32,35,42,43,51,52</sup> also used the Hypercarb HPLC system and showed that the analysis of the bulk IPC materials does not reveal the peaks corresponding to minor components like random EPR, segmented EPC and PE homopolymer.

Several authors<sup>28,29,31,51,93</sup> have reported that HT-HPLC has superior separation capabilities over crystallization-based techniques like TREF, CRYSTAF and CEF, since it can also provide CCD of amorphous polyolefins. Macko and co-workers<sup>31,37,110</sup> carried out comparative studies between HT-HPLC and CRYSTAF for the analysis of blends of EPR and IPC materials. In their studies they indicated that HT-HPLC can detect minor differences in ethylene contents and they separated copolymers according to their microstructural properties. The CRYSTAF technique showed characterisation results similar to HT-HPLC only for IPC materials due to a high percentage of crystalline components i.e. iPP. They further demonstrated that the extent of adsorption of iPP in the Hypercarb column increases with increasing molar mass.

Mekap *et al.*<sup>111</sup> used the HT-HPLC system with porous graphite (Hypercarb) as the stationary phase to determine the critical conditions for PE materials. Four combinations of strong/weak solvent pairs were identified and their critical mobile phase compositions were successfully determined at a temperature of 160 °C. Several studies have shown that the HT-HPLC system can be hyphenated with other techniques like SEC, FT-IR and NMR to enrich the information obtained on the CCD of different classes of polyolefin materials. Pasch and co-workers<sup>35,45,52,71</sup> have done extensive work using a HT-HPLC system coupled to FT-IR spectroscopy through a LC-transform interface. From their work, FT-IR data have confirmed that IPC and EPR copolymers can be separated according to the ethylene content of the eluting fractions. The recent work done by Cheruthazhekatt and Pasch<sup>112</sup> on EPR copolymers with high comonomer contents has proved that the HT-HPLC system can be modified for improved separation in polyolefin analyses. In their work, they developed a chromatographic method named high temperature size exclusion-liquid adsorption chromatography (SEC-LAC). The new SEC-LAC

method was coupled to FT-IR to quantify small amounts of iPP homopolymer in EPR copolymers.

## 2.3 References

1. C. Kock, M. Gahleitner, A. Schausberger, E. Ingolic. *Journal of Applied Polymer Science* **2012**, *128*, 1484-1496.
2. H. Pasch, M. I. Malik, T. Macko. *Advances in Polymer Science* **2013**, *251*, 77-140.
3. R. A. García, B. Coto, M. T. Expósito, I. Suarez, A. Fernández-Fernández, S. Caveda. *Macromolecular Research* **2011**, *19*, 778-788.
4. M. Sun, D. Gao, H. Zhang, H. Zou, M. Xu, S. Zhang, J. Li, J. Liu. *Journal of Applied Polymer Science* **2014**, *131*, 8705-8713.
5. J. K. Lee, J. H. Lee, K. H. Lee, B. S. Jin. *Journal of Applied Polymer Science* **2001**, *81*, 695-700.
6. V. Agarwal, T. B. Van Erp, L. Balzano, M. Gahleitner, M. Parkinson, L. E. Govaert, V. Litvinov, A. P. M. Kentgens. *Polymer* **2014**, *55*, 896-905.
7. M. Gahleitner, C. Tranninger, P. Doshev. *Journal of Applied Polymer Science* **2013**, *130*, 3028-3037.
8. C. Kock, N. Aust, C. Grein, M. Gahleitner. *Journal of Applied Polymer Science* **2013**, *130*, 287-296.
9. M. Pires, R. S. Mauler, S. A. Liberman. *Journal of Applied Polymer Science* **2004**, *92*, 2155-2162.
10. Y. Shang-Guan, F. Chen, Q. Zheng. *Science China Chemistry* **2012**, *55*, 698-712.
11. Y. Yokoyama, T. Ricco. *Journal of Applied Polymer Science* **1997**, *66*, 1007-1014.
12. R. Zacur, G. Goizueta, N. Capiati. *Polymer Engineering and Science* **2000**, *40*, 1921-1930.
13. R. Zacur, G. Goizueta, N. Capiati. *Polymer Engineering and Science* **1999**, *39*, 921-929.
14. Z. S. Petrović, J. Budinski-Simendić, V. Divjaković, Ž. Škrbić. *Journal of Applied Polymer Science* **1996**, *59*, 301-310.
15. L. Botha, P. Sinha, S. Joubert, H. Duveskog, A. J. van Reenen. *European Polymer Journal* **2014**, *59*, 94-104.
16. L. Botha, A. J. van Reenen. *European Polymer Journal* **2013**, *49*, 2202-2213.
17. S. Mncwabe, N. Luruli, E. Marantos, P. Nhlapo, L. Botha. *Macromolecular Symposia* **2012**, *313-314*, 33-42.
18. C. Grein, M. Gahleitner, K. Bernreitner. *Express Polymer Letters* **2012**, *6*, 688-696.
19. F. M. Mirabella Jr. *Polymer* **1993**, *34*, 1729-1735.
20. Z. Q. Fan, Y. Q. Zhang, J. T. Xu, H. T. Wang, L. X. Feng. *Polymer* **2001**, *42*, 5559-5566.
21. S. Thanyapruksanon, S. Thongyai, P. Prasertdam. *Journal of Applied Polymer Science* **2007**, *103*, 3609-3616.
22. A. J. van Reenen, N. C. Basson. *Express Polymer Letters* **2012**, *6*, 427-436.

23. W. Rungswang, P. Saendee, B. Thitisuk, T. Pathaweeisariyakul, W. Cheevasrirungruang. *Journal of Applied Polymer Science* **2013**, *128*, 3131-3140.
24. M. Swart, A. J. van Reenen. *Journal of Applied Polymer Science* **2015**, *132*, 41783.
25. N. Manabe, Y. Yokota, H. Nakatani, S. Suzuki, B. Liu, M. Terano. *Journal of Applied Polymer Science* **2006**, *100*, 1831-1835.
26. H. Pasch, E. de Goede, P. Mallon. *Macromolecular Symposia* **2012**, *312*, 174-190.
27. S. Podzimek. *Journal of Applied Polymer Science* **2014**, *131*, 40111.
28. R. Chitta, T. Macko, R. Brüll, C. Boisson, E. Cossoul, O. Boyron. *Macromolecular Chemistry and Physics* **2015**, *216*, 721-732.
29. R. Chitta, T. Macko, R. Brüll, G. van Doremaele, L. C. Heinz. *Journal of Polymer Science, Part A: Polymer Chemistry* **2011**, *49*, 1840-1846.
30. T. Macko, R. Brüll, R. G. Alamo, F. J. Stadler, S. Losio. *Analytical and Bioanalytical Chemistry* **2011**, *399*, 1547-1556.
31. T. Macko, R. Brüll, Y. Wang, B. Coto, I. Suarez. *Journal of Applied Polymer Science* **2011**, *122*, 3211-3217.
32. H. Pasch, A. Albrecht, R. Brüll, T. Macko, W. Hiller. *Macromolecular Symposia* **2009**, *282*, 71-80.
33. S. Cheruthazhekatt, H. Pasch. *Polymer* **2014**, *55*, 5358-5369.
34. S. Cheruthazhekatt, H. Pasch. *Analytical and Bioanalytical Chemistry* **2014**, *406*, 2999-3007.
35. S. Cheruthazhekatt, T. F. J. Pijpers, V. B. F. Mathot, H. Pasch. *Analytical and Bioanalytical Chemistry* **2013**, *405*, 8995-9007.
36. R. Chitta, A. Ginzburg, T. Macko, R. Brüll, G. van Doremaele. *LC-GC Europe* **2012**, *25*, 352-358.
37. T. Macko, A. Ginzburg, K. Remerie, R. Brüll. *Macromolecular Chemistry and Physics* **2012**, *213*, 937-944.
38. A. Albrecht, R. Brüll, T. Macko, P. Sinha, H. Pasch. *Macromolecular Chemistry and Physics* **2008**, *209*, 1909-1919.
39. E. de Goede, P. E. Mallon, H. Pasch. *Macromolecular Materials and Engineering* **2012**, *297*, 26-38.
40. E. de Goede, P. E. Mallon, K. Rode, H. Pasch. *Macromolecular Materials and Engineering* **2011**, *296*, 1018-1027.
41. S. de Goede, R. Brüll, H. Pasch, N. Marshall. *E-Polymers* **2004**, 1-9.
42. S. Cheruthazhekatt, T. F. J. Pijpers, G. W. Harding, V. B. F. Mathot, H. Pasch. *Macromolecules* **2012**, *45*, 5866-5880.
43. S. Cheruthazhekatt, T. F. J. Pijpers, G. W. Harding, V. B. F. Mathot, H. Pasch. *Macromolecules* **2012**, *45*, 2025-2034.
44. E. de Goede, P. Mallon, H. Pasch. *Macromolecular Materials and Engineering* **2010**, *295*, 366-373.
45. A. Albrecht, L. C. Heinz, D. Lilge, H. Pasch. *Macromolecular Symposia* **2007**, *257*, 46-55.

46. T. Macko, U. Schulze, R. Brüll, A. Albrecht, H. Pasch, T. Fónagy, L. Häussler, B. Iván. *Macromolecular Chemistry and Physics* **2008**, *209*, 404-409.
47. C. Piel, A. Albrecht, C. Neubauer, C. W. Klampfl, J. Reussner. *Analytical and Bioanalytical Chemistry* **2013**, *400*, 2607-2613.
48. S. Cheruthazhekatt, T. F. J. Pijpers, V. B. F. Mathot, H. Pasch. *Macromolecular Symposia* **2013**, *330*, 22-29.
49. Z. Fu, J. Xu, Y. Zhang, Z. Fan. *Journal of Applied Polymer Science* **2005**, *97*, 640-647.
50. K. Jeon, Y. L. Chiari, R. G. Alamo. *Macromolecules* **2008**, *41*, 95-108.
51. S. Cheruthazhekatt, H. Pasch. *Analytical and Bioanalytical Chemistry* **2013**, *405*, 8607-8614.
52. S. Cheruthazhekatt, G. W. Harding, H. Pasch. *Journal of Chromatography A* **2013**, *1286*, 69-82.
53. G. Liu, X. Zhang, Y. Liu, X. Li, H. Chen, K. Walton, G. Marchand, D. Wang. *Polymer* **2013**, *54*, 1440-1447.
54. Y. Liu, S. Bo, Y. Zhu, W. Zhang. *Journal of Applied Polymer Science* **2005**, *97*, 232-239.
55. Y. D. Zhang, C. J. Wu, S. N. Zhu. *Polymer Journal* **2002**, *34*, 700-708.
56. J. C. Randall. *Macromolecules* **1978**, *11*, 33-36.
57. G. J. Ray, P. E. Johnson, J. R. Knox. *Macromolecules* **1977**, *10*, 773-778.
58. A. Tynys, I. Fonseca, M. Parkinson, L. Resconi. *Macromolecules* **2012**, *45*, 7704-7710.
59. M. Hehn, K. Maiko, H. Pasch, W. Hiller. *Macromolecules* **2013**, *46*, 7678-7686.
60. W. Hiller, P. Sinha, M. Hehn, H. Pasch. *Progress in Polymer Science* **2014**, *39*, 979-1016.
61. H. Pasch, L. C. Heinz, T. Macko, W. Hiller. *Pure and Applied Chemistry* **2008**, *80*, 1747-1762.
62. E. B. Berda, T. W. Baughman, K. B. Wagener. *Journal of Polymer Science, Part A: Polymer Chemistry* **2006**, *44*, 4981-4989.
63. V. B. F. Mathot, M. F. J. Pijpers. *Thermochimica Acta* **1989**, *151*, 241-259.
64. V. B. F. Mathot, R. L. Scherrenberg, T. F. J. Pijpers. *Polymer* **1998**, *39*, 4541-4559.
65. G. vanden Poel, V. B. F. Mathot. *Thermochimica Acta* **2007**, *461*, 107-121.
66. S. Cheruthazhekatt, D. D. Robertson, M. Brand, A. van Reenen, H. Pasch. *Analytical Chemistry* **2013**, *85*, 7019-7023.
67. M. H. Ha, B. K. Kim. *Polymer Engineering and Science* **2004**, *44*, 1858-1865.
68. X. Y. Lu, J. J. Yi, S. T. Chen, F. H. Zu, R. B. Li. *Chinese Journal of Polymer Science* **2012**, *30*, 122-129.
69. C. H. Stephens, B. C. Poon, P. Ansems, S. P. Chum, A. Hiltner, E. Baer. *Journal of Applied Polymer Science* **2006**, *100*, 1651-1658.
70. S. Liberman, A. P. De Azeredo, F. P. Dos Santos, M. A. Da Silva, B. Monrabal, N. Mayo. *Macromolecular Symposia* **2013**, *330*, 30-41.
71. H. Pasch, R. Brüll, U. Wahner, B. Monrabal. *Macromolecular Materials and Engineering* **2000**, *279*, 46-51.

72. L. Lu, H. Fan, B. G. Li, S. Zhu. *Industrial and Engineering Chemistry Research* **2009**, *48*, 8349-8355.
73. Y. Xue, Y. Fan, S. Bo, X. Ji. *European Polymer Journal* **2011**, *47*, 1646-1653.
74. G. Shen, H. Shen, B. Xie, W. Yang, M. Yang. *Journal of Applied Polymer Science* **2013**, *129*, 2103-2111.
75. D. G. Papageorgiou, G. Z. Papageorgiou, D. N. Bikiaris, K. Chrissafis. *European Polymer Journal* **2013**, *49*, 1577-1590.
76. L. Wild, R. Ranganath, A. Barlow. *Journal of Applied Polymer Science* **1977**, *21*, 3331-3343.
77. L. Wild, T. Ryle. *American Chemical Society, Polymer Preprints, Division of Polymer Chemistry* **1977**, *18*, 182-187.
78. B. Monrabal. *Advances in Polymer Science* **2013**, *257*, 203-252.
79. B. Monrabal, J. Sancho-Tello, N. Mayo, L. Romero. *Macromolecular Symposia* **2007**, *257*, 71-79.
80. J. Nieto, T. Oswald, F. Blanco, J. B. P. Soares, B. Monrabal. *Journal of Polymer Science, Part B: Polymer Physics* **2001**, *39*, 1616-1628.
81. B. Monrabal, P. Del Hierro. *Analytical and Bioanalytical Chemistry* **2011**, *399*, 1557-1561.
82. N. Aust, M. Gahleitner, K. Reichelt, B. Raninger. *Polymer Testing* **2006**, *25*, 896-903.
83. S. Cheruthazhekatt, H. Pasch. *Macromolecular Symposia* **2014**, *337*, 51-57.
84. S. Anantawaraskul, J. B. P. Soares, P. M. Wood-Adams, B. Monrabal. *Polymer* **2003**, *44*, 2393-2401.
85. B. Monrabal. *Macromolecular Symposia* **1996**, *110*, 81-86.
86. B. Monrabal. *Journal of Applied Polymer Science* **1994**, *52*, 491-499.
87. B. Monrabal, J. Blanco, J. Nieto, J. B. P. Soares. *Journal of Polymer Science, Part A: Polymer Chemistry* **1999**, *37*, 89-93.
88. S. Anantawaraskul, J. B. P. Soares, P. Jirachathorn, J. Limtrakul. *Journal of Polymer Science, Part B: Polymer Physics* **2006**, *44*, 2749-2759.
89. S. Anantawaraskul, J. B. P. Soares, P. M. Wood-Adams. *Advances in Polymer Science* **2005**, *182*, 1-54.
90. S. Anantawaraskul, P. Somnukguande, J. B. P. Soares. *Macromolecular Symposia* **2009**, *282*, 205-215.
91. J. B. P. Soares. *Macromolecular Symposia* **2007**, *257*, 1-12.
92. J. B. P. Soares, S. Anantawaraskul. *Journal of Polymer Science, Part B: Polymer Physics* **2005**, *43*, 1557-1570.
93. S. Cheruthazhekatt, N. Mayo, B. Monrabal, H. Pasch. *Macromolecular Chemistry and Physics* **2013**, *214*, 2165-2171.
94. H. Pasch. *Polymers for Advanced Technologies* **2015**, *26*, 771-784.
95. T. Macko, R. Brüll, R. G. Alamo, Y. Thomann, V. Grumel. *Polymer* **2009**, *50*, 5443-5448.
96. T. Macko, F. Cutillo, V. Busico, R. Brüll. *Macromolecular Symposia* **2010**, *298*, 182-190.
97. T. Macko, H. Pasch. *Macromolecules* **2009**, *42*, 6063-6067.



98. T. Macko, H. Pasch, R. Brüll. *Journal of Chromatography A* **2006**, *1115*, 81-87.
99. T. Macko, H. Pasch, Y. Wang. *Macromolecular Symposia* **2009**, *282*, 93-100.
100. H. Pasch, B. Trathnigg. *HPLC of Polymers*; Springer: New York, **1998**.
101. A. Roy, M. D. Miller, D. M. Meunier, A. Willem Degroot, W. L. Winniford, F. A. van Damme, R. J. Pell, J. W. Lyons. *Macromolecules* **2010**, *43*, 3710-3720.
102. H. Pasch, M. I. Malik. *Advanced Separation Techniques for Polyolefins*; Springer: New York, **2014**.
103. R. Chitta, R. Brüll, T. Macko, V. Monteil, C. Boisson, E. Grau, A. Leblanc. *Macromolecular Symposia* **2010**, *298*, 191-199.
104. A. Ginzburg, T. Macko, V. Dolle, R. Brüll. *Journal of Chromatography A* **2010**, *1217*, 6867-6874.
105. E. Uliyanchenko, S. van der Wal, P. J. Schoenmakers. *Polymer Chemistry* **2012**, *3*, 2313-2335.
106. R. Chitta, A. Ginzburg, G. van Doremale, T. Macko, R. Brüll. *Polymer* **2011**, *52*, 5953-5960.
107. A. Ginzburg, T. Macko, V. Dolle, R. Brüll. *European Polymer Journal* **2011**, *47*, 319-329.
108. A. Ginzburg, T. Macko, F. Malz, M. Schroers, I. Troetsch-Schaller, J. Strittmatter, R. Brüll. *Journal of Chromatography A* **2013**, *1285*, 40-47.
109. V. Dolle, A. Albrecht, R. Brüll, T. Macko. *Macromolecular Chemistry and Physics* **2011**, *212*, 959-970.
110. T. Macko, R. Brüll, Y. Zhu, Y. Wang. *Journal of Separation Science* **2010**, *33*, 3446-3454.
111. D. Mekap, T. Macko, R. Brüll, R. Cong, A. W. deGroot, A. Parrott, P. J. C. H. Cools, W. Yau. *Polymer* **2013**, *54*, 5518-5524.
112. S. Cheruthazhekatt, H. Pasch. *Polymer* **2015**, *64*, 1-7.

## Chapter 3: Experimental Work

---

### 3 Experimental Procedures: Analytical Techniques

*This chapter discusses and explains the analytical experimental procedures used to separate and characterize both ethylene-propylene rubbers (EPR) and vis-broken impact polypropylene copolymers (IPC) materials. Different combinations of the various analytical techniques were used in each part of the study to obtain comprehensive information on the materials.*

#### 3.1 Temperature Rising Elution Fractionation (TREF)

Preparative TREF was carried out using an instrument developed and built in-house. Approximately 3.0 g of polymer and 2.0 wt% Irganox 1010 (Ciba Specialty Chemicals, Switzerland) were dissolved in 300 mL of xylene at 130 °C in a glass reactor. The dissolution time was between 3 – 4 hrs. The reactor was then transferred to a temperature-controlled oil bath and filled with sand (white quartz, Sigma-Aldrich, South Africa), used as a crystallization support. The oil bath and support were both preheated to 130 °C. The oil bath was then cooled to temperature of 20 °C at a controlled rate of 1 °C/h in order to facilitate the controlled crystallization of the polymer<sup>1,2</sup>. The crystallized mixture was then packed into a stainless steel column which was inserted into a modified gas chromatography oven for the elution step. Xylene (preheated) was used as eluent in order to collect the fractions at predetermined intervals (30, 60, 90 and 130 °C) as the temperature of the oven was raised. The fractions were isolated by precipitation in acetone, followed by drying to a constant weight for an overnight period.

#### 3.2 Differential Scanning Calorimetry (DSC)

Melting and crystallization behaviours of the samples were measured on a TA Instruments Q100 DSC system, calibrated with indium metal according to standard procedures. A sample mass of ~5.0 mg was used for the analysis. A scanning rate of 10 °C/min was applied across the temperature range of -70 – 200 °C. The samples were subjected to three cycles with the first cycle (first heating) used to erase the thermal history of the samples<sup>3</sup>. Data obtained during the second (cooling) and third (heating) cycles were used for all thermal analysis calculations. Measurements were conducted in a nitrogen atmosphere at a purge gas flow rate of 50 mL/min.

#### 3.3 Crystallization Analysis Fractionation (CRYSTAF)

CRYSTAF experiments were carried out using a commercial CRYSTAF apparatus Model 200 (Polymer Char, Valencia, Spain). For each sample, approximately 20 mg was dissolved in 35

mL of 1,2,4-trichlorobenzene (TCB) at 160 °C. Dissolution was carried out for 120 – 180 minutes depending on the ethylene content of the sample. Dissolution and crystallization was carried out under agitation in stainless steel reactors, equipped with automatic stirring and filtration devices. After dissolution, the temperature was decreased from 100 °C to approximately 30 °C at a rate of 0.1 °C/min. Fractions were taken automatically and the concentration of the solution was determined by an infrared detector as function of temperature, using 3.5  $\mu\text{m}$  as the chosen wavelength.

### **3.4 High Temperature Size Exclusion Chromatography (HT-SEC)**

Molar mass measurements for all samples were performed at 150 °C using a PL GPC 220 high temperature chromatograph (Polymer Laboratories, Church Stretton, UK) equipped with a differential refractive index (RI) detector. The column set used consisted of three 300 $\times$ 7.5 mm i.d. PLgel Olexis columns together with a 50 $\times$ 7.5 mm PLgel Olexis guard column (Polymer Laboratories, Church Stretton, UK). The eluent used was TCB at a flow rate of 1.0 mL/min with 0.0125 wt% 2,6-ditertbutyl-4-methylphenol (BHT) added as a stabilizer. Samples with mass of ~2 mg were dissolved at 160 °C in TCB at a concentration of 1 mg/mL for 2 – 3 hr (depending on the ethylene content of the sample) and 200  $\mu\text{L}$  of each sample was injected. Narrowly distributed polystyrene standards (Polymer Laboratories, Church Stretton, UK) were used for calibration.

### **3.5 High Temperature High Performance Liquid Chromatography (HT-HPLC)**

The separations were conducted on a high temperature solvent gradient interaction chromatograph (SGIC) constructed by Polymer Char (Valencia, Spain), comprising of an autosampler, two separate ovens, switching valves and two pumps equipped with vacuum degassers (Agilent, Waldbronn, Germany). One oven was used for the HPLC column, while the second oven is the location of the injector and a switching valve. The autosampler is a separate unit connected to the injector through a heated transfer line. A high-pressure binary gradient pump was used for HPLC in the first dimension.

An evaporative light scattering detector (ELSD, model PL-ELS 1000, Polymer Laboratories, Church Stretton, England) was used with the following parameters: a gas flow rate of 1.5 L/min, a nebuliser temperature of 160 °C, and an evaporator temperature of 270 °C. HT-HPLC was carried out using a Hypercarb column (Hypercarb®, Thermo Scientific, Dreieich, Germany) with the following parameters: 100 $\times$ 4.6 mm id., packed with porous graphite particles with a particle diameter of 5 $\mu\text{m}$ , a surface area of 120 m<sup>2</sup>/g, and a pore size of 250 Å. The flow rate of

the mobile phase was 0.5 mL/min. The column was placed in the column oven maintained at 160 °C. The HPLC separations were accomplished by applying a linear gradient<sup>4,5</sup> from 1-decanol to TCB as shown in Fig. 3.1. The volume fraction of TCB was linearly increased to 100% within 10 min after the sample injection and then held constant for 25 min. Finally, the initial chromatographic conditions were re-established with 100% 1-decanol. The dwell and void volumes of 1.7 ml and 1.1 ml, respectively were measured according the method described by Ginzburg et al<sup>6,7</sup>. This reflects that there is an isocratic elution of 1-decanol (1.7 ml) before the start of gradient hits the column<sup>8</sup>. Samples were injected at a concentration of 1 – 1.2 mg/mL, with 20 µL of each sample being injected.

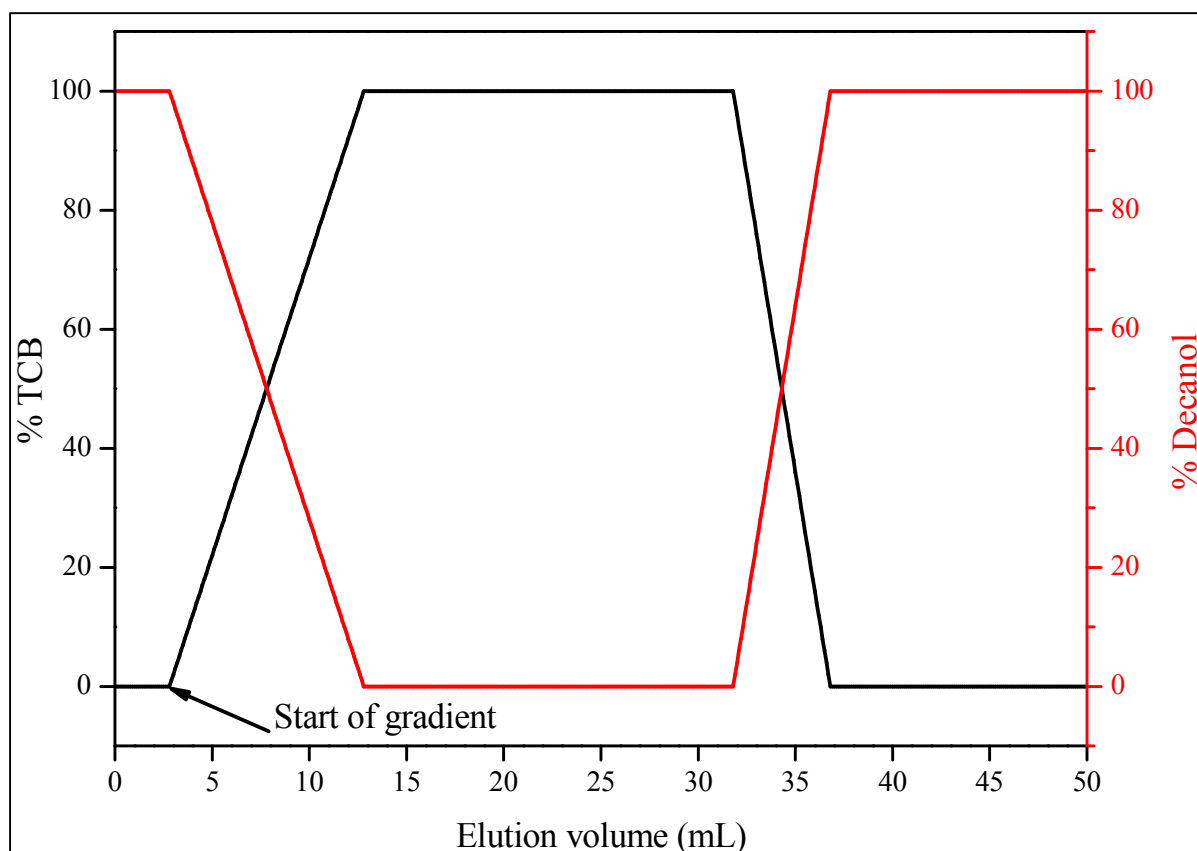


Figure 3.1: Linear gradient profile for the mobile composition in HPLC separations.

### 3.5.1 Collection of HPLC fractions by the LC Transform Interface

An LC-Transform series model 303 (Lab Connections) was coupled to the high temperature SGIC instrument in order to collect the HPLC eluate. Samples were dissolved at 160 °C in 1-decanol at a concentration of 1 – 1.2 mg/mL, with 110 µL of each sample being injected. The HPLC column outlet was connected to the LC transform interface through a heated transfer line

set at 160 °C. The fractions were deposited by rotating a Germanium disc (sample target in the LC-Transform) at a speed of 10 °/min. The disc stage and nozzle temperatures of the LC-Transform were set to 160 °C. The pressure was set at ~10 atm to obtain uniform deposition of the sample on the disc.

### 3.5.2 FTIR analyses of the deposited fractions

FTIR analyses of the deposited HPLC fractions were performed on a Thermo Nicolet iS10 Spectrometer (Thermo Scientific, Waltham, MA), equipped with the LC-Transform FTIR interface connected to a standard transmission base plate. Spectra were recorded in the absorbance format at a resolution of 8 cm<sup>-1</sup> with 16 scans being recorded for each spectrum. Thermo Scientific OMNIC software (version 8.1) was used for data collection and processing.

### 3.6 Fourier Transform Infrared Spectroscopy (FTIR)

FTIR analyses of the samples were performed on a Thermo Nicolet iS10 Spectrometer (Thermo Scientific, Waltham, MA). Spectra were recorded in the absorbance format at a resolution of 8 cm<sup>-1</sup> with 16 scans being recorded for each spectrum. Thermo Scientific OMNIC software (version 8.1) was used for data collection and processing.

### 3.7 High Temperature <sup>13</sup>C NMR Spectroscopy

<sup>13</sup>C NMR spectra were measured on a 400-MHz Varian Unity Inova NMR spectrometer, at a resonance frequency of 150 MHz for carbon. Deuterated 1,1,2,2-tetrachloroethane-d<sub>2</sub> (95.5+ atom% D, Sigma-Aldrich) at δ 74.3 ppm as internal reference, was used as a solvent for the sample preparation (at a concentration of 6 wt%). The dissolution time was between 3 – 4 hr, depending on the ethylene content of the sample. Analyses were carried out at 120 °C in nitrogen atmosphere, with an acquisition time of 0.79 s and pre-acquisition delay time of 15 s with more than 2500 scans. This had led to total analysis time of 6 to 10 hr per sample.

### 3.8 References

1. S. Cheruthazhekatt, H. Pasch. *Macromolecular Symposia* **2014**, 337, 51-57.
2. M. Swart, A. J. van Reenen. *Journal of Applied Polymer Science* **2015**, 132, 41783.
3. H. Pasch, R. Brüll, U. Wahner, B. Monrabal. *Macromolecular Materials and Engineering* **2000**, 279, 46-51.

4. T. Macko, H. Pasch. *Macromolecules* **2009**, *42*, 6063-6067.
5. S. Cheruthazhekatt, H. Pasch. *Analytical and Bioanalytical Chemistry* **2013**, *405*, 8607-8614.
6. A. Ginzburg, T. Macko, V. Dolle, R. Brüll. *European Polymer Journal* **2011**, *47*, 319-329.
7. A. Ginzburg, T. Macko, F. Malz, M. Schroers, I. Troetsch-Schaller, J. Strittmatter, R. Brüll. *Journal of Chromatography A* **2013**, *1285*, 40-47.
8. S. Cheruthazhekatt, G. W. Harding, H. Pasch. *Journal of Chromatography A* **2013**, *1286*, 69-82.

## Chapter 4: Molecular Heterogeneity of EPR Copolymers

---

### 4 Molecular Heterogeneity of Ethylene-Propylene Rubbers: New Insights through Advanced Crystallisation-based and Chromatographic Techniques

*This chapter outlines the work done on the separation and characterization of ethylene-propylene rubber (EPR) copolymers using advanced fractionation methods. The importance of the TREF procedure for both isolating and concentrating minor components of the bulk samples is highlighted in the present work. In general, the combination of the various analytical techniques proved that EPR copolymers with high ethylene contents have complex molecular compositions and are not completely amorphous. This work has been published as the following research article: Phiri, M.J.; Cheruthazhekatt, S.; Dimeska, A.; Pasch, H., Molecular Heterogeneity of Ethylene-Propylene Rubbers: New Insights through Advanced Crystallization-based and Chromatographic Techniques. *Journal of Polymer Science Part A: Polymer Chemistry* 2015, 53, 863-874.*

#### 4.1 Summary of the Research Study

Ethylene-propylene rubber (EPR) forms the most critical phase of impact polypropylene copolymers (IPC) since it contributes significantly to the impact resistance of the IPC. EPR copolymers with high ethylene contents have been assumed to be completely amorphous random copolymers based on their bulk sample analyses using crystallisation-based techniques such as CRYSTAF<sup>1-3</sup>. As such, the comprehensive analysis of the microstructure of EPR copolymers has not been extensively explored in previous work. The main aim of the present study was to explore advanced fractionation techniques namely SEC, TREF, CRYSTAF, DSC, HPLC and HPLC-FTIR for the elucidation of the molecular structure of a set of EPR samples. In the current study, five EPR samples prepared by a Ziegler-Natta catalyst system were separated and characterised by both crystallisation-based and chromatographic techniques. The EPR samples had different ethylene contents, which were in the range of 25 – 66 mol % as determined by <sup>13</sup>CNMR spectroscopy.

The CRYSTAF analyses revealed that there is little or no detectable amount of crystallizing material in the bulk samples in the temperature range between 30 – 100 °C and the samples could be regarded to be completely amorphous. This observation was made from the remaining soluble material collected below 30 °C, which indicates the end of the crystallization process.

However, the results of the DSC analyses indicated the presence of long crystallizable sequences of either ethylene or propylene units within the bulk samples. Samples with lower ethylene contents (25 – 45 mol %) have copolymer components with broad chemical compositions ranging from segmented ethylene-propylene copolymers (EPC) at ~120 °C and propylene-rich copolymers or low tacticity isotactic polypropylene (iPP) at ~150 °C. On the other hand, samples with higher ethylene contents (45 – 66 mol %) have only one peak at 120 °C due to formation of EPC material. The intensity of the peak was observed to increase with larger amounts of ethylene in the bulk samples. In order to obtain a comprehensive chemical composition distribution (CCD) of the samples, HT-HPLC was used since the separation occurs above the melting and crystallization temperatures of the EPR samples. The results of HT-HPLC showed that samples with lower and higher ethylene contents contain propylene-rich and ethylene-rich copolymers, respectively. The latter was confirmed by the longer retention time on the column suggesting that there is strong interaction with the long ethylene sequences. This showed that one technique was not sufficient to characterize complex materials like EPR copolymers comprehensively.

Therefore, the bulk samples were fractionated by preparative TREF and analysed by a variety of complementary techniques to obtain comprehensive information on the molecular complexity of the EPR copolymers. Figure 4.1 presents the fractionation by TREF and the analyses of the 90 °C TREF fractions of the EPR samples using SEC, HPLC, CRYSTAF and DSC. Interestingly, there were significant amounts of crystallising material in the samples as indicated by the presence of the 90 and 130 °C TREF fractions, see Fig 4.1A. It was found that the TREF fractions collected above 120 °C contain only PE or PP homopolymers. Considering the high amounts of comonomers it was rather unexpected to find homopolymers in these rubber materials. The major phase present in the EPR copolymers was found to contain random ethylene-propylene (EP) copolymers making ~60 % of the bulk material, as seen by the largest percentage collected at the TREF temperature of 30 °C. TREF was able to isolate and preconcentrate the minor components within the bulk samples which were not easily achievable with other methods. The TREF fractions were very complex regarding their molecular compositions since co-crystallization and co-elution took place during the experimental procedure. As such, there was a need to determine the detailed CCD of the fractions using further analyses techniques.



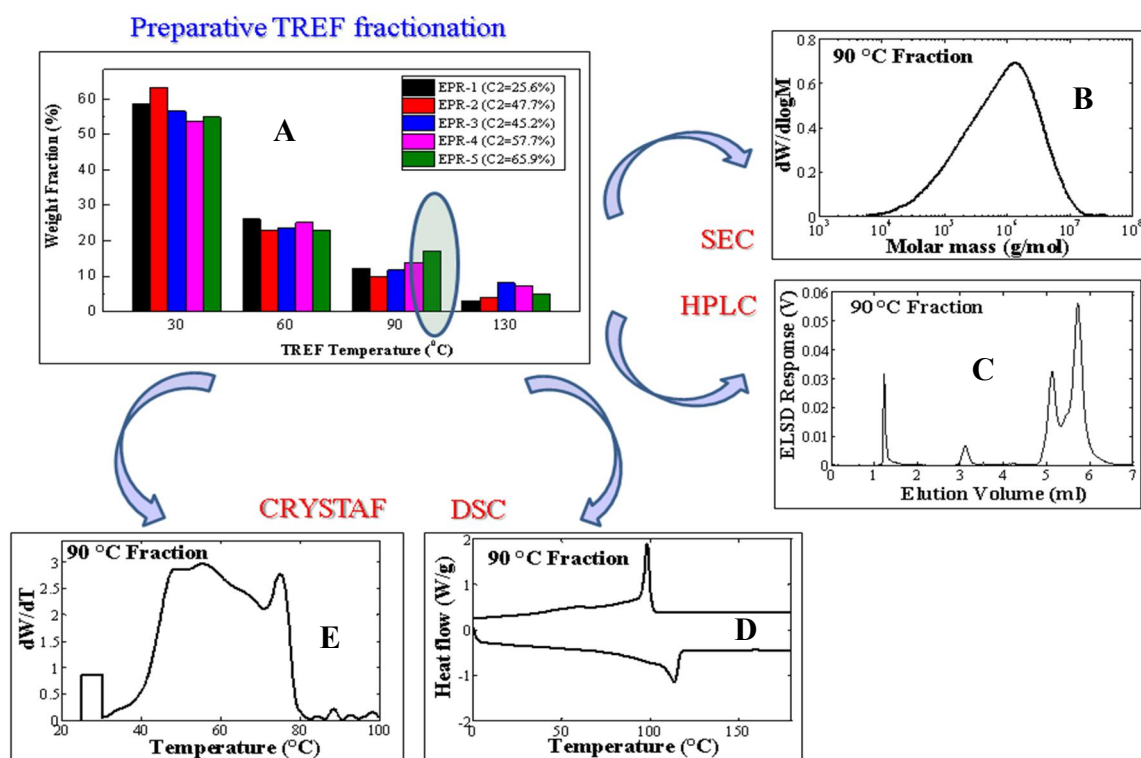


Figure 4.1: prep-TREF fractionation results of EPR copolymers (A) and analyses of the 90 °C TREF fraction using SEC (B), HT-HPLC (C), DSC (D) and CRYSTAF (E).

For all TREF fractions, unimodal molar mass distributions (MMD) were obtained using HT-SEC. The broadness of the MMD curves was found to decrease with increasing TREF temperature indicating a lower heterogeneity in the late eluting fractions. The 30 °C TREF fractions were confirmed by HT-HPLC to contain random EP copolymers and the elution volumes of the fractions were found to depend on the ethylene contents of their respective bulk samples. All samples eluted after start of the gradient. However, due to the amorphous nature of the 30 °C TREF fractions, DSC and CRYSTAF were not able to characterize these fractions. The mid-elution TREF fractions at 60 °C showed the existence of EP components with large crystallisable sequences when using the DSC<sup>4</sup> with multiple melting and crystallization peaks. The crystallization temperatures ( $T_c$ ) for the fractions occurred at ~70 °C which was about a difference of 30 °C from their melting temperatures ( $T_m$ ). This difference further proved that these TREF fractions are composed of random units of propylene and ethylene with different sequence lengths; they consequently take a long time to crystallize.

The CRYSTAF curves for the 90 °C TREF fractions showed multi-modal distribution behaviors for the crystallization temperature range between 40 – 80 °C. There were three distinct peaks that were observed for these TREF fractions. The first set of peaks which appeared at ~45 °C was attributed to presence of random EPC copolymers. It was assumed to

be caused by high amounts of terminal methyl groups from the low molar mass copolymers that have small contents of propylene units. In a previous study by Nieto et al<sup>5</sup>, it was found that terminal methyl groups reduce the overall crystallinity of polymer materials in a similar manner as short-chain branches from comonomer incorporation. The second set of peaks at ~60 °C was probably due to propylene-rich copolymers. The last set of peaks which appeared at around 75 °C was due to ethylene-rich EP copolymers and their intensities increased with the ethylene content of the bulk samples. The 90 °C TREF fractions are the most important fractions in these EPR samples, since they form the interphase between the amorphous part (EP rubber) and highly crystalline materials (iPP and PE).

The 130 °C TREF fractions contained both crystalline EPC and iPP homopolymer as determined by DSC, with two melting peaks at 120 and 160 °C, respectively. However, there was a single peak for  $T_c$  reflecting that there was co-crystallization taking place within the eluting TREF fractions. The HPLC chromatograms obtained for the 130 °C TREF fractions showed three distinct set of peaks at different elution volume regions. All the samples showed the presence of low molar mass iPP which elutes in 100 % 1-decanol before the start of gradient. The second set of elution peaks appeared immediately after the start of the gradient and they were due to high molar mass of iPP. The last set of peaks which results from the presence of PE homopolymer appears at an elution volume of ~ 6.0 mL. The results of HT-HPLC showed a comprehensive separation and characterization for both amorphous and crystalline TREF fractions.

In order to obtain additional microstructural information on the separated fractions, HT-HPLC was coupled to FT-IR spectroscopy using the LC transform interface. The FT-IR data confirmed that the TREF fractions were separated according to the ethylene content of the eluted samples<sup>6</sup>. From HPLC of the 130 °C TREF fractions, the early eluting samples were observed to contain the low molar mass iPP reflected by the presence of methyl (CH<sub>3</sub>) stretches with absorption bands at 2956 and 2871 cm<sup>-1</sup>. The late eluting component from HPLC showed more intense peaks for the methylene (CH<sub>2</sub>) stretches with absorption bands at 2920 and 2850 cm<sup>-1</sup>. Moreover, the CH<sub>2</sub> split peaks at 720 – 730 cm<sup>-1</sup> reflected the presence of crystalline ethylene sequences from the PE homopolymer. The result proved that material that elutes after the start of the TCB gradient is composed of ethylene segments which increase with HPLC elution volume. The overall results illustrate the capability of HT-HPLC coupled to FTIR spectroscopy to separate and characterize the EPR samples according to the comprehensive microstructure properties.

From the HPLC results, it was confirmed that the lengths of propylene and ethylene sequences in the chain influence their interaction with the Hypercarb stationary phase, thus making ethylene-rich copolymers and PE homopolymer to elute at later elution volumes. In overall, the combination of preparative TREF and various advanced analytical techniques proved that EPR copolymers are not completely amorphous through a comprehensive analyses done in the present study.

## 4.2 References

1. T. Macko, R. Brüll, Y. Wang, B. Coto, I. Suarez. *Journal of Applied Polymer Science* **2011**, *122*, 3211-3217.
2. T. Macko, A. Ginzburg, K. Remerie, R. Brüll. *Macromolecular Chemistry and Physics* **2012**, *213*, 937-944.
3. S. Cheruthazhekatt, N. Mayo, B. Monrabal, H. Pasch. *Macromolecular Chemistry and Physics* **2013**, *214*, 2165-2171.
4. E. de Goede, P. Mallon, H. Pasch. *Macromolecular Materials and Engineering* **2010**, *295*, 366-373.
5. J. Nieto, T. Oswald, F. Blanco, J. B. P. Soares, B. Monrabal. *Journal of Polymer Science, Part B: Polymer Physics* **2001**, *39*, 1616-1628.
6. S. Cheruthazhekatt, G. W. Harding, H. Pasch. *Journal of Chromatography A* **2013**, *1286*, 69-82.

# Molecular Heterogeneity of Ethylene-Propylene Rubbers: New Insights Through Advanced Crystallization-Based and Chromatographic Techniques

Mohau Justice Phiri,<sup>1</sup> Sadiqali Cheruthazhett,<sup>1</sup> Anita Dimeska,<sup>2</sup> Harald Pasch<sup>1</sup>

<sup>1</sup>Department of Chemistry and Polymer Science, Stellenbosch University, 7602 Matieland, South Africa

<sup>2</sup>Lummas Novolen Technology GmbH, Carl-Bosch-Str. 38, 67056 Ludwigshafen, Germany

Correspondence to: H. Pasch (E-mail: [hpasch@sun.ac.za](mailto:hpasch@sun.ac.za))

Received 21 October 2014; accepted 8 December 2014; published online 13 January 2015

DOI: 10.1002/pola.27512

**ABSTRACT:** For a long time ethylene-propylene rubber (EPR) copolymers with high comonomer contents were believed to be amorphous materials with a random copolymer composition. This is not completely correct as has been shown by temperature rising elution fractionation (TREF) combined with differential scanning calorimetry (DSC), crystallization analysis fractionation (CRYSTAF), and high temperature–high-performance liquid chromatography (HT-HPLC). When using only conventional crystallization-based fractionation methods, the comprehensive compositional analysis of EPR copolymers was impossible due to the fact that large fractions of these copolymers do not crystallize under CRYSTAF conditions. In the present work, HT-HPLC was used for the separation of the EPR copolymers according to their ethylene and propylene distributions along the polymer chains. These investigations showed the existence of long ethylene sequences in the bulk samples which was further confirmed by DSC. The results on the bulk samples prompted us to conduct preparative fractionations of EPR copolymers having varying ethylene contents using TREF. Surprisingly, significant amounts of crystallizing materials were obtained that were analyzed using a multistep protocol. CRYSTAF and DSC analyses of the TREF fractions

revealed the presence of components with large crystallizable sequences that had not been detected by the bulk samples analyses. HT-HPLC provided a comprehensive separation and characterization of both the amorphous and the crystalline TREF fractions. The TREF fractions eluting at higher temperatures showed the presence of ethylene-rich copolymers and PE homopolymer. In order to obtain additional structural information on the separated fractions, HT-HPLC was coupled to Fourier transform-infrared (FT-IR) spectroscopy. The FT-IR data confirmed that the TREF fractions were separated according to the ethylene contents of the eluted samples. Preparative TREF analysis together with a combination of various analytical methods proved to be useful tools in understanding the complex molecular composition of these rubber samples. © 2015 Wiley Periodicals, Inc. *J. Polym. Sci., Part A: Polym. Chem.* **2015**, *53*, 863–874

**KEYWORDS:** differential scanning calorimetry; ethylene-propylene rubber; fractionation of polymers; FT-IR spectroscopy; high temperature–high performance liquid chromatography; microstructure; polyolefins; preparative temperature rising elution fractionation

**INTRODUCTION** Ethylene-propylene rubbers (EPR) are widely used as the stress concentrators or absorbers that prevent crack propagation in the continuous matrix of isotactic polypropylene (iPP) homopolymer.<sup>1</sup> The specific composition of the dispersed rubber particles leads to an improved interphase bonding in the matrix of the material.<sup>1,2</sup> Other studies have suggested that the rubber particles cause a decrease in domain size of the crystalline polymer thus increasing the overall impact strength.<sup>3–5</sup> These improved materials, frequently named “impact polypropylene copolymers (IPC)” exhibit enhanced toughness properties in a wide temperature range and they are used in applications such as automobile parts, appliances and other industrial uses.<sup>2,4–7</sup>

The EPR copolymers used in this study were prepared using a Ziegler-Natta catalyst system that is typically used in the dual-reactor IPC process. Due to multiple active sites of the catalyst, copolymers with very broad molar mass distribution (MMD) and chemical composition distribution (CCD) are produced. Furthermore, the EPR copolymers have comonomer (ethylene) contents between 25 and 66%. Studies have shown that in this percentage range, the samples are regarded to be noncrystallizing and amorphous.<sup>6,8,9</sup> It was also found that the crystallization temperatures as measured from crystallization fractionation analysis (CRYSTAF) were below 35 °C, further suggesting amorphous behavior of EPR.<sup>8</sup> However, due to the high reactivity of ethylene, one

© 2015 Wiley Periodicals, Inc.

has to consider small quantities of various materials including highly branched to linear polyethylene homopolymer and ethylene-propylene segmented copolymers to be present in EPR.<sup>5–7,10–12</sup> Due to this complexity, the investigation of the molecular composition of EPR copolymers is in the focus of this study.

The importance of the compositional analysis arises from the fact that MMD and CCD play major roles in the microstructure and phase separation behavior of EPR copolymers. High temperature size exclusion chromatography (HT-SEC) has been used extensively for the determination of MMD of the EPR copolymers and other polyolefins.<sup>8–11,13–15</sup> In terms of CCD analysis, there are various analytical techniques that have been used effectively for characterization of high comonomer content EPR copolymers.<sup>4,6,8–11</sup> Nuclear magnetic resonance (<sup>13</sup>C-NMR) and Fourier transform-infrared (FT-IR) spectroscopy have been used for characterization of the EPR copolymers and average comonomer contents are mostly estimated by these techniques.<sup>2,6,8,16–18</sup> Another approach to chemical composition analysis is the use of differential scanning calorimetry (DSC) for analyzing the melting and crystallization behaviors of EPR copolymers<sup>2,10,13</sup> and the observation of glass transition temperatures which decrease with increasing ethylene content.<sup>16,18</sup> DSC is a simple and widely used method, however, the crystallization behavior is strongly influenced by the thermal history of the sample.<sup>15,19–23</sup> Solution crystallization-based techniques, such as temperature rising elution fractionation (TREF)<sup>10,24–27</sup> and crystallization analysis fractionation (CRYSTAF),<sup>15,28–31</sup> have been utilized to analyze CCD of EPR copolymers with high ethylene contents. It has been indicated by both techniques that these copolymers are completely amorphous or contain only very small amounts of crystallizing material. As a result EPRs with high comonomer contents cannot be fully separated and characterized through these techniques. The main limitation of these techniques is the fact that they can fractionate and analyze only the crystallizable part of the material.<sup>6,32,33</sup>

A comprehensive solvent-gradient chromatographic technique which permits separation and characterization to occur above the melting and crystallization temperatures of polyolefins has been used to avoid the problems of co-crystallization effects that take place in DSC, TREF, and CRYSTAF.<sup>6,11,34–37</sup> The recently developed high temperature-high performance liquid chromatography (HT-HPLC) allows the analysis of both the amorphous and the crystalline fractions since the separation depends on the interaction or adsorption of the macromolecules with the stationary phase.<sup>14,27,38–44</sup> For EPR copolymers it had been reported that on a graphitic stationary phase the separation depends mainly on the ethylene content of the sample.<sup>11,26,35,40–42</sup> The HPLC chromatograms of EPR copolymers with high ethylene contents had shown multimodal elution profiles that indicate the complexity of these samples.<sup>8</sup> Thus the need to find a comprehensive method to fully characterize the EPR copolymers is of great importance in both academia and industry.

**TABLE 1** Details on the Composition of the Bulk EPR Samples

Sample ID	Ethylene Content (C <sub>2</sub> ) by NMR (wt %)	<i>M<sub>w</sub></i> <sup>a</sup> by SEC (kg/mol)	<i>M<sub>w</sub></i> / <i>M<sub>n</sub></i>
EPR 1	25.6	851	8.6
EPR 2	37.7	497	16.3
EPR 3	45.2	1946	24.4
EPR 4	57.7	857	13.2
EPR 5	65.9	1001	13.5

<sup>a</sup> Molar masses are polystyrene equivalents.

In this study we demonstrate the capabilities of the combination of DSC, CRYSTAF, and HT-HPLC with FT-IR spectroscopy for the separation and characterization of EPR copolymers produced by a Ziegler-Natta catalyst system. For the first time it will be shown that the combination of preparative TREF and a range of advanced analytical techniques can provide detailed information on EPR copolymers with high comonomer contents in terms of thermal, crystallization, and microstructural properties.

## EXPERIMENTAL

### Materials

Xylene (>99% purity) and 1-decanol (>99% purity) were purchased from Chemical & Laboratory suppliers and Aldrich, respectively, and used as received. HPLC grade 1,2,4-trichlorobenzene (TCB) was purchased from Sigma Aldrich and filtered through a 0.2 μm membrane filter before use. Five model ethylene-propylene rubber (EPR) samples were obtained from Lummus Novolen Technology GmbH (Germany) and they were designated as EPR-1, EPR-2, EPR-3, EPR-4, and EPR-5. These EPR samples were prepared in a lab scale polymerization reactor using a Ziegler-Natta catalyst system. The gas phase copolymerizations were carried out for 60 min at a temperature of 60 °C and a pressure of 13.8 bar. Their bulk ethylene contents and molar masses are given in Table 1.

### Temperature Rising Elution Fractionation

Preparative TREF was carried out using an instrument developed and built in-house. Approximately 3.0 g of polymer and 2.0 wt % Irganox 1010 (Ciba Specialty Chemicals, Switzerland) were dissolved in 300 mL of xylene at 130 °C in a glass reactor. The reactor was then transferred to a temperature-controlled oil bath and filled with sand (white quartz, Sigma-Aldrich, South Africa), used as a crystallization support. The oil bath and support were both preheated to 130 °C. The oil bath was then cooled at a controlled rate of 1 °C/h in order to facilitate the controlled crystallization of the polymer. The crystallized mixture was then packed into a stainless steel column which was inserted into a modified gas chromatography oven for the elution step. Xylene (pre-heated) was used as eluent in order to collect the fractions

at predetermined intervals as the temperature of the oven was raised. The fractions were isolated by precipitation in acetone, followed by drying to a constant weight. The TREF fractionations were repeated once a good reproducibility was obtained.

### Differential Scanning Calorimetry

Melting and crystallization behaviors of the samples were measured on a TA Instruments Q100 DSC system, calibrated with indium metal according to standard procedures. A scanning rate of 10 °C/min was applied across the temperature range of 0 to 200 °C. Data obtained during the second heating cycle were used for all thermal analysis calculations. Measurements were conducted in a nitrogen atmosphere at a purge gas flow rate of 50 mL/min.

### Crystallization Analysis Fractionation

CRYSTAF experiments were carried out using a commercial CRYSTAF apparatus Model 200 (Polymer Char, Valencia, Spain). For each sample, approximately 20 mg was dissolved in 35 mL of 1,2,4-trichlorobenzene (TCB). Crystallization was carried out under agitation in stainless steel reactors, equipped with automatic stirring and filtration devices. After dissolution, the temperature was decreased from 100 °C to approximately 30 °C at a rate of 0.1 °C/min. Fractions were taken automatically and the concentration of the solution was determined by an infrared detector, using 3.5 μm as the chosen wavelength.

### High Temperature Size Exclusion Chromatography

Molar mass measurements for all samples were performed at 150 °C using a PL GPC 220 high temperature chromatograph (Polymer Laboratories, Church Stretton, UK) equipped with a differential refractive index (RI) detector. The column set used consisted of three 300 × 7.5 mm i.d. PLgel Olexis columns together with a 50 × 7.5 mm PLgel Olexis guard column (Polymer Laboratories, Church Stretton, UK). The eluent used was TCB at a flow rate of 1.0 mL/min with 0.0125 wt % 2,6-ditertbutyl-4-methylphenol (BHT) added as a stabilizer. Samples were dissolved at 160 °C in TCB at a concentration of 1 mg/mL for 1 to 2 h (depending on the sample type) and 200 μL of each sample was injected. Narrowly distributed polystyrene standards (Polymer Laboratories, Church Stretton, UK) were used for calibration. The accuracy of the molar mass determinations was ±5%.

### Chromatographic System

All chromatographic experiments were performed using a new chromatographic system for high-temperature two-dimensional liquid chromatography constructed by Polymer Char (Valencia, Spain), comprising of an autosampler, two separate ovens, switching valves, and two pumps equipped with vacuum degassers (Agilent, Waldbronn, Germany). One oven was used for the HPLC column, while the second oven is the location of the injector and a switching valve. The autosampler is a separate unit connected to the injector through a heated transfer line. A high-pressure binary gradient pump was used for HPLC in the first dimension.

### High Temperature HPLC

The separations were conducted on a high temperature solvent gradient interaction chromatograph (SGIC) constructed by Polymer Char (Valencia, Spain). An evaporative light scattering detector (ELSD, model PL-ELS 1000, Polymer Laboratories, Church Stretton, England) was used with the following parameters: A gas flow rate of 1.5 L/min, a nebuliser temperature of 160 °C, and an evaporator temperature of 270 °C. HT-HPLC was carried out using a Hypercarb column (Hypercarb®, Thermo Scientific, Dreieich, Germany) with the following parameters: 100 × 4.6 mm id., packed with porous graphite particles with a particle diameter of 5 μm, a surface area of 120 m<sup>2</sup>/g, and a pore size of 250 Å. The flow rate of the mobile phase was 0.5 mL/min. The column was placed in the column oven maintained at 160 °C. The HPLC separations were accomplished by applying a linear gradient from 1-decanol to TCB. The volume fraction of TCB was linearly increased to 100% within 10 min after the sample injection and then held constant for 25 min. Finally, the initial chromatographic conditions were re-established with 100% 1-decanol. Samples were injected at a concentration of 1 to 1.2 mg/mL, with 20 μL of each sample being injected.

### Collection of HPLC Fractions by the LC Transform Interface

An LC-Transform series model 303 (Lab Connections) was coupled to the SGIC instrument in order to collect the HPLC eluate. Samples were dissolved at 160 °C in 1-decanol at a concentration of 1 to 1.2 mg/mL, with 110 μL of each sample being injected. The HPLC column outlet was connected to the LC transform interface through a heated transfer line set at 160 °C. The fractions were deposited by rotating a Germanium disc (sample target in the LC-Transform) at a speed of 10°/min. The disc stage and nozzle temperatures of the LC-Transform were set to 160 °C.

### FT-IR Analyses of the Deposited Fractions

FT-IR analyses of the deposited HPLC fractions were performed on a Thermo Nicolet iS10 Spectrometer (Thermo Scientific, Waltham, MA), equipped with the LC-Transform FT-IR interface connected to a standard transmission base plate. Spectra were recorded at a resolution of 8 cm<sup>-1</sup> with 16 scans being recorded for each spectrum. Thermo Scientific OMNIC software (version 8.1) was used for data collection and processing.

## RESULTS AND DISCUSSION

The molecular compositions of the EPR copolymers were studied using different analytical techniques as will be presented here. Firstly, CRYSTAF was used to study the crystallization behavior of the samples in solution, employing TCB as the solvent. Secondly, in order to examine the crystallization and melting characteristics of these EPR, standard DSC was utilized. These techniques were used to find out if the samples were amorphous rubbers. Lastly, the chemical composition distributions of the samples were studied using adsorption chromatography which operates above any

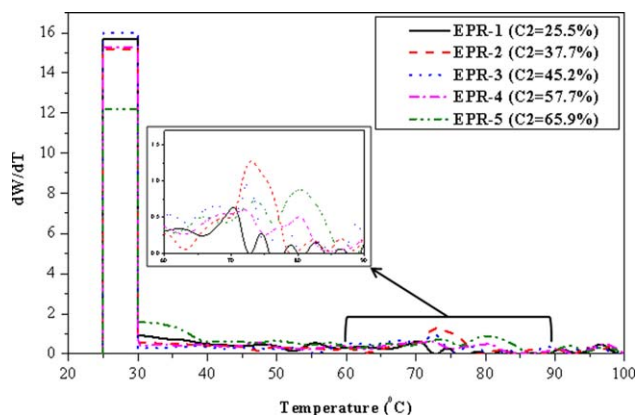


**FIGURE 1** CRYSTAF curves of EPR samples obtained in the temperature range between 30 and 100 °C, insert represents the zoomed parts of the curves between 60 and 90 °C. [Color figure can be viewed in the online issue, which is available at [wileyonlinelibrary.com](http://wileyonlinelibrary.com).]

melting temperatures and separates based on the ethylene content of the samples.

The solution crystallization curves as obtained by CRYSTAF are presented in Figure 1. For the interpretation of the crystallization curves, the following must be taken into consideration: crystallizable polymer material precipitates out of solution between 30 and 100 °C with macromolecules having the longest ethylene and propylene sequences precipitating at the highest temperatures. At the end of the crystallization (precipitation) process at 30 °C, all polymer material remaining in solution forms the amorphous part and is presented as an rectangular area in the crystallization curve.<sup>29</sup> From Figure 1, it can be observed that there is almost no polymer material crystallizing in the temperature range between 30 and 100 °C. Most of the material is located in the soluble fraction. Therefore, it can be assumed that the EPR samples are practically amorphous because of the large amounts of soluble fractions below 30 °C. However, when zooming into the region between 60 and 90 °C, as illustrated by the insert in Figure 1, there are small crystallizable amounts of EPR that vary in chemical composition.

The DSC results for the bulk samples are illustrated in Figure 2(a) using the second heating data to study the melting behavior of the EPR samples. Surprisingly, all samples showed melting events above room temperature. EPR-1 exhibits a broad melting region between 80 and 150 °C as shown in Figure 2(a). The broadness of the melting region is a clear indication for the complex chemical composition of this sample. Fractions that melt at lower temperatures belong to copolymer species with higher ethylene contents while the fractions with higher propylene contents melt at higher temperatures. On the other hand, samples EPR-2 and EPR-3 exhibit two distinct melting regions with sharp intense peaks and low intensity peaks at approximately 120 and 160 °C, respectively. The first set of peaks is attributed to the presence of ethylene-propylene crystalline (EPC) copolymers and intensities of the peaks increase with

increasing ethylene contents of the samples. The second set of peaks at 160 °C is due to presence of isotactic polypropylene (iPP).<sup>13</sup> Samples EPR-4 and EPR-5 exhibit only one sharp peak at 120 °C which is also due to the presence of EPC. The increased intensity of this peak correlates also with the ethylene content of the samples.

The crystallization behavior of the EPR samples follows the same trend as the melting behavior as can be seen in Figure 2(b). The first cooling data were used in this case. There are multiple crystallization peaks that might be due to components with distinctively different chemical compositions. Samples EPR-4 and EPR-5 show one single crystallization peak at around 100 °C.

The DSC results of the bulk samples do not reveal all details of the molecular complexity of these samples. In order to obtain more comprehensive chemical composition information, HT-HPLC was used. The separation in this case takes place above the melting and crystallization temperatures of the EPR samples.

The chromatograms of the EPR samples are shown in Figure 3, where after a short isocratic elution period using 1-decanol the TCB gradient starts at 2.7 mL. The results indicate that all bulk samples elute after the start of the gradient

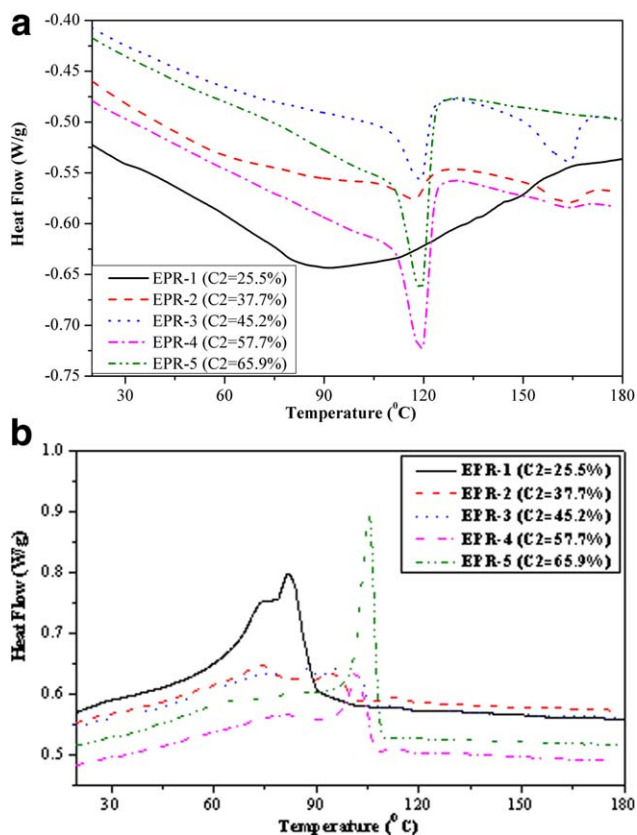


**FIGURE 2** DSC curves for the EPR samples, (a) second heating curves at scan rate of 10 °C/min, (b) first cooling curves at scan rate of 10 °C/min. [Color figure can be viewed in the online issue, which is available at [wileyonlinelibrary.com](http://wileyonlinelibrary.com).]

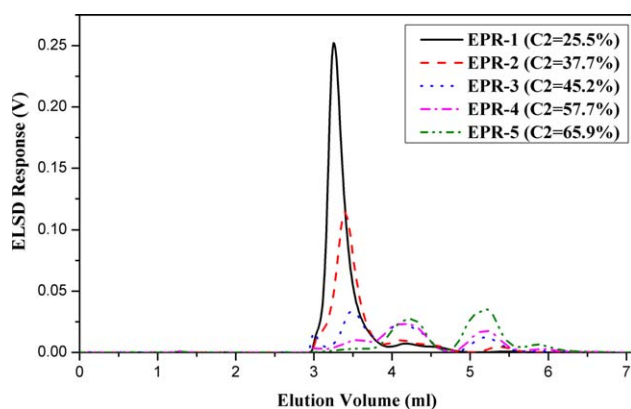


**FIGURE 3** HT-HPLC chromatograms obtained after isocratic and gradient elution (1-decanol to TCB) for the EPR bulk samples. [Color figure can be viewed in the online issue, which is available at [wileyonlinelibrary.com](http://wileyonlinelibrary.com).]

elution and there is no noticeable material that elutes in 100% 1-decanol. This indicates clearly, that the samples do not contain any low molar mass amorphous PP. EPR-1 and EPR-2 having lower  $C_2$  contents are assumed to consist mainly of propylene-rich material. This is confirmed by the appearance of sharp elution peaks between elution volumes of 3 and 4 mL. EPR-2 shows a small peak at an elution volume of about 5 mL which indicates components with higher ethylene contents. Sample EPR-3 shows the presence of high molar iPP as indicated by the small peak eluting at the start of the gradient. Moreover, there is also evidence of the existence of longer ethylene sequences in samples EPR-3 to EPR-5 at higher elution volumes. The present elution behavior is characteristic for EP copolymers with complex ethylene and propylene unit distributions.<sup>11</sup> Samples EPR-4 and EPR-5 are most strongly retained on the column as seen from the elution volumes at 4 to 7 mL. The chromatograms of these bulk samples do not reveal the presence of PE homopolymer. It can be assumed, however, that the small fraction eluting close to 6 mL is due to PE or copolymer fractions with very high ethylene contents.

The inconclusive results that were obtained on the bulk samples prompted a preparative TREF to be carried out so that amorphous and crystalline components can be analyzed separately.

Figure 4 shows preparative TREF results of the five EPR bulk samples, representing the weight percentage of each fraction as function of elution temperature. There are quantifiable amounts for all the TREF fractions collected at different temperatures that can be subjected to further investigations. The TREF results prove that the bulk samples are not completely amorphous as has been suggested by the CRYSTAF analyses. According to the TREF results, the samples contain only 55 to 65 wt % of true amorphous material, see TREF fractions at 30 °C. The fractions that are eluting at higher temperatures did crystallize in the first TREF step and are, therefore, not amorphous. The fact that these crystallizable fractions have not been seen in CRYSTAF has two

reasons: (1) in TREF xylene is used as the solvent while in CRYSTAF TCB is used and (2) co-crystallization effects manifest themselves differently in TREF and CRYSTAF. As has been shown in previous investigations, TREF does not fractionate purely based on chemical composition.<sup>13,44</sup> Co-crystallization takes place and the resulting TREF fractions are still very complex regarding their molecular structures. Still, due to the simple experimental setup and the fact that preparative fractionations can be conducted easily, TREF is the preferred first step in the analysis of complex polyolefins such as the present EPRs. Another advantage of TREF is that minor components can be isolated and preconcentrated which is not easily possible by other methods.

After the TREF experiments, there is the need to determine the detailed compositional and microstructural characteristics of the collected fractions. Thus, further analyses using various analytical techniques are done and discussed in the following sections. As a first step, the molar masses of all fractions were determined by HT-SEC, Figure 5 presenting the corresponding molar mass distributions.

As can be seen in Figure 5 and Table 2, there are no major differences between the samples in terms of molar masses. All fractions exhibit unimodal MMDs; the molar mass dispersities vary between 5 and 18. There is no clear trend or correlation between molar mass and TREF elution temperature. As the molar masses are quite high it can be assumed that the molar mass has only a minor influence on the TREF elution behavior.

In order to prove that the TREF fractions exhibit different crystallizabilities, they were subjected to CRYSTAF investigations. As can be seen in Figure 6, CRYSTAF confirms the assumption that the 30 °C TREF fractions are completely amorphous. In contrast to the analysis of the bulk samples (see Fig. 1), the measurement of the TREF fractions shows that the samples contain significant amounts of highly crystalline materials as is signified by the 130 °C TREF fractions that are crystallizing between 70 and 85 °C. These TREF fractions can be assigned to PE and/or PP homopolymers as well as copolymers with very high comonomer (ethylene or propylene) contents.

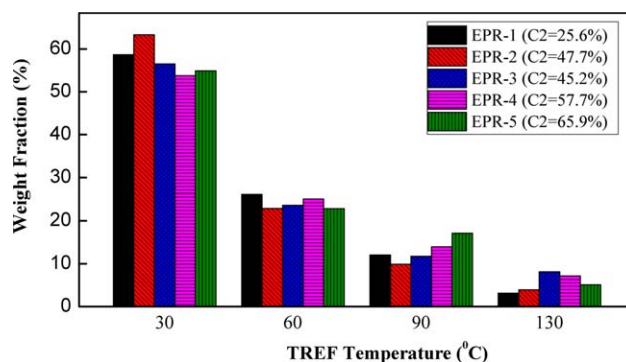


**FIGURE 4** TREF results for five EPR bulk samples, indicating the overall weight percentages as a function of elution temperature. [Color figure can be viewed in the online issue, which is available at [wileyonlinelibrary.com](http://wileyonlinelibrary.com).]



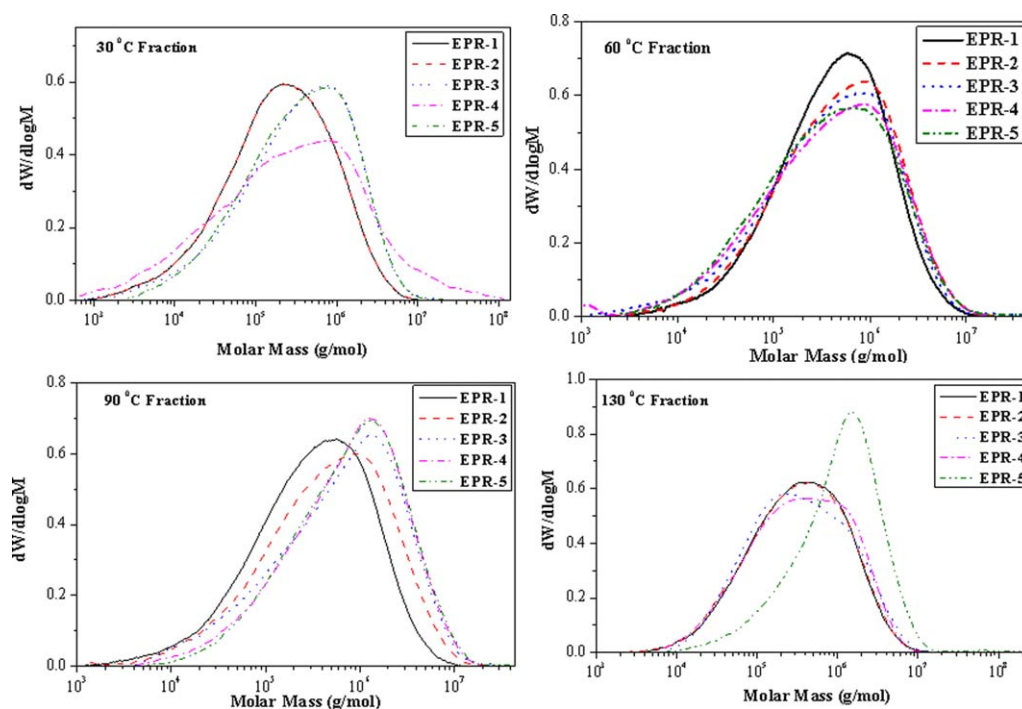


**FIGURE 5** Molar mass distributions for all TREF fractions of the EPR samples as obtained by HT-SEC, molar masses are polystyrene equivalents. [Color figure can be viewed in the online issue, which is available at [wileyonlinelibrary.com](http://wileyonlinelibrary.com).]

**TABLE 2** Summary of the HT-SEC Results of the TREF Fractions

Sample	TREF Fraction (°C)	$M_n^a$ (kg/mol)	$M_w^a$ (kg/mol)	$M_w/M_n$
EPR-1	30	48	488	10.1
	60	143	803	5.6
	90	86	694	8.0
	130	122	715	5.9
EPR-2	30	80	810	10.1
	60	133	973	7.3
	90	60	1076	17.9
	130	116	704	6.1
EPR-3	30	59	825	14.0
	60	80	926	11.6
	90	142	1417	10.0
	130	132	791	6.0
EPR-4	30	29	422	14.7
	60	43	486	11.2
	90	197	1501	7.6
	130	123	781	6.3
EPR-5	30	91	815	9.0
	60	97	946	9.8
	90	242	1582	6.5
	130	338	2197	6.5

<sup>a</sup> Molar masses are polystyrene equivalents.

The CRYSTAF curves for the 90 °C TREF fractions show multimodal crystallization peaks between 40 and 80 °C. There are three distinct peaks that can be observed for these TREF fractions (see Fig. 6). The first set of peaks which appears around 45 °C are attributed to random EPC copolymers which is in agreement with findings of Nieto et al.<sup>31</sup> The second set of peaks at approximately 60 °C is probably due to propylene-rich copolymers. Long sequences of propylene increase the crystallinity as compared with random EP copolymers. The last set of peaks which appears at around 75 °C is due to ethylene-rich EP copolymers. The increased intensity of this set of peaks corresponds to the increased ethylene content of the bulk samples (see Tab. 1). The 90 °C TREF fractions are semi-crystalline in nature and they are most important fractions in EPRs that constitute the dispersed phase in IPC, since they form the interphase between the dispersed amorphous part (EP rubber) and the highly crystalline continuous phase of iPP.<sup>41</sup>

A detailed analysis of the 130 °C TREF fractions provides further subtle information on the molecular structure of the samples. Samples EPR-1, EPR-2 and EPR-3 show single maximum crystallization peaks whereas samples EPR-4 and EPR-5 show two distinct crystallization peaks. The first crystallization peak at about 75 °C is most prominent in the samples with lower  $C_2$  contents while the last crystallization peak at about 85 °C appears only in the samples with the highest  $C_2$  contents. As has been shown for the bulk samples, there are indications for the presence of PP homopolymer in the samples with lower  $C_2$  contents, see Figure 2. In agreement with these findings, the crystallization peak appearing at about

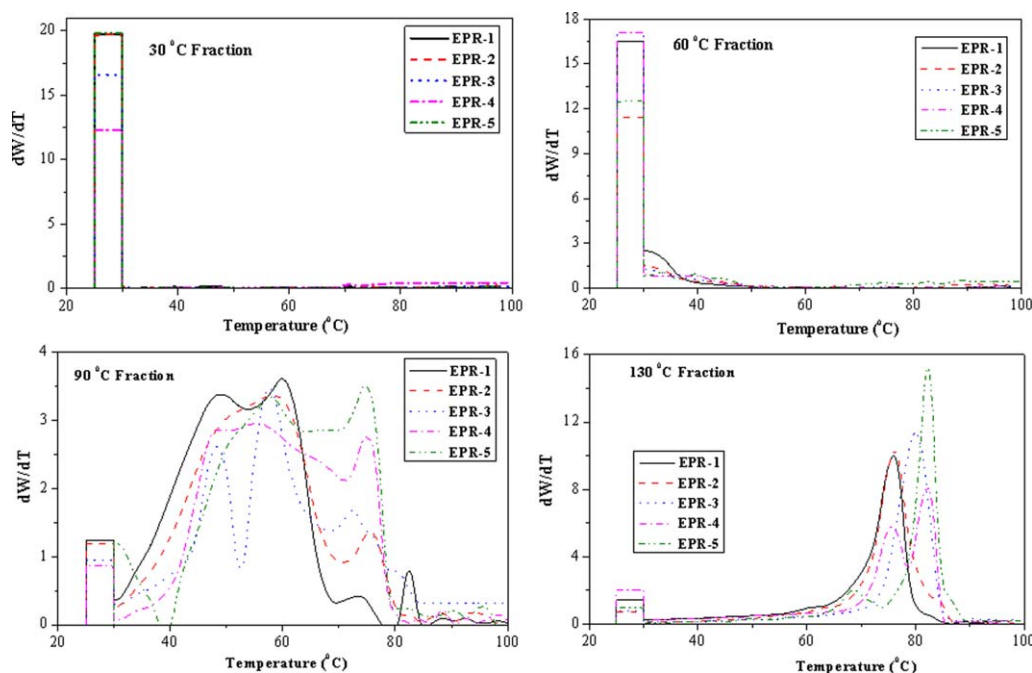


**FIGURE 6** CRYSTAF curves for the TREF fractions of the EPR samples obtained at crystallization temperatures between 30 and 100 °C. [Color figure can be viewed in the online issue, which is available at [wileyonlinelibrary.com](http://wileyonlinelibrary.com).]

75 °C is assigned to PP. PE homopolymer could not be directly identified from the DSC curves of the bulk samples. However, the crystallization temperature of PE in CRYSTAF is between 80 and 85 °C and, therefore, the last crystallization peak at about 85 °C is tentatively assigned to PE. This assignment is in agreement with the HPLC results for the bulk samples where a small late eluting peak for PE is found for sample EPR-5, see Figure 3. The bimodal peak pattern for sample EPR-4 indicates the presence of both PP and EP in the 130 °C TREF fraction.

Further complementary information on the composition of the TREF fractions is obtained by DSC. The DSC melting and crystallization curves of all TREF fractions with scan rates of 10 °C/min are displayed in Figure 7. There are no melting or crystallization peaks that can be observed for the 30 °C TREF fractions. This behavior was expected, since these fractions did neither crystallize nor melt in the TREF fractionation and the CRYSTAF analysis. Therefore, the DSC results confirm that the 30 °C TREF fractions contain entirely amorphous random ethylene-propylene copolymer molecules.

The 60 °C TREF fractions exhibit multiple melting and crystallization peaks that indicate complex copolymer compositions. These correspond to segmented copolymer structures that have longer propylene sequences (e.g. sample EPR-1) or longer ethylene sequences (e.g. EPR-5). The “PP-like” nature of the 60 °C TREF fraction of EPR-1 is indicated by transition temperatures of  $T_m \sim 100$  °C and  $T_c \sim 60$  °C, while the ‘PE-like’ nature of the 60 °C TREF fraction of EPR-5 is indicated by transition temperatures of  $T_m \sim 90$  °C and  $T_c \sim 75$  °C.<sup>44</sup> This behavior is even more pronounced in the 90 °C TREF fractions as can be seen from the corresponding melting curves.

The DSC results for the 130 °C TREF fractions provide a significantly more conclusive idea on the molecular composition as compared with the CRYSTAF findings. All fractions exhibit two distinct melt endotherms, one at about 125 °C and the other one between 150 and 165 °C. In excellent agreement with the all previous analyses these can be assigned to PE and PP homopolymers, respectively. As would one expect, the PE peak is most prominent in the samples that have the highest  $C_2$  contents, i.e. samples EPR-4 and EPR-5. It has to be pointed out, however, that even these samples seem to contain small amounts of PP homopolymer which is indicated by small melting peaks around 160 °C. In contrast, the samples with the lowest  $C_2$  contents, i.e. samples EPR-1 and EPR-2, show the most intense peaks for PP. Unexpectedly, even these samples seem to contain some PE homopolymer as is indicated by the peak at 125 °C.

The analytical methods that have been used so far are based on the observation of melting or crystallization events. As has been shown for the bulk samples, HT-HPLC provides distinctively different structural information since separation in this case is entirely based on differences in chemical composition. The separations are conducted at temperatures above the melting or crystallization points and, hence, sample crystallinity does not influence the method.

The HT-HPLC chromatograms for all TREF fractions are shown in Figure 8.

The chromatograms obtained for the 130 °C TREF fractions provide very clear confirmation of the CRYSTAF and DSC findings. Three distinct sets of peaks at different elution volumes can be identified. All fractions show the presence of

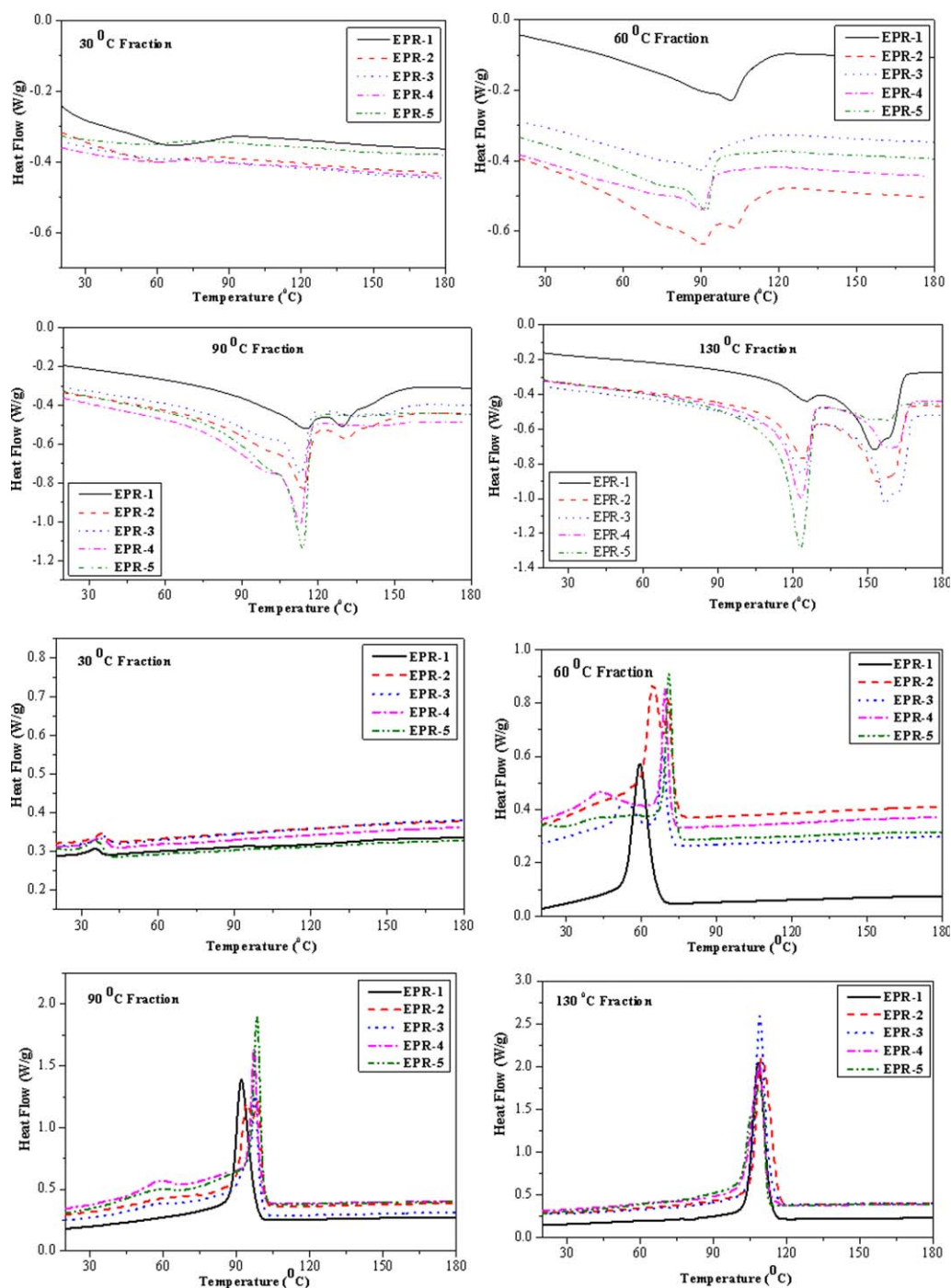


**FIGURE 7** Second heating (a) and first cooling curves (b) for all TREF fractions of the EPR samples as obtained from DSC at a scan rate of 10 °C/min. [Color figure can be viewed in the online issue, which is available at [wileyonlinelibrary.com](http://wileyonlinelibrary.com).]

low molar mass iPP which elutes in 100% 1-decanol before the start of the solvent gradient. The second set of elution peaks appears immediately after the start of the gradient and can be assigned to high molar mass iPP. The relative intensity of these peaks decreases with increasing  $C_2$  contents of the bulk samples. This peak is practically not observed for sample EPR-5 having the highest  $C_2$  content.

The latest eluting peaks which are due to PE homopolymer appear at elution volumes of around 5.8 mL.<sup>38,41</sup> These peaks are only obtained for samples EPR-4 and EPR-5 and the peak intensity increases with increasing  $C_2$  contents of the bulk samples. In contrast to the CRYSTAF results of the 130 °C TREF fractions, HT-HPLC allows for the effective and baseline separation of iPP and PE irrespective of crystallinity.

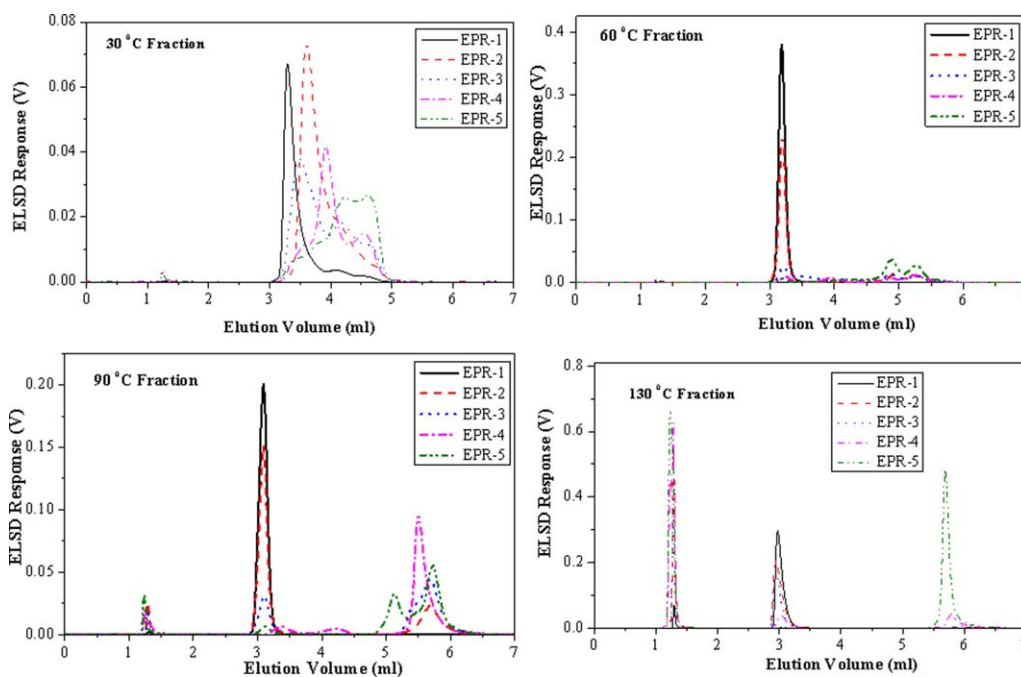


**FIGURE 8** HT-HPLC chromatograms for the TREF fractions of the EPR samples, solvent gradient elution (1-decanol to TCB) after an initial isocratic step. [Color figure can be viewed in the online issue, which is available at [wileyonlinelibrary.com](http://wileyonlinelibrary.com).]

The HT-HPLC chromatograms of the 30 °C TREF fractions show that all components elute after the start of the solvent gradient confirming that material is retained on the stationary phase. Very small elution peaks at about 1.4 mL indicate that the fractions might contain minute amounts of low molar mass (amorphous) PP. The elution volumes for all fractions are between 3 and 5 mL and show multimodal elution patterns indicating their complex chemical composition. As has been suggested by the CRYSTAF and DSC investigations, the components are amorphous random EP copolymers with different ethylene contents. As has been found previously, separation occurs according to increasing ethylene contents in the copolymers.<sup>6,11,14</sup> This is confirmed by the present investigations. The 30 °C TREF fraction of sample EPR-1 having the lowest C<sub>2</sub> content elutes mainly between 3 and 4 mL which is due to the fact that this fraction contains mainly propylene-rich macromolecules. In contrast, the 30 °C TREF fraction of sample EPR-5 having the highest C<sub>2</sub> content elutes mainly between 4 and 5 mL. This is clear proof for the assumption that this fraction contains mainly ethylene-rich macromolecules.

The 60 °C and 90 °C TREF fractions apparently contain significant amounts of co-crystallizing (high molar mass, low crystallinity) PP or propylene-rich copolymer fractions eluting close to 3 mL in addition to copolymer fractions that elute later. The amount of the early eluting fractions correlates with the C<sub>2</sub> contents of the samples meaning that these components appear mainly in samples EPR-1 and EPR-2 but are not seen in samples EPR-4 and EPR-5. The amounts of late eluting (segmented) EP copolymer fractions increase with increasing C<sub>2</sub> contents from EPR-1 to EPR-5.

The preceding results provided only qualitative information on the composition of the TREF fractions. Quantitative information on the defined compositional distribution within the individual components of the separated fractions is not provided by the currently used evaporative light scattering detector since this detector only monitors the relative concentration of the eluting species. For a strict quantification it would be necessary to calibrate the ELSD specifically for PE and PP and estimate the detector response for the copolymer fractions.

For a more quantitative estimate, HT-HPLC was coupled with FT-IR spectroscopy as an effective and affordable method to determine the exact chemical composition of the separated fractions from HPLC. The procedure for the exact compositional analysis (distribution of ethylene and propylene) was accomplished as explained in our previous work.<sup>34,41,44</sup> The results of the HT-HPLC-FT-IR analysis for a number of selected TREF fractions are shown in Figures 9 and 10.

There is small shift in HPLC elution volume axis for the Gram-Schmidt (GS) concentration profile as compared with the ELSD profile which is caused by a larger volume of the transfer capillary used to connect the LC transform interface to the HT-HPLC instrument. The start of the solvent gradient corresponds to about 3.5 mL. For the 30 °C TREF fraction of EPR-3, see Figure 9(a), a decrease in the propylene content across the GS concentration profile is observed whereas there is an increase of the ethylene content towards late eluting fractions. This is also observed for the 60 and 90 °C TREF fractions but not for the 130 °C TREF fraction which only consists of PP. The TREF fraction of EPR-5 collected at

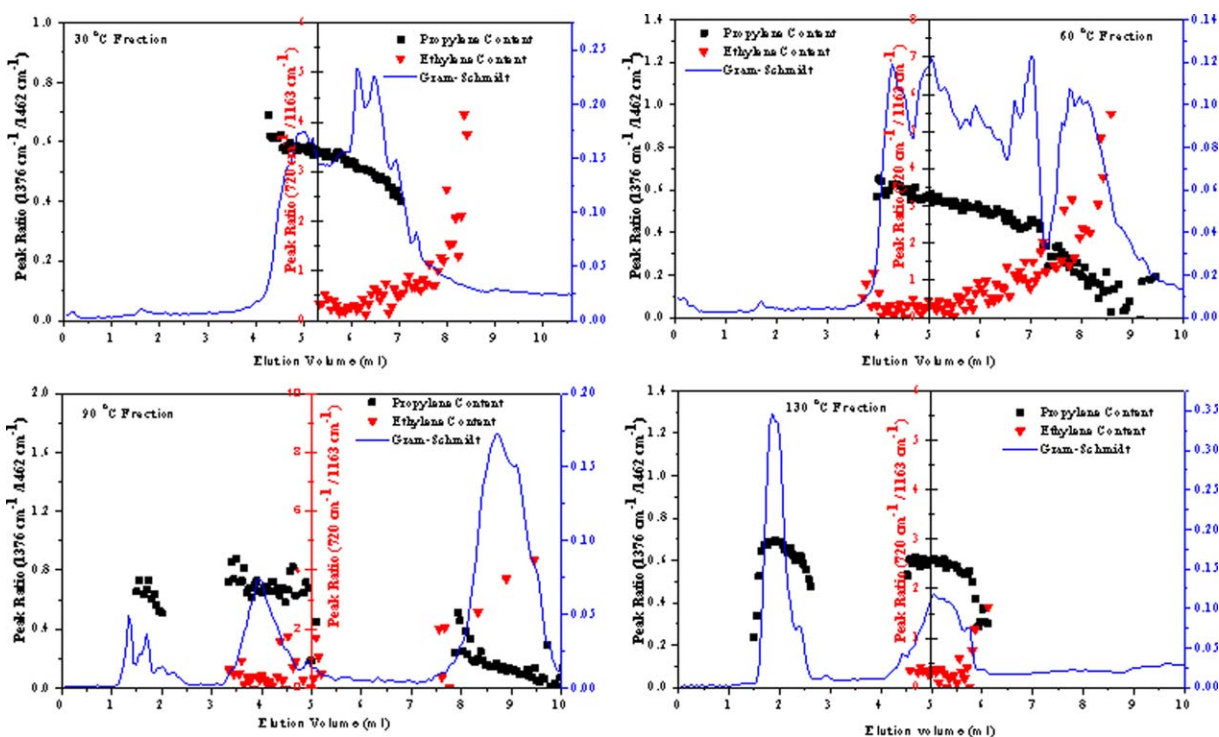


**FIGURE 9** Analysis of all TREF fractions of EPR-3 using HT-HPLC coupled to FT-IR spectroscopy, illustrating propylene and ethylene distributions as function of elution volume. [Color figure can be viewed in the online issue, which is available at [wileyonlinelibrary.com](http://wileyonlinelibrary.com).]

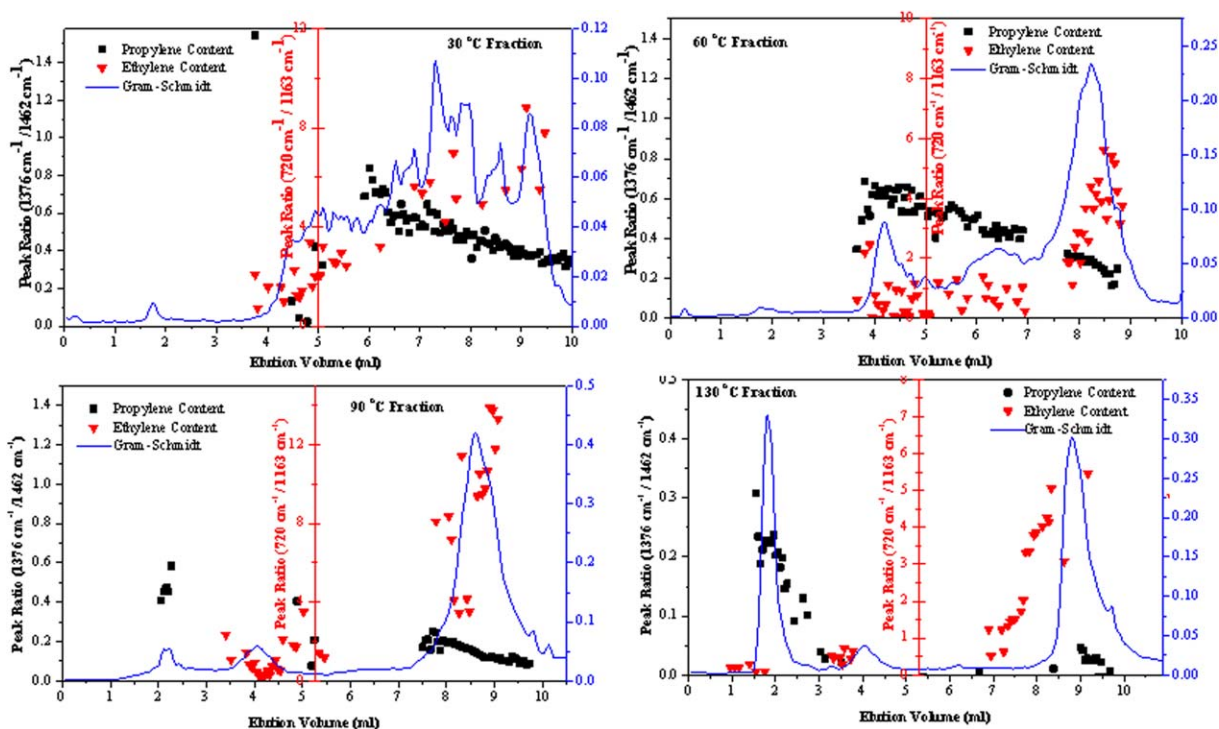


**FIGURE 10** Analysis of all TREF fractions of EPR-5 using HT-HPLC coupled to FT-IR spectroscopy, illustrating propylene and ethylene distributions as function of elution volume. [Color figure can be viewed in the online issue, which is available at [wileyonlinelibrary.com](http://wileyonlinelibrary.com).]

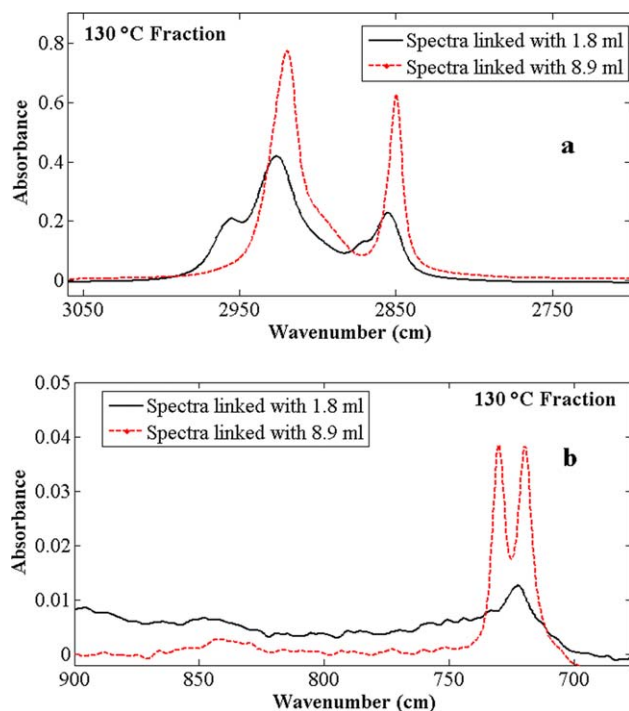


**FIGURE 11** Selected regions of the FT-IR spectra of the 130 °C TREF fraction of EPR-5, (a) higher wavenumbers and (b) lower wavenumbers showing selected methyl and methylene absorptions. [Color figure can be viewed in the online issue, which is available at [wileyonlinelibrary.com](http://wileyonlinelibrary.com).]

130 °C as shown in Figure 10 indicates two distinct sharp peaks at elution volumes of 1.8 and 8.9 mL, respectively. For the first eluting component, the ethylene content is almost zero, whereas the propylene content is at its maximum value. The ethylene content increases with increasing elution volume starting at around 7.0 mL until it reaches its maximum at roughly 9.0 mL. The propylene content in this late eluting part is very low and approaches zero. As shown and proven by other authors, these results confirm that the adsorption/desorption mechanism on the Hypercarb stationary phase is according to the ethylene and propylene contents of the samples.

In order to confirm the assignments and prove the chemical structure of the eluted components, the individual FT-IR spectra at peak maximum of each component were further examined and analyzed. The spectral data were taken for the two corresponding fractions for both the higher and lower wavenumber regions. The spectrum linked with an elution volume of 1.8 mL, shown in Figure 11(a), reflects the presence of CH<sub>3</sub> stretches with absorption bands at 2956 and 2871 cm<sup>-1</sup> which are not present in the spectrum linked to the late eluting component at 8.9 mL. This result further confirms that the first eluting component is predominantly PP homopolymer. On the other hand, the spectrum linked to an elution volume of 8.9 mL shows more intense peaks for the CH<sub>2</sub> stretches with absorption

bands at 2920 and 2850 cm<sup>-1</sup>. This spectral behavior is due to the presence of PE homopolymer. Moreover, the CH<sub>2</sub> split peaks at 720 to 730 cm<sup>-1</sup> as shown in Figure 11(b) reflect the presence of crystalline ethylene sequences. This result further proves that the late eluting material is mainly PE. The overall results illustrate the capability of HT-HPLC coupled to FT-IR spectroscopy to separate and characterize the EPR samples comprehensively according to the molecular properties.

## CONCLUSIONS

Ethylene-propylene copolymers have complex molecular structures with multiple distributions in terms of chemical composition, molar mass, and sequence distribution. EPRs are an integral part of impact polypropylene copolymers (IPC) where they constitute the dispersed phase in a polypropylene matrix. The size of the rubber particles and their molecular structure are responsible for the favorable impact properties of IPC.

For a long time it was believed that EPRs are mostly amorphous materials with random distributions of the monomer units across the macromolecular chains. Recently it was shown, however, that EPRs exhibit a much more complex molecular structure consisting of random and segmented copolymer species as well as fractions of homopolymers. The present study was aimed at using advanced multiple fractionation and analysis techniques to reformulate EPRs that are typically part of complex IPC formulations.

In a first step, EPR bulk samples were analyzed by HT-SEC, DSC, CRYSTAF, and HT-HPLC and it was shown that the samples contain significant amounts of crystallizable components in addition to the expected amorphous random EP copolymers. Indications for the presence of segmented propylene-rich and ethylene-rich copolymer fractions were found along with measurable amounts of PP homopolymer.

More detailed molecular information was obtained by conducting preparative TREF as a prefractionation procedure. TREF suffers from co-crystallization effects, however, it provides sufficient amounts of materials for further analytical studies. The TREF fractions are still very complex regarding molecular composition and, thus, must be fractionated further using complementary methods. A comprehensive approach entailing HT-SEC, CRYSTAF, DSC, HT-HPLC, and FT-IR investigations provided very detailed structural information on the TREF fractions. It was proven that EPRs varying over a large range of chemical compositions are composed of random and segmented copolymer molecules, polyethylene and polypropylene in various ratios.

The present investigations show that only a comprehensive and multidimensional analytical protocol is able to unravel the molecular structure of complex olefin copolymers. Further work will be directed towards fractionating the random and segmented copolymer structures and analyzing sequence distributions by NMR spectroscopy.

## ACKNOWLEDGMENTS

The authors thank SASOL, South Africa, and Lummus Novolen Technology GmbH, Germany, for the financial support of this work. The EPR samples provided by Lummus Novolen Technology GmbH are also gratefully acknowledged.

## REFERENCES AND NOTES

- Z. S. Petrović, J. Budinski-Simendić, V. Divjaković, Ž. Škrbić, *J. Appl. Polym. Sci.* **1996**, *59*, 301–310.
- M. Pires, R. S. Mauler, S. A. Liberman, *J. Appl. Polym. Sci.* **2004**, *92*, 2155–2162.
- J. K. Lee, J. H. Lee, K. H. Lee, B. S. Jin, *J. Appl. Polym. Sci.* **2001**, *81*, 695–700.
- L. Botha, A. J. van Reenen, *Eur. Polym. J.* **2013**, *49*, 2202–2213.
- C. Kock, M. Gahleitner, A. Schausberger, E. Ingolic, *J. Appl. Polym. Sci.* **2012**, *128*, 1484–1496.
- S. Cheruthazhekatt, H. Pasch, *Anal. Bioanal. Chem.* **2013**, *405*, 8607–8614.
- C. Kock, N. Aust, C. Grein, M. Gahleitner, *J. Appl. Polym. Sci.* **2013**, *130*, 287–296.
- T. Macko, A. Ginzburg, K. Remerie, R. Brüll, *Macromol. Chem. Phys.* **2012**, *213*, 937–944.
- T. Macko, R. Brüll, Y. Wang, B. Coto, I. Suarez, *J. Appl. Polym. Sci.* **2011**, *122*, 3211–3217.
- E. De Goede, P. Mallon, H. Pasch, *Macromol. Mater. Eng.* **2010**, *295*, 366–373.
- S. Cheruthazhekatt, G. W. Harding, H. Pasch, *J. Chromatogr. A* **2013**, *1286*, 69–82.
- S. Thanyapruksanon, S. Thongyai, P. Praserttham, *J. Appl. Polym. Sci.* **2007**, *103*, 3609–3616.
- S. Cheruthazhekatt, T. F. J. Pijpers, G. W. Harding, V. B. F. Mathot, H. Pasch, *Macromolecules* **2012**, *45*, 5866–5880.
- H. Pasch, A. Albrecht, R. Brüll, T. Macko, W. Hiller, *Macromol. Symp.* **2009**, *282*, 71–80.
- H. Pasch, R. Brüll, U. Wahner, B. Monrabal, *Macromol. Mater. Eng.* **2000**, *279*, 46–51.
- Z. Fu, J. Xu, Y. Zhang, Z. Fan, *J. Appl. Polym. Sci.* **2005**, *97*, 640–647.
- G. H. Zohuri, M. M. Mortazavi, R. Jamjah, S. Ahmadjo, *J. Appl. Polym. Sci.* **2004**, *93*, 2597–2605.
- S. D. Kim, Y. Choi, W. Choi, C. Choi, Y. S. Chun, *Macromol. Symp.* **2012**, *312*, 27–33.
- V. B. F. Mathot, M. F. J. Pijpers, *Thermochim. Acta* **1989**, *151*, 241–259.
- M. H. Ha, B. K. Kim, *Polym. Eng. Sci.* **2004**, *44*, 1858–1865.
- E. B. Berda, T. W. Baughman, K. B. Wagener, *J. Polym. Sci., Part A: Polym. Chem.* **2006**, *44*, 4981–4989.
- G. Vanden Poel, V. B. F. Mathot, *Thermochim. Acta* **2007**, *461*, 107–121.
- V. B. F. Mathot, R. L. Scherrenberg, T. F. J. Pijpers, *Polymer* **1998**, *39*, 4541–4559.
- S. Mncwabe, N. Luruli, E. Marantos, P. Nhlapo, L. Botha, *Macromol. Symp.* **2012**, –313314, 33–42.
- N. Aust, M. Gahleitner, K. Reichelt, B. Raninger, *Polym. Test.* **2006**, *25*, 896–903.
- S. Cheruthazhekatt, T. F. J. Pijpers, V. B. F. Mathot, H. Pasch, *Macromol. Symp.* **2013**, *330*, 22–29.
- S. Cheruthazhekatt, H. Pasch, *Macromol. Symp.* **2014**, *337*, 51–57.
- S. Anantawaraskul, P. Somnukguandee, J. B. P. Soares, J. Limtrakul, *J. Polym. Sci., Part B: Polym. Phys.* **2009**, *47*, 866–876.
- J. B. P. Soares, S. Anantawaraskul, *J. Polym. Sci., Part B: Polym. Phys.* **2005**, *43*, 1557–1570.
- B. Monrabal, *Adv. Polym. Sci.* **2013**, *257*, 203–252.
- J. Nieto, T. Oswald, F. Blanco, J. B. P. Soares, B. Monrabal, *J. Polym. Sci., Part B: Polym. Phys.* **2001**, *39*, 1616–1628.
- B. Monrabal, P. Del Hierro, *Anal. Bioanal. Chem.* **2011**, *399*, 1557–1561.
- A. Albrecht, L. C. Heinz, D. Lilge, H. Pasch, *Macromol. Symp.* **2007**, *257*, 46–55.
- H. Pasch, M. I. Malik, T. Macko, *Adv. Polym. Sci.* **2013**, *251*, 77–140.
- T. Macko, H. Pasch, *Macromolecules* **2009**, *42*, 6063–6067.
- L.-C. Heinz, H. Pasch, *Polymer* **2005**, *46*, 12040–12045.
- T. Macko, H. Pasch, R. Brüll, *J. Chromatogr. A* **2006**, *1115*, 81–87.
- T. Macko, R. Brüll, R. G. Alamo, Y. Thomann, V. Grumel, *Polymer* **2009**, *50*, 5443–5448.
- A. Ginzburg, T. Macko, V. Dolle, R. Brüll, *Eur. Polym. J.* **2011**, *47*, 319–329.
- R. Chitta, A. Ginzburg, T. Macko, R. Brüll, G. Van Doremale, *LC-GC Eur.* **2012**, *25*, 352–358.
- S. Cheruthazhekatt, N. Mayo, B. Monrabal, H. Pasch, *Macromol. Chem. Phys.* **2013**, *214*, 2165–2171.
- T. Macko, R. Brüll, Y. Zhu, Y. Wang, *J. Sep. Sci.* **2010**, *33*, 3446–3454.
- A. Albrecht, R. Brüll, T. Macko, P. Sinha, H. Pasch, *Macromol. Chem. Phys.* **2008**, *209*, 1909–1919.
- S. Cheruthazhekatt, T. F. J. Pijpers, G. W. Harding, V. B. F. Mathot, H. Pasch, *Macromolecules* **2012**, *45*, 2025–2034.

## Chapter 5: Homogeneity of Metallocene EPR Copolymers

---

### 5 On the Homogeneity of Metallocene Ethylene-Propylene Copolymers as Investigated by Multiple Fractionation Techniques

*In this chapter, three metallocene-based ethylene-propylene rubber (EPR) copolymers are fractionated and characterized by multiple fractionation methods to determine their homogeneity. Upon the fractionation of the samples by preparative TREF, the analyses of the individual fractions reveal a remarkably high chemical heterogeneity within the bulk samples. The present study shows that the combination of various analytical techniques is the essential tool to understand the complex nature of the molecular composition of metallocene-based EPR copolymers. This work has been published as the following research article: Phiri, M.J.; Dimeska, A.; Pasch, H., On the Homogeneity of Metallocene Ethylene-Propylene Copolymers as Investigated by Multiple Fractionation Techniques. *Macromolecular Chemistry and Physics*, 2015, 216, 1619-1628.*

#### 5.1 Summary of the Research Study

It has been proven by numerous techniques that ethylene-propylene copolymers synthesised by metallocene catalysts exhibit narrow molar mass (MMD)<sup>1-3</sup> and chemical composition distributions (CCD)<sup>1</sup> when analysed as bulk samples. Hence, there (apparently) has never been a need to fractionate such homogeneous materials into individual fractions. However, based on our previous work done on the Ziegler-Natta EPR copolymers with high comonomer contents, there were unexpected PE and PP homopolymers detected from the bulk samples upon fractionation procedures such as TREF. This observation prompted us to carry out comprehensive analyses to reveal the chemical composition heterogeneity of metallocene EPR with high ethylene contents. A number of advanced techniques namely SEC, TREF, CRYSTAF, DSC, HPLC and <sup>13</sup>C NMR were used for the analyses of the EPR samples having different amounts of ethylene contents in the range of 30 – 50 mol %.

In the first step of characterization, the bulk samples were analysed by various analytical techniques to determine their bulk chemical composition and molar mass homogeneities. SEC, DSC and HPLC showed that the EPR samples exhibit both narrow MMDs and CCDs. The three samples showed similar melting temperatures ( $T_m$ ) with values of ~154 °C and this was characteristic of EP copolymers having long sequences of propylene units. HPLC chromatograms showed no observable or quantifiable material that eluted in 100 % of 1-



decanol, however after the start of the gradient with TCB, all the material that was adsorbed on the column eluted in the volume range of 3.5 – 4.5 mL. It was comprehended that the peak elution volumes for the samples increase with their ethylene content. The amorphous phase was the major part present in these EPR samples as determined by the CRYSTAF technique. In addition, there was a small amount of crystallizing material in the crystallization temperature range of 30 – 90 °C suggesting the complexity in the chemical compositions of the EPR copolymers

The overall results of the bulk sample analyses revealed that these EPR samples have different chemical compositions among them. Furthermore, based on our previous work in Chapter 4, it was determined that EPR samples with high comonomer contents have minor components that cannot be detected from the bulk sample analysis, as such preparative TREF was found to be essential. Subsequently, the bulk samples were fractionated by preparative TREF so that further analyses could be performed on the fractions. TREF showed similar results to those obtained by CRYSTAF with the amorphous phase constituting the largest percentage of the material. The TREF fractions collected at 30 °C consisted of ~ 80 % of the overall bulk samples material and this percentage is found to increase with the ethylene content of the bulk samples. Interestingly, highly crystalline material was collected at a TREF temperature of 130 °C. It was unexpected for metallocene-based EPR copolymers with such high ethylene contents to indicate the presence of iPP homopolymer. On the other hand, the percentages of segmented ethylene-propylene (EP) copolymers as contained in the 90 °C fractions were the lowest among all TREF fractions hence some of the analyses were not performed due to very low quantities.

All the TREF fractions showed unimodal MMDs and the molar masses of the fractions increased with higher TREF temperatures. However, the TREF fractions collected at 60 and 90 °C had slightly higher dispersity values as compared to other fractions due to large number of molecules which had resulted from the co-crystallization and co-elution that took place during the TREF experiments. DSC and CRYSTAF showed that the 30 and 60 °C TREF fractions contained random EP copolymers which were completely amorphous according to the fact that there were no observable crystallization peaks detected in both DSC and CRYSTAF. The 90 °C TREF fractions contained either propylene-rich copolymer or low molar mass iPP with low tacticity due the melting peak around 150 °C that was seen in DSC. The 90 °C fractions exhibit melt enthalpies of about 18 J/g indicating EP copolymers. Furthermore, the 130 °C TREF fractions showed melting peaks at around 160 °C suggesting

that the fractions consist mainly of high molar mass iPP<sup>4</sup>. Since there is no disruption in the tacticity of the iPP, its  $T_m$  shifted to higher values as compared to EP copolymers. These results were confirmed by CRYSTAF showing a crystallization temperature of  $\sim 80$  °C corresponding to iPP homopolymer. There was a shift in peak maximum to higher temperatures with the ethylene content of the bulk samples. The shift was expected since it had been shown that material containing more PE crystallises first and faster as compared to PP-rich material when using the CRYSTAF technique<sup>5-7</sup>. These CRYSTAF results further proved that the TREF fractions from the metallocene-based EPR copolymers had entirely different chemical composition distributions (CCD).

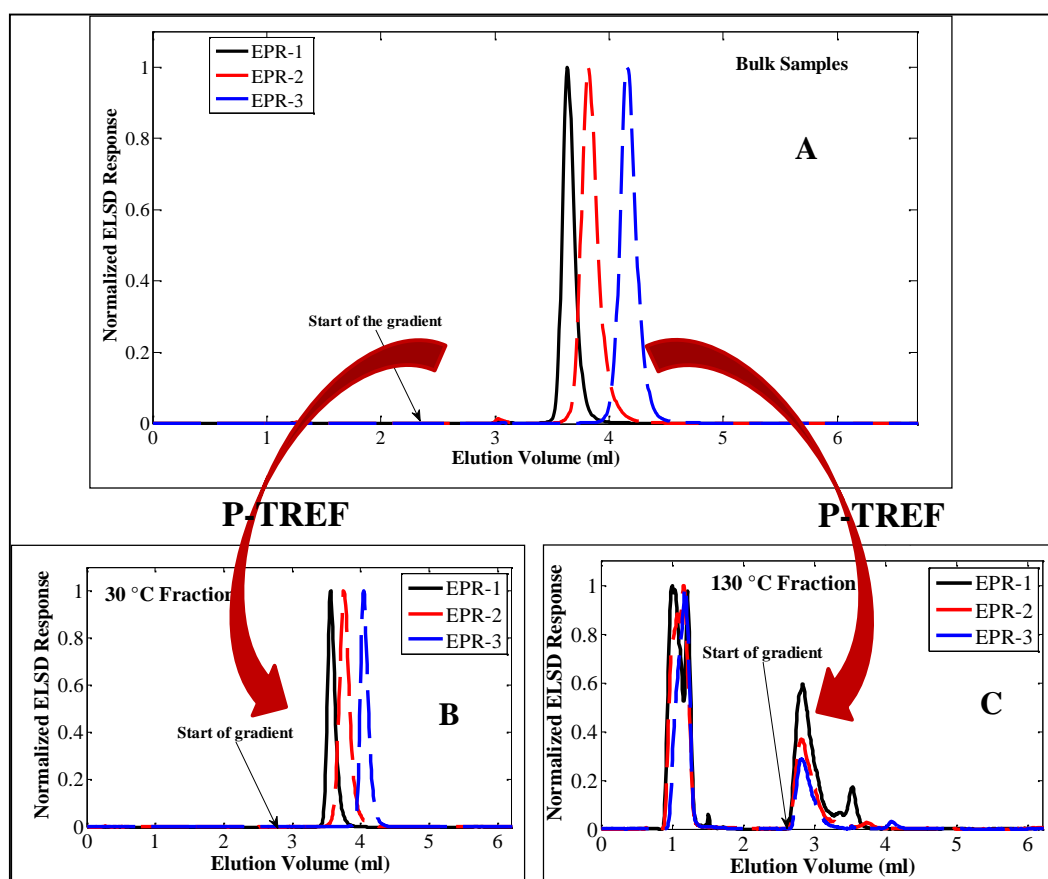


Figure 5.1: HT-HPLC chromatograms for the bulk EPR samples (A), and the 30 (B) and 130 °C (C) TREF fractions, solvent gradient elution (1-decanol to TCB) after an initial isocratic step.

In contrast to other techniques, HPLC separated and characterized both the amorphous and crystalline fractions since the separation in HPLC depends mainly on the interaction of the EP copolymers with the graphitic stationary phase. The HPLC results on the three bulk samples and their selected TREF fractions are presented in Figure 5.1. The HPLC results of the 30 and

60 °C TREF fractions showed similar chemical compositions as their corresponding bulk samples. These TREF fractions were assumed to consist of EP copolymers with random propylene and ethylene sequences along the macromolecules. On the other hand, the late eluting TREF fractions (90 and 130 °C) showed entirely different chemical compositions compared to the bulk samples and this behaviour was unexpected from samples prepared by a metallocene catalyst system. For the 90 °C TREF fractions, the materials that eluted in 100 % of 1-decanol were mainly due to low molar mass of iPP. After the start of the gradient with TCB, the material that eluted at 3.5 – 4.5 mL had similar compositions as the bulk samples. The components that eluted immediately (~2.7 mL) after the start of the gradient from the 130 °C TREF fractions were due to high mass of iPP. As depicted in the Fig. 5.1, HPLC revealed the heterogeneity of the metallocene-catalysed EPR copolymers.

The <sup>13</sup>C NMR results confirmed the heterogeneity observed by the HPLC analyses. In addition, the comonomer contents and the monomer sequence distributions of all TREF fractions were calculated and it was found that the 30 and 60 °C fractions contain similar EP sequences. However, minor differences in the sequence distributions were observed with minute amounts of EP junctions such as PEP, EPE, PPE and EEP. It was assumed that these junctions play a major role in the crystallinity of these fractions as observed from TREF experiments. However, the 130 °C TREF fractions were found to have three peaks corresponding to carbon atoms of the propylene repeating units. The <sup>13</sup>C NMR spectra showed three major signals due to CH<sub>2</sub> (~47 ppm), CH (~30 ppm) and CH<sub>3</sub> (~23 ppm) which were entirely different from the spectra obtained for the lower TREF fractions. This suggests that the 130 °C TREF fractions contained iPP homopolymer as it has been seen from DSC, CRYSTAF and HPLC analyses.

In summary, the present work showed that a remarkably high chemical heterogeneity is present in the metallocene-based EPR samples as evidenced by prep-TREF fractionation and the further analysis of the fractions by advanced analytical methods including HT-HPLC as well as <sup>13</sup>C NMR. The combination of various analytical techniques proved to be a useful tool in understanding the molecular structures of these complex EPR copolymers.

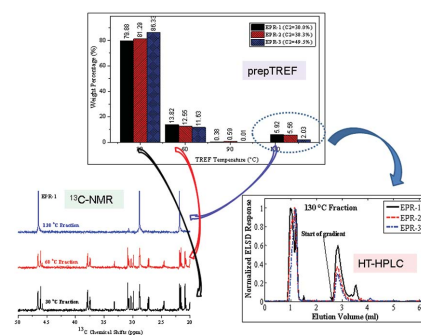
## 5.2 References

1. R. Chitta, A. Ginzburg, T. Macko, R. Brüll, G. van Doremaele. *LC-GC Europe* **2012**, 25, 352-358.
2. T. Macko, A. Ginzburg, K. Remerie, R. Brüll. *Macromolecular Chemistry and Physics* **2012**, 213, 937-944.
3. S. Podzimek. *Journal of Applied Polymer Science* **2014**, 131, 40111.
4. S. Cheruthazhekatt, T. F. J. Pijpers, G. W. Harding, V. B. F. Mathot, H. Pasch. *Macromolecules* **2012**, 45, 2025-2034.
5. B. Monrabal. *Macromolecular Symposia* **1996**, 110, 81-86.
6. B. Monrabal, P. Del Hierro. *Analytical and Bioanalytical Chemistry* **2011**, 399, 1557-1561.
7. H. Pasch, R. Brüll, U. Wahner, B. Monrabal. *Macromolecular Materials and Engineering* **2000**, 279, 46-51.

# On the Homogeneity of Metallocene Ethylene–Propylene Copolymers as Investigated by Multiple Fractionation Techniques

Mohau Justice Phiri, Anita Dimeska, Harald Pasch\*

The chemical heterogeneity of ethylene–propylene copolymers by multiple fractionation techniques is addressed. Three metallocene copolymer samples with different ethylene contents, ranging from 30 to 50 mol% are analyzed using bulk methods to confirm their molecular heterogeneity. In a second step, the samples are fractionated by temperature rising elution fractionation (TREF) to obtain fractions at 30, 60, 90, and 130 °C. These fractions are subsequently analyzed regarding their thermal and molecular properties. Differential scanning calorimetry, crystallization analysis fractionation, and high-temperature high performance liquid chromatography (HT-HPLC) results reveal that the TREF fractions collected at 130 °C are mainly due to polypropylene homopolymer, which is rather unexpected considering the high ethylene contents of the bulk samples. Most importantly, HT-HPLC reveals a remarkably high chemical heterogeneity of the fractions and thus the bulk samples. Solution  $^{13}\text{C}$ -NMR provides the comonomer contents and sequence distributions of the fractions. These indicate that the same TREF fractions from different samples have distinctively different chemical compositions.



## 1. Introduction

Ethylene–propylene (EP) copolymers produced by metallocene catalysts system have been proven to have narrow molar mass distributions (MMD) and low chemical heterogeneities.<sup>[1,2]</sup> Metallocene catalysts are unique in that they have single active sites for polymerizations to take place.<sup>[2–4]</sup> As such metallocene-catalyzed EP copolymers

have found lots of attention in research as it is interesting to study structure-property relations as compared to samples prepared by Ziegler–Natta catalysts.<sup>[1,3,5–7]</sup> Recent developments in both reactor and catalyst technologies have allowed to synthesize EP copolymers with very broad chemical compositions.<sup>[5,8,9]</sup> These have complex structures and elastomeric properties for samples with high ethylene contents.<sup>[5,8,10]</sup>

In order to obtain comprehensive compositional information about such complex EP copolymers, both MMD and chemical composition distribution (CCD) must be determined simultaneously. The MMD of such copolymers is typically determined using high-temperature size exclusion chromatography (HT-SEC).<sup>[5,11–15]</sup> There are numerous analytical techniques available for the determination of the chemical composition of EP copolymers including Fourier transform infrared

M. J. Phiri, Prof. H. Pasch  
Department of Chemistry and Polymer Science  
Stellenbosch University  
7602 Matieland, South Africa  
E-mail: [hpasch@sun.ac.za](mailto:hpasch@sun.ac.za)  
Dr. A. Dimeska  
Lummas Novolen Technology GmbH  
Carl-Bosch-Str. 38, 67056 Ludwigshafen, Germany

spectroscopy (FTIR) and  $^{13}\text{C}$  NMR spectroscopy for estimating average chemical compositions of bulk samples.<sup>[5,9,13,15]</sup> In a few cases  $^{13}\text{C}$  NMR has been used for the direct quantification of polymer microstructures.<sup>[4,5,15]</sup> Monomer sequence distributions revealed information about both chain initiation and termination reactions in EP copolymers produced by metallocene catalysts.<sup>[16–18]</sup>

Thermal analysis is another way to get compositional information of EP copolymers and differential scanning calorimetry (DSC) has been used extensively to determine melting and crystallization behaviors. For EPR copolymers with high comonomer contents, Jeon et al. stated that an increase in the ethylene content causes a decrease in overall crystallinity since the ethylene units act as a defect that disrupts crystallizable sequence lengths of the polypropylene chain.<sup>[5]</sup> Even though DSC is a simple and fast technique, it suffers from cocrystallization effects in the analysis of polyolefins.<sup>[8,19]</sup>

Solution crystallization-based techniques like temperature rising elution fractionation (TREF) have been largely utilized for the analysis of CCD of many polyolefin systems.<sup>[20–25]</sup> Preparative TREF (being tedious and time consuming) separates and concentrates minor constituents within the bulk sample. In our recent work on the analysis of Ziegler–Natta EP copolymers with high comonomer contents,<sup>[26]</sup> we found that there are minor homopolymer fractions of iPP and PE in late eluting TREF fractions. These materials were not observed in the analyses of the bulk samples. Fractions collected from preparative TREF can be further analyzed by other analytical techniques.<sup>[13,19,23,25]</sup>

One of those, high-temperature high performance liquid chromatography (HT-HPLC) had shown superior capabilities for being able to analyze both amorphous and crystalline materials.<sup>[11,13,15,19,27–30]</sup> The separation in HT-HPLC depends mainly on the chemical composition of the polyolefin<sup>[29–32]</sup> and in EP copolymers separation is according to the ethylene content of the sample.<sup>[13,16,33,34]</sup> Several studies had been done on HT-HPLC of metallocene EP copolymers but their focus was on the bulk samples.<sup>[15,33–35]</sup> Fractionation of metallocene EP copolymers by TREF and subsequent HT-HPLC analysis has not been reported in the literature. In the present study, three metallocene EP copolymers with high comonomer contents are fractionated using preparative TREF. The resulting fractions together with the bulk samples are analyzed using multiple analytical techniques, namely DSC, FTIR, CRYSTAF (crystallization analysis fractionation), HT-HPLC, and solution  $^{13}\text{C}$  NMR. The combination of these analytical techniques proved to be an essential tool for understanding the complex microstructural properties of complex EP copolymers.

■ Table 1. Details on the composition of the bulk EPR samples.

Sample name	Ethylene content ( $\text{C}_2$ ) by NMR [mol%]	$M_w^a$ by SEC [kg mol $^{-1}$ ]	$M_w/M_n$
EPR-1	30.0	586	3.12
EPR-2	38.3	445	4.99
EPR-3	49.5	449	5.41

<sup>a</sup>)Molar masses are polystyrene equivalents.

## 2. Experimental Section

### 2.1. Materials

Xylene (>99% purity) and 1-decanol (>99% purity) were purchased from Chemical & Laboratory suppliers and Aldrich, respectively, and used as received. HPLC grade 1,2,4-trichlorobenzene (TCB) was purchased from Sigma-Aldrich and filtered through a 0.2  $\mu\text{m}$  membrane filter before use. Three model ethylene–propylene rubber (EPR) samples designated as EPR-1, EPR-2, and EPR-3 were prepared in a lab scale polymerization reactor using a supported metallocene catalyst system. The gas phase copolymerizations were carried out for 60 min at a temperature of 60 °C and a pressure of 13.8 bar. The different compositions of the model EPR samples were achieved by adjusting the monomer feeding ratios in the reactor, accordingly. Their bulk ethylene contents and molar masses are given in Table 1.

### 2.2. Temperature Rising Elution Fractionation

Preparative TREF was carried out using an instrument developed and built in-house. Approximately 3.0 g of polymer and 2.0 wt% Irganox 1010 (Ciba Specialty Chemicals, Switzerland) were dissolved in 300 mL of xylene at 130 °C in a glass reactor. The reactor was then transferred to a temperature-controlled oil bath and filled with sand (white quartz, Sigma-Aldrich, South Africa), used as a crystallization support. The oil bath and support were both preheated to 130 °C. The oil bath was then cooled at a controlled rate of 1 °C h $^{-1}$  in order to facilitate the controlled crystallization of the polymer. The crystallized mixture was then packed into a stainless steel column which was inserted into a modified gas chromatography oven for the elution step. Xylene (preheated) was used as eluent in order to collect the fractions at predetermined intervals as the temperature of the oven was raised. The fractions were isolated by precipitation in acetone, followed by drying to a constant weight.

### 2.3. Differential Scanning Calorimetry

Melting and crystallization behaviors of the samples were measured on a TA Instruments Q100 DSC system, calibrated with indium metal according to standard procedures. A scanning rate of 10 °C min $^{-1}$  was applied across the temperature range of –70 to 200 °C. Data obtained during the second heating cycle were used for all thermal analysis calculations. Measurements were conducted in a nitrogen atmosphere at a purge gas flow rate of 50 mL min $^{-1}$ .

## 2.4. Crystallization Analysis Fractionation

CRYSTAF experiments were carried out using a commercial CRYSTAF apparatus Model 200 (Polymer Char, Valencia, Spain). For each sample, approximately 20 mg was dissolved in 35 mL of TCB. Crystallization was carried out under agitation in stainless steel reactors, equipped with automatic stirring and filtration devices. After dissolution, the temperature was decreased from 100 °C to approximately 30 °C at a rate of 0.1 °C min<sup>-1</sup>. Fractions were taken automatically and the concentration of the solution was determined by an infrared detector, using 3.5 μm as the chosen wavelength.

## 2.5. High-Temperature Size Exclusion Chromatography

Molar mass measurements for all samples were performed at 150 °C using a PL GPC 220 high temperature chromatograph (Polymer Laboratories, Church Stretton, UK) equipped with a differential refractive index (RI) detector. The column set used consisted of three 300 × 7.5 mm i.d. PLgel Olexis columns together with a 50 × 7.5 mm PLgel Olexis guard column (Polymer Laboratories, Church Stretton, UK). The eluent used was TCB at a flow rate of 1.0 mL min<sup>-1</sup> with 0.0125 wt% 2,6-ditertbutyl-4-methylphenol (BHT) added as a stabilizer. Samples were dissolved at 160 °C in TCB at a concentration of 1 mg mL<sup>-1</sup> for 1–2 h (depending on the sample type) and 200 μL of each sample was injected. Narrowly distributed polystyrene standards (Polymer Laboratories, Church Stretton, UK) were used for calibration.

## 2.6. High-Temperature High Performance Liquid Chromatography

The separations were conducted on a high temperature solvent gradient interaction chromatograph (SGIC) constructed by Polymer Char (Valencia, Spain), comprising of an autosampler, two separate ovens, switching valves, and two pumps equipped with vacuum degassers (Agilent, Waldbronn, Germany). One oven was used for the HPLC column, while the second oven is the location of the injector and a switching valve. The autosampler is a separate unit connected to the injector through a heated transfer line. A high-pressure binary gradient pump was used for HPLC in the first dimension.

An evaporative light scattering detector (ELSD, model PL-ELS 1000, Polymer Laboratories, Church Stretton, England) was used with the following parameters: a gas flow rate of 1.5 L min<sup>-1</sup>, a nebuliser temperature of 160 °C, and an evaporator temperature of 270 °C. HT-HPLC was carried out using a Hypercarb column (Hypercarb, Thermo Scientific, Dreieich, Germany) with the following parameters: 100 × 4.6 mm i.d., packed with porous graphite particles with a particle diameter of 5 μm, a surface area of 120 m<sup>2</sup> g<sup>-1</sup>, and a pore size of 250 Å. The flow rate of the mobile phase was 0.5 mL min<sup>-1</sup>. The column was placed in the column oven maintained at 160 °C. The HPLC separations were accomplished by applying a linear gradient from 1-decanol to TCB. The volume fraction of TCB was linearly increased to 100% within 10 min after the sample injection and then held constant for 25 min. Finally, the initial chromatographic conditions were re-established with 100% 1-decanol. The dwell and void volumes

of 1.7 and 1.1 mL, respectively, were measured according to the method described by Ginzburg et al.<sup>[28]</sup> This reflects that there is an isocratic elution of 1-decanol (1.7 mL) before the start of gradient hits the column.<sup>[13]</sup> Samples were injected at a concentration of 1–1.2 mg mL<sup>-1</sup>, with 20 μL of each sample being injected.

## 2.7. Fourier Transform Infrared Spectroscopy

FTIR analyses of the samples were performed on a Thermo Nicolet iS10 Spectrometer (Thermo Scientific, Waltham, MA). Spectra were recorded at a resolution of 8 cm<sup>-1</sup> with 16 scans being recorded for each spectrum. Thermo Scientific OMNIC software (version 8.1) was used for data collection and processing.

## 2.8. High Temperature <sup>13</sup>C NMR Spectroscopy

<sup>13</sup>C NMR spectra were measured on a 400 MHz Varian Unity Inova NMR spectrometer, at a resonance frequency of 150 MHz for carbon. Deuterated 1,1,2,2-tetrachloroethane-d<sub>2</sub> (95.5+ atom% D, Sigma-Aldrich) at δ 74.3 ppm as internal reference, was used as a solvent for the sample preparation (at a concentration of 6 wt%). Analyses were carried out at 120 °C in nitrogen atmosphere, with an acquisition time of 0.79 s and preacquisition delay time of 15 s. This had led to total analysis time of 6 to 10 h per sample.

## 3. Results and Discussion

Evaluating the “homogeneity” of a polyolefin sample means analyzing its molar mass and chemical heterogeneity as well as its melting and crystallization behaviors. This is typically done by SEC (molar mass), HPLC (chemical composition), and DSC (melting and crystallization). If these methods provide narrow and unimodal distribution curves then these findings suggest that the sample is rather homogeneous or has a low molecular dispersity.

Figure 1 presents the SEC, HPLC, and DSC results for the bulk samples. As can be seen in Figure 1a, the samples exhibit unimodal narrow molar mass distributions. The peak maximum molar masses are very similar indicating that the ethylene–propylene ratio did not significantly influence the molar mass, see also Table 1. This is in agreement with previous findings that showed that metallocene catalysts produce polymers with narrow and unimodal molar mass distributions.<sup>[5,15,34]</sup>

HPLC separates the samples according to the ethylene–propylene ratio and provides an idea on the chemical composition distribution. Similar to SEC, very narrow elution profiles are obtained. The elution order is EPR-3 > EPR-2 > EPR-1 which is in agreement with the increasing ethylene content of the samples, see Figure 1b.

The EPR samples were further analyzed by DSC with a scan rate of 10 °C min<sup>-1</sup> to determine the thermal

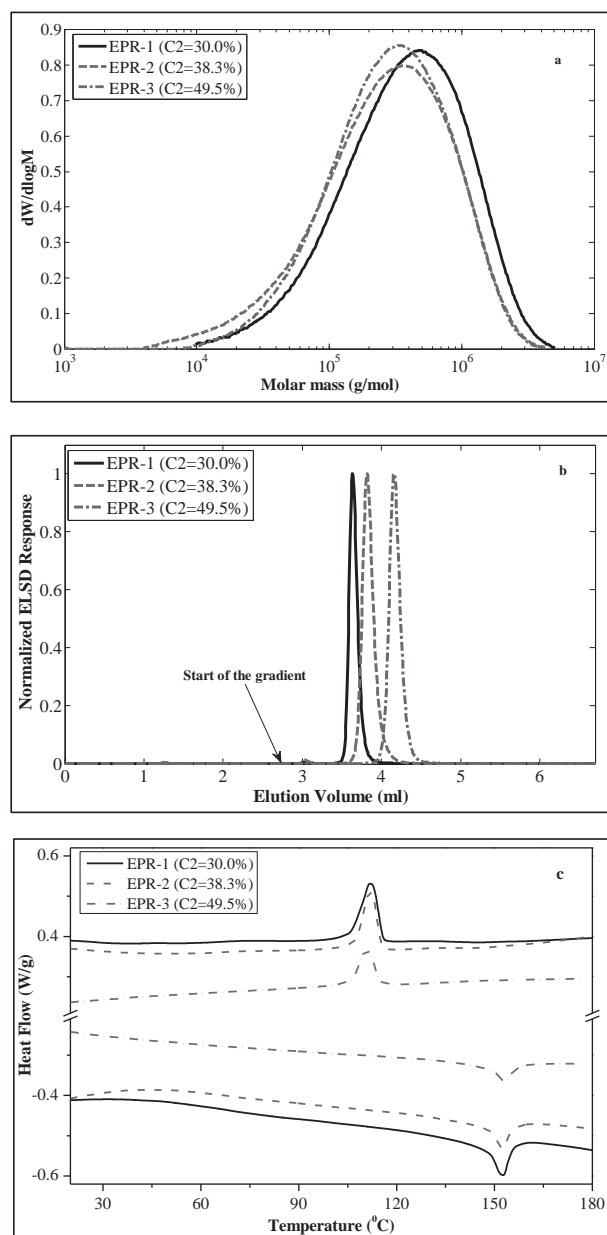


Figure 1. Bulk analysis of samples EPR-1, EPR-2, and EPR-3 by a) SEC, b) HPLC, and c) DSC.

properties, see Figure 1c and Table 2. As can be seen, the three samples have similar melting temperatures ( $T_m$ ) with values of  $\approx 153$  °C which are characteristic of propylene-rich EP copolymers having long sequences of propylene units. The crystallization temperatures ( $T_c$ ) are at approximately 111 °C and they are identical for all samples. The average crystallinities of the samples were estimated based on the melt enthalpies as shown in Table 2. With increasing ethylene contents the melting peak areas decrease reflecting the lower crystallinity for samples with higher ethylene contents. As is known, the inclusion

Table 2. Thermal properties of the EPR samples as obtained from first cooling and second heating measurements of DSC with a scan rate of  $10$  °C  $\text{min}^{-1}$ .

Sample name	$T_m$ [°C]	$T_c$ [°C]	$T_g$ [°C]	$\Delta H$ [J $\text{g}^{-1}$ ]
EPR-1	152.71	111.96	-39.63	2.87
EPR-2	152.64	111.79	-43.44	1.76
EPR-3	153.24	111.08	-50.80	0.89

of ethylene units in the polypropylene chains causes a reduction in crystallizable sequence lengths of iPP.<sup>[1,5]</sup>

The observed glass transition temperatures ( $T_g$ ) in Table 2 show noticeable differences and  $T_g$  is found to decrease with increasing ethylene content. This is in agreement with the lower crystallinity at higher ethylene contents. Several studies have proved that EP copolymers with lower  $T_g$  values have higher impact resistance. It is important to notice that despite similar  $T_m$  and  $T_c$  of these samples, they do have significantly different  $T_g$  that would affect their impact resistance properties.

The analyses of the bulk samples by SEC, HPLC, and DSC suggest that they have narrow molecular heterogeneities. In the present comonomer range the molar masses and the melting/crystallization temperatures are not significantly affected by the chemical composition. In contrast, the HPLC elution behavior and the glass transition temperatures are influenced by the chemical composition. Most importantly, CRYSTAF results show that the samples consist of a very high percentage of noncrystallizable material. The soluble fractions increase with increasing ethylene contents of the copolymers, see Figure 2, and these results are consistent with the lower melt enthalpies obtained by DSC as shown in Table 2.

A more detailed investigation of the samples was conducted with preparative TREF fractionations as the first step followed by the separation and characterization of individual components. The prep TREF profiles for the

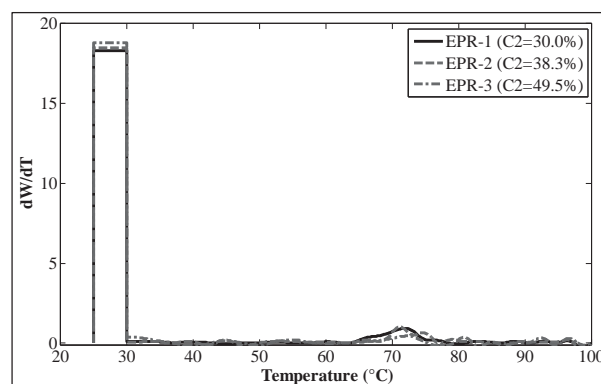


Figure 2. CRYSTAF curves for the bulk EPR samples obtained at crystallization temperatures of 30–100 °C.



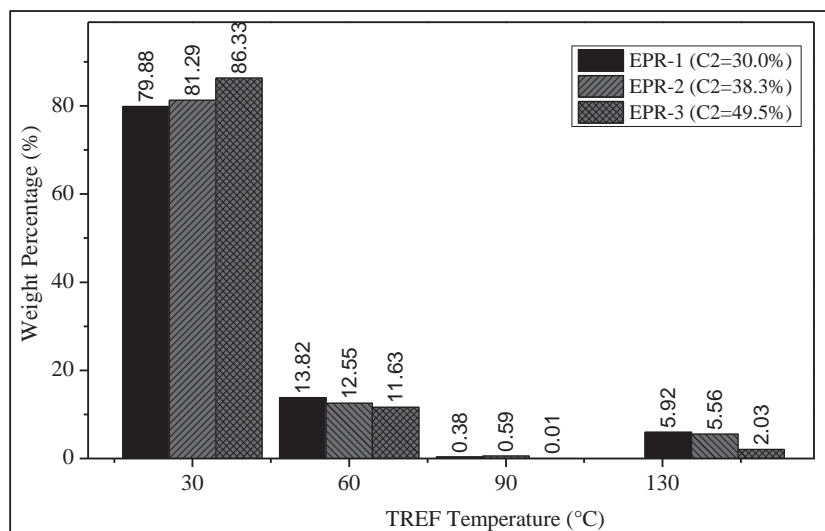


Figure 3. Preparative TREF results for EPR-1, EPR-2 and EPR-3, indicating the overall weight percentages of each fraction as a function of elution temperature.

material collected at 130 °C contained mostly iPP homopolymer.

The results of the molar mass analyses of the TREF fractions are summarized in Table 3. Similar to the results for the bulk samples, all the TREF fractions showed unimodal MMDs. The molar masses of the fractions increase with higher TREF temperature suggesting that either there is a molar mass influence on the TREF fractionations or the chemical composition influences the molar masses. At higher TREF temperatures the propylene content of the copolymer fractions is higher.

The thermal analysis was done on all the TREF fractions and no distinct melting and crystallization events were observed for the fractions collected at 30 and 60 °C. This behavior indicates that these TREF fractions are completely

amorphous or have a low crystallinity. The DSC results of the 90 and 130 °C TREF fractions are shown in Figure 4. The 90 °C TREF fraction of the EPR-3 was not analysed by DSC due to the low quantity that was obtained by TREF. The observed  $T_m$  for these fractions is seen at 150 and 160 °C, respectively. It was concluded that the 90 °C TREF fractions consist of EP copolymer species with long propylene sequences while the 130 °C TREF fractions are due to iPP. The melt enthalpies that were determined for the 90 and 130 °C fractions are shown in Table 4. In agreement with the previous statements, the 130 °C fractions exhibit a melt enthalpy of roughly 70 J g<sup>-1</sup> which is in agreement

three samples are presented in Figure 3. This figure presents a very interesting insight into the complexity of the samples. In agreement with the CRYSTAF results it is seen that noncrystallizable (amorphous) material makes about 80 wt% of the total samples. 11–14 wt% are segmented copolymers while 2–6 wt% are highly crystalline material, probably iPP or propylene-rich copolymer fractions. The percentage of non-crystallizable material is found to increase with the ethylene content of the bulk samples. These results are consistent with the  $T_g$  measurements of the bulk samples. In our previous work on EPR samples with high ethylene contents,<sup>[26]</sup> we had seen that TREF

Table 3. Molar masses of the TREF fractions for the three EPR samples as measured by HT-SEC.

Sample name	TREF fraction [°C]	$M_w^a$ [kg mol <sup>-1</sup> ]	$M_n^a$ [kg mol <sup>-1</sup> ]	$M_w/M_n$
EPR-1	30	399	159	2.51
	60	405	128	3.15
	90	405	114	3.54
	130	718	271	2.65
EPR-2	30	385	150	2.56
	60	343	83	4.12
	90	396	64	6.22
	130	576	99	5.84
EPR-3	30	359	111	3.24
	60	360	96	3.75
	90	NA	NA	NA
	130	498	112	4.43

<sup>a</sup>) Molar masses are polystyrene equivalents. NA: not analyzed due to low quantity of sample.

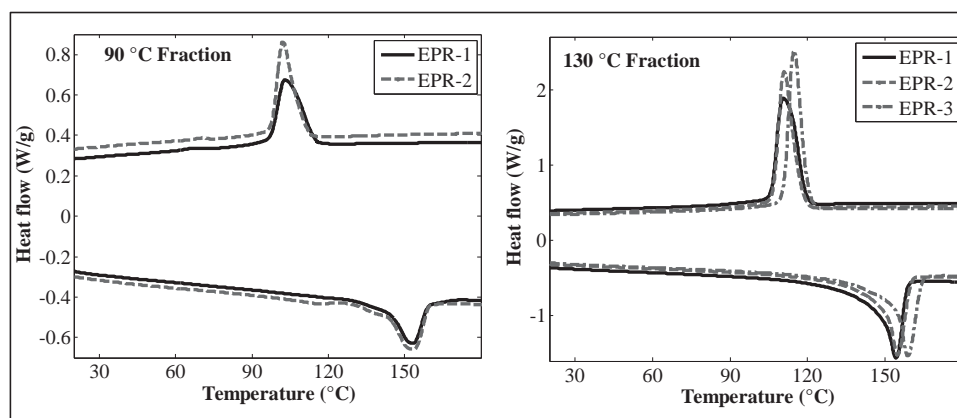


**Figure 4.** DSC curves for the TREF fractions of EPR samples showing first cooling and second heating measurements at a scan rate of  $10\text{ °C min}^{-1}$ ,  $90\text{ °C}$  fraction of EPR-3 was not analyzed due its low quantity.

with the melt enthalpy of iPP ( $70.8\text{ J g}^{-1}$  for 100% iPP). The  $90\text{ °C}$  fractions exhibit melt enthalpies of about  $18\text{ J g}^{-1}$  indicating EP copolymers.

In the next step, the DSC results which were obtained from the solid phase were contrasted to crystallization results obtained from solution using CRYSTAF. The normalized CRYSTAF results of the fractions are presented in Figure 5 showing crystallization temperatures between  $30$  and  $100\text{ °C}$ . The TREF fractions collected at both  $30$  and  $60\text{ °C}$  show no observable or quantifiable peaks in the crystallization region. According to CRYSTAF, these fractions are mostly amorphous with almost all material appearing in the soluble fractions at  $30\text{ °C}$ . These results are consistent with the DSC analyses that indicate the  $30$  and  $60\text{ °C}$  fractions to be completely amorphous. The  $130\text{ °C}$  fractions show unimodal crystallization peaks between  $65$  and  $85\text{ °C}$  for all EPR samples with a very small portion of amorphous material observed at  $30\text{ °C}$ . The lowest amount of solubles and the highest crystallization temperature are obtained for sample EPR-3. This finding is in agreement with the DSC results that show the highest  $T_m$  and  $T_c$  for sample EPR-3. At the same time the highest melt enthalpy is obtained for this sample.

**Table 4.** Thermal properties for TREF fractions of the EPR samples as obtained from first cooling and second heating measurements of DSC with scan rate of  $10\text{ °C min}^{-1}$ .

Sample name	TREF fraction	$T_m$ [°C]	$T_c$ [°C]	$\Delta H$ [J g <sup>-1</sup> ]
EPR-1	90	153.17	102.98	17.11
	130	154.36	110.60	68.25
EPR-2	90	153.55	102.13	18.02
	130	154.95	110.98	69.04
EPR-3	130	158.99	114.80	74.75

The results from DSC and CRYSTAF showed that there are some differences between TREF fractions collected at the same temperatures. Both techniques suffer from cocrystallization effects and, therefore, these results are not completely conclusive.

A chromatographic technique, HT-HPLC, which separates and characterizes EP copolymers based on their ethylene contents was employed for a more conclusive microstructure analysis. This technique operates above the crystallization temperature of the samples and, therefore, avoids the shortcomings of both DSC and CRYSTAF. Figure 6 shows the normalized results of the HT-HPLC experiments obtained with solvent gradient elution using a 1-decanol/TCB mobile phase. For the  $30$  and  $60\text{ °C}$  TREF fractions all materials elute after the start of the solvent gradient. This indicates that the fractions contain only EP copolymer molecules and no iPP homopolymer.

The HPLC chromatograms of the  $30$  and  $60\text{ °C}$  TREF fractions show that the peak maximum elution volume increases with increasing  $C_2$  content of the bulk sample. Based on the present separation mechanism, increasing elution volumes mean increasing  $C_2$  contents. This in turn means that TREF fractions from different samples that are collected at similar temperatures have different chemical compositions. This is very unusual at least for the  $60\text{ °C}$  TREF fractions because for a long time it was believed that TREF fractions collected at similar temperatures have the same chemical compositions. A similar situation is observed for the  $90\text{ °C}$  TREF fractions. The copolymer fractions eluting between  $3$  and  $4\text{ mL}$  again appear in the order of increasing  $C_2$  bulk content. Different from the  $60\text{ °C}$  TREF fractions, these fractions contain small amounts of lower molar mass iPP that elute before the start of the gradient.

As is known from previous work,<sup>[26]</sup> the  $130\text{ °C}$  TREF fractions consist mainly of lower and higher molar mass iPP. This can be seen by the characteristic elution pattern

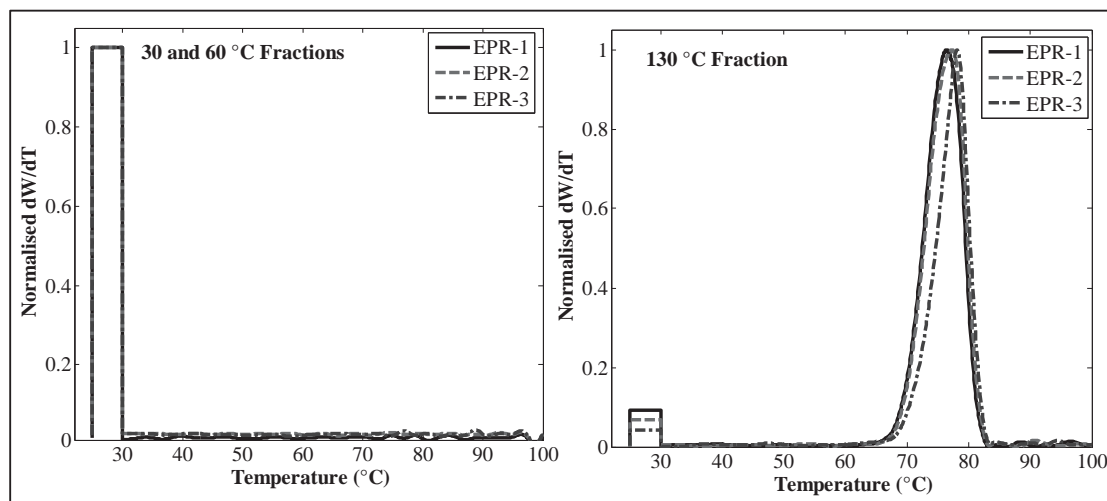


Figure 5. CRYSTAF curves for the TREF fractions of the EPR samples obtained at crystallization temperatures between 30–100 °C. The 90 °C fractions of the samples were not analyzed due their low quantity.

between 1 and 3 mL. Small amounts of EP copolymer elute at 3–4 mL.

It is interesting to note that the differences seen in the HPLC traces of the 90 °C TREF fractions are not seen in DSC, see Figure 4. This indicates that HPLC is more sensitive toward subtle differences in the chemical compositions of the present TREF fractions. In addition, the HPLC analyses of the TREF fractions reveal more details as can be seen by comparing the HPLC traces of the bulk samples with those of the 130 °C TREF fractions. While iPP was not detected in the bulk sample analyses, it was clearly seen

in the fractions. As shown in our previous work<sup>[26]</sup> on EPR samples with high comonomer contents, preparative TREF combined with HPLC proves again to be a powerful tool in revealing the heterogeneity at molecular level of such complex samples.

For conclusive information on the chemical composition of the TREF fractions it was worthwhile to determine the ethylene content of the fractions together with the concentrations of ethylene and propylene sequences using solution NMR. Figure 7 shows the <sup>13</sup>C NMR spectra for the TREF fractions of EPR-1 and EPR-2. The spectra

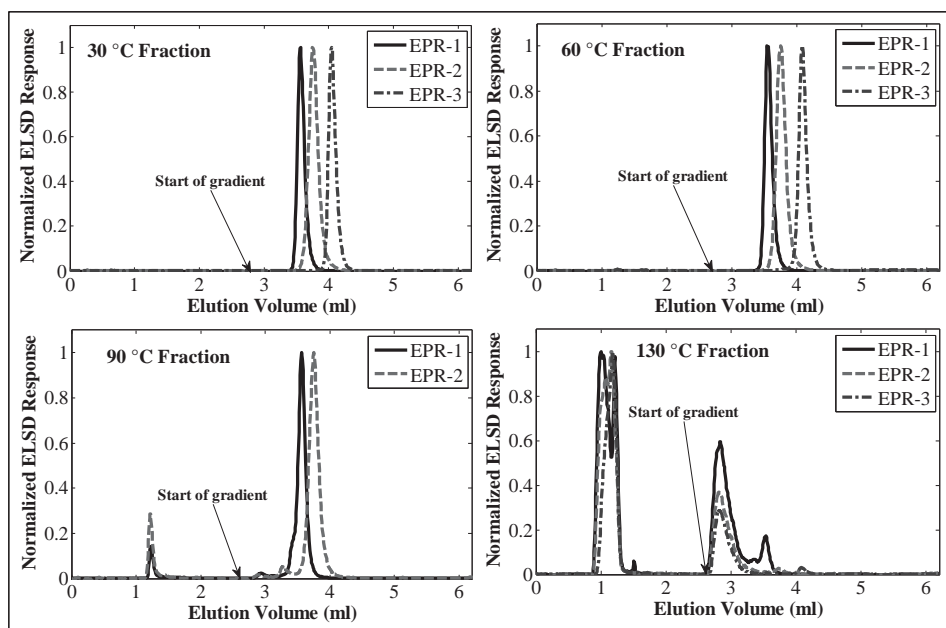
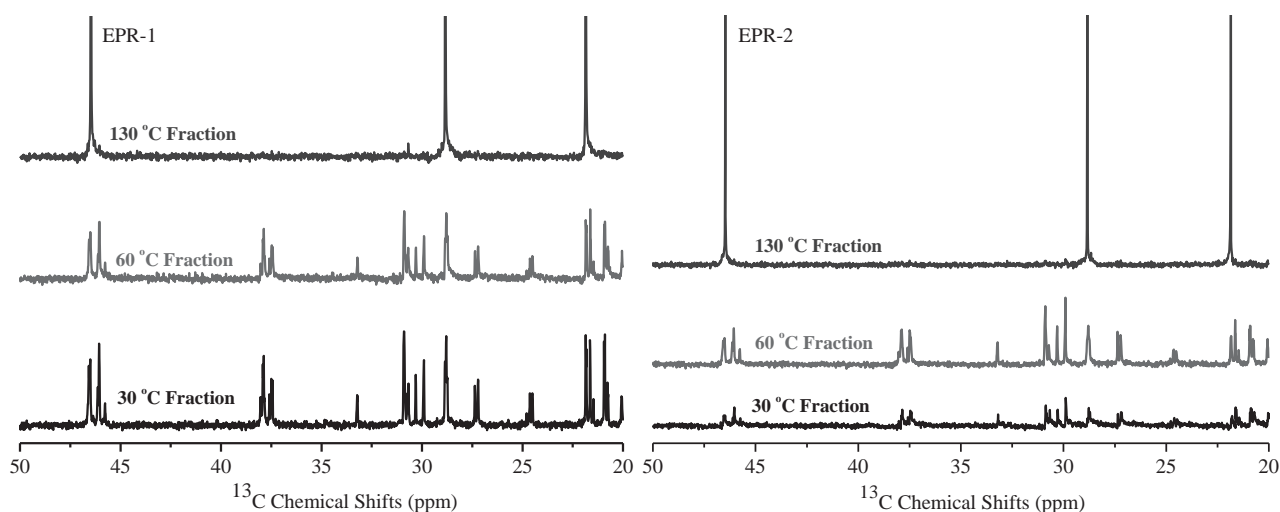


Figure 6. HT-HPLC chromatograms for the TREF fractions of the three EPR samples, solvent gradient elution (1-decanol to TCB) after an initial isocratic step. The 90 °C fraction of EPR-3 was not analyzed due its low quantity.



**Figure 7.**  $^{13}\text{C}$  NMR spectra for the TREF fractions of the EPR-1 and EPR-2 obtained at high temperature (120 °C), the 90 °C fractions of the samples were not analyzed due their low quantity.

were obtained at a temperature of 120 °C with acquisition times of 0.79 s. The TREF fractions collected at 130 °C show spectra with three major signals due to  $\text{CH}_2$  ( $\approx 47$  ppm),  $\text{CH}$  ( $\approx 29$  ppm), and  $\text{CH}_3$  ( $\approx 22$  ppm). These spectra are entirely different from the spectra obtained for the lower TREF fractions. The assignment of the peaks, the comonomer content and the monomer sequences distributions were estimated based on the relationships established by both Ray et al.<sup>[36]</sup> and Randall.<sup>[37]</sup> The three distinct signals observed for the 130 °C TREF fractions correspond to the carbon atoms of the propylene repeating unit and, therefore, these fractions can be assigned to iPP. These results are in good agreement with the HPLC results of 130 °C TREF fractions.

The numerous peaks observed for the 30 and 60 °C TREF fractions indicate that a variety of longer ethylene and propylene sequences are present in these fractions. The quantitative analysis of these segments is summarized in Table 5.

More detailed information on the microstructure of the TREF fractions is obtained from the sequence analysis by  $^{13}\text{C}$  NMR. The analysis of the 130 °C TREF fractions proves that these fractions are almost pure PP. The 30 and 60 °C TREF fractions contain a variety of ethylene–propylene sequences including longer PPP sequences. It is interesting to observe that there are no distinct differences between the 30 and the 60 °C TREF fraction in each sample. Comparing the sequence distributions of different samples, a

**Table 5.**  $^{13}\text{C}$  NMR monomer and sequences distribution for the TREF fractions of three EPR samples.

Sample ID	EPR-1			EPR-2			EPR-3		
	TREF fraction [°C]	30	60	130	30	60	130	30	60
P (%)		66.3	67.0	98.5	61.1	59.6	98.4	48.6	51.0
E (%)		33.7	33.0	1.5	38.9	40.4	1.6	51.4	49.0
PP (%)		45.5	46.7	98.5	36.7	37.6	98.4	23.9	25.2
PE + EP (%)		41.0	38.8	0.0	45.5	43.5	0.0	44.9	46.0
EE (%)		13.5	14.5	1.5	17.9	18.9	1.6	31.3	28.8
PPP (%)		30.2	32.7	98.5	20.1	22.3	98.4	11.7	12.0
PPE (%)		30.8	29.2	0.0	33.8	31.0	0.0	27.7	27.7
EPE (%)		5.3	5.1	0.0	7.2	6.3	0.0	9.1	11.3
EEE (%)		6.2	6.9	1.5	10.0	9.9	1.6	19.7	18.3
PEE (%)		16.9	16.6	0.0	18.2	19.3	0.0	21.7	20.6
PEP (%)		10.5	9.5	0.0	10.7	11.2	0.0	10.1	10.1

clear trend to ethylene-rich sequences (EEE, PEE) can be seen from sample EPR-1 to EPR-3 which correlates with the increasing ethylene content of the bulk samples.

In agreement with the HPLC results the NMR analyses show that TREF fractions from different samples taken at the same TREF temperature do not have the same composition. With increasing ethylene contents of the bulk samples the corresponding TREF fractions also exhibit increasing ethylene contents. This is a clear proof of the previous statement that TREF is not an absolute fractionation method but depends on the composition of the sample.

#### 4. Conclusions

Metallocene-catalyzed ethylene–propylene copolymers are assumed to exhibit single and narrow distributions in terms of molar mass, chemical composition, and sequence distributions. This statement was mainly based on the investigation of bulk samples.

The current study was aimed at examining how homogenous metallocene-catalyzed EP copolymers are based on multiple fractionation and analysis techniques. It was found that the present copolymers exhibit quite complex molecular compositions. The structural information that was obtained by advanced analytical methods goes far beyond the details that are obtained by bulk methods.

In a first step, the EPR bulk samples were analyzed using various analytical techniques, namely, HT-SEC, DSC, FTIR, and HT-HPLC and rather narrow distributions in terms of molar mass and chemical composition were found for the samples. HT-HPLC was found to be very sensitive regarding the ethylene content of the samples.

Preparative TREF was conducted to obtain in depth knowledge about the molecular structure of the EPR samples. The resulting TREF fractions were analyzed by HT-SEC, DSC, CRYSTAF, HT-HPLC, and solution  $^{13}\text{C}$ -NMR. The fractions showed homogenous distributions only in terms of molar mass, however, a significant heterogeneity in chemical composition was found. In addition to a large variety of copolymer structures, significant amounts of iPP were detected. HT-HPLC and  $^{13}\text{C}$ -NMR proved to be the most useful techniques since they are able to analyze both amorphous and crystalline fractions.

The present findings show that TREF is not an absolute technique that, for a given copolymer system, fractionates independently of the bulk sample composition. The combination of various analytical techniques proved to be a necessary tool in understanding the molecular structure of these complex EPR copolymers.

Acknowledgements: The authors thank SASOL, South Africa, and Lummus Novolen Technology GmbH, Germany, for the

financial support of this work. The high temperature  $^{13}\text{C}$  NMR measurements done by Dr. J. Brand and E. Malherbe are gratefully acknowledged.

Received: April 10, 2015; Revised: May 27, 2015;  
Published online: June 18, 2015; DOI: 10.1002/macp.201500135

Keywords: differential scanning calorimetry; ethylene–propylene copolymers; high-temperature HPLC; metallocene catalyst; NMR; temperature rising elution fractionation

- [1] C. H. Stephens, B. C. Poon, P. Ansems, S. P. Chum, A. Hiltner, E. Baer, *J. Appl. Polym. Sci.* **2006**, *100*, 1651.
- [2] C. Piel, F. G. Karssenbergh, W. Kaminsky, V. B. F. Mathot, *Macromolecules* **2005**, *38*, 6789.
- [3] A. Shamiri, M. H. Chakrabarti, S. Jahan, M. A. Hussain, W. Kaminsky, P. V. Aravind, W. A. Yehye, *Materials* **2014**, *7*, 5069.
- [4] C. Gabriel, E. Kokko, B. Löfgren, J. Seppälä, H. Münstedt, *Polymer* **2002**, *43*, 6383.
- [5] K. Jeon, Y. L. Chiari, R. G. Alamo, *Macromolecules* **2008**, *41*, 95.
- [6] C. Kock, N. Aust, C. Grein, M. Gahleitner, *J. Appl. Polym. Sci.* **2013**, *130*, 287.
- [7] C. Kock, M. Gahleitner, A. Schausberger, E. Ingolic, *J. Appl. Polym. Sci.* **2012**, *128*, 1484.
- [8] M. Pires, R. S. Mauler, S. A. Liberman, *J. Appl. Polym. Sci.* **2004**, *92*, 2155.
- [9] Z. Fu, J. Xu, Y. Zhang, Z. Fan, *J. Appl. Polym. Sci.* **2005**, *97*, 640.
- [10] G. Liu, X. Zhang, Y. Liu, X. Li, H. Chen, K. Walton, G. Marchand, D. Wang, *Polymer* **2013**, *54*, 1440.
- [11] T. Macko, H. Pasch, *Macromolecules* **2009**, *42*, 6063.
- [12] H. Pasch, R. Brüll, U. Wahner, B. Monrabal, *Macromol. Mater. Eng.* **2000**, *279*, 46.
- [13] S. Cheruthazhekatt, G. W. Harding, H. Pasch, *J. Chromatogr. A* **2013**, *1286*, 69.
- [14] P. Stepan, *J. Appl. Polym. Sci.* **2013**, *131*, 40111.
- [15] T. MacKo, A. Ginzburg, K. Remerie, R. Brüll, *Macromol. Chem. Phys.* **2012**, *213*, 937.
- [16] S. Cheruthazhekatt, H. Pasch, *Anal. Bioanal. Chem.* **2013**, *405*, 8607.
- [17] A. Tynys, I. Fonseca, M. Parkinson, L. Resconi, *Macromolecules* **2012**, *45*, 7704.
- [18] V. Agarwal, T. B. Van Erp, L. Balzano, M. Gahleitner, M. Parkinson, L. E. Govaert, V. Litvinov, A. P. M. Kentgens, *Polymer* **2014**, *55*, 896.
- [19] S. Cheruthazhekatt, T. F. J. Pijpers, G. W. Harding, V. B. F. Mathot, H. Pasch, *Macromolecules* **2012**, *45*, 2025.
- [20] J. B. P. Soares, S. Anantawaraskul, *J. Polym. Sci., Part B: Polym. Phys.* **2005**, *43*, 1557.
- [21] B. Monrabal, L. Romero, *Macromol. Chem. Phys.* **2014**, *215*, 1818.
- [22] B. Monrabal, P. Del Hierro, *Anal. Bioanal. Chem.* **2011**, *399*, 1557.
- [23] Y. Xue, Y. Fan, S. Bo, X. Ji, *Eur. Polym. J.* **2011**, *47*, 1646.
- [24] N. Aust, M. Gahleitner, K. Reichelt, B. Raninger, *Polym. Test.* **2006**, *25*, 896.
- [25] E. De Goede, P. Mallon, H. Pasch, *Macromol. Mater. Eng.* **2010**, *295*, 366.
- [26] M. J. Phiri, S. Cheruthazhekatt, A. Dimeska, H. Pasch, *J. Polym. Sci., Part A: Polym. Chem.* **2015**, *53*, 863.

- [27] A. Albrecht, L. C. Heinz, D. Lilge, H. Pasch, *Macromol. Symp.* **2007**, *257*, 46.
- [28] A. Ginzburg, T. MacKo, V. Dolle, R. Brüll, *Eur. Polym. J.* **2011**, *47*, 319.
- [29] H. Pasch, M. I. Malik, T. Macko, *Adv. Polym. Sci.* **2013**, *251*, 77.
- [30] S. Cheruthazhekatt, N. Mayo, B. Monrabal, H. Pasch, *Macromol. Chem. Phys.* **2013**, *214*, 2165.
- [31] T. MacKo, R. Brüll, Y. Zhu, Y. Wang, *J. Sep. Sci.* **2010**, *33*, 3446.
- [32] D. Mekap, T. MacKo, R. Brüll, R. Cong, A. W. deGroot, A. Parrott, P. J. C. H. Cools, W. Yau, *Polymer* **2013**, *54*, 5518.
- [33] R. Chitta, A. Ginzburg, T. MacKo, R. Brüll, G. Van Doremaele, *LC-GC Eur.* **2012**, *25*, 352.
- [34] R. Chitta, T. MacKo, R. Brüll, G. Van Doremaele, L. C. Heinz, *J. Polym. Sci., Part A: Polym. Chem.* **2011**, *49*, 1840.
- [35] T. MacKo, R. Brüll, Y. Wang, B. Coto, I. Suarez, *J. Appl. Polym. Sci.* **2011**, *122*, 3211.
- [36] G. J. Ray, P. E. Johnson, J. R. Knox, *Macromolecules* **1977**, *10*, 773.
- [37] J. C. Randall, *Macromolecules* **1978**, *11*, 33.

## Chapter 6: Compositional Heterogeneity of Vis-broken IPC

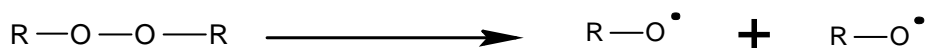
### 6 Exploring the Compositional Heterogeneity of Vis-broken Impact Polypropylene Copolymers using Advanced Fractionation Methods

*This chapter presents the research work done on the fractionation and characterization of vis-broken impact polypropylene copolymers (IPC) using various analytical techniques. Four vis-broken IPC samples were used to study the effect of an organic peroxide on the molecular properties of the IPC materials. In conclusion, an effective multidimensional analytical approach was established in the present study to explore compositional heterogeneities in the vis-broken IPC materials. This work is prepared for publication and the manuscript is attached.*

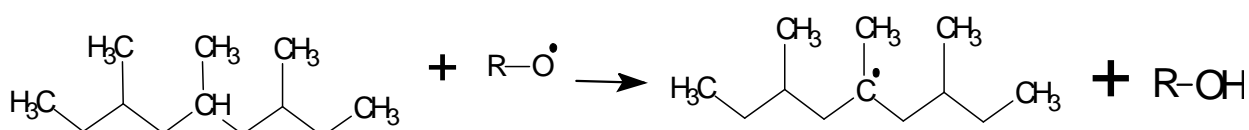
#### 6.1 Summary of the Research Study

Vis-broken impact polypropylene copolymers (IPC) are known to have decreased molar masses and melt viscosities due to the action of organic peroxides during the vis-breaking process<sup>1-3</sup>. An increase in the melt flow rates of the vis-broken IPC is related to their high solubility properties<sup>4</sup> due to changes in chemical composition. There is limited previous work done to evaluate the effect of the peroxide on the microstructural properties of the vis-broken IPC materials. Therefore, the aim of the present study was to explore the molecular composition of vis-broken IPC using multiple fractionation techniques. Scheme 1 presents the general mechanism for the degradation of ethylene-propylene (EP) copolymers under the influence of a peroxide<sup>5,6</sup>. For illustration purposes, the scheme is based on the attack at the propylene units. The final products from the degradation depend mainly on the type of polymer, type and concentration of peroxide and presence of other additives<sup>5</sup>.

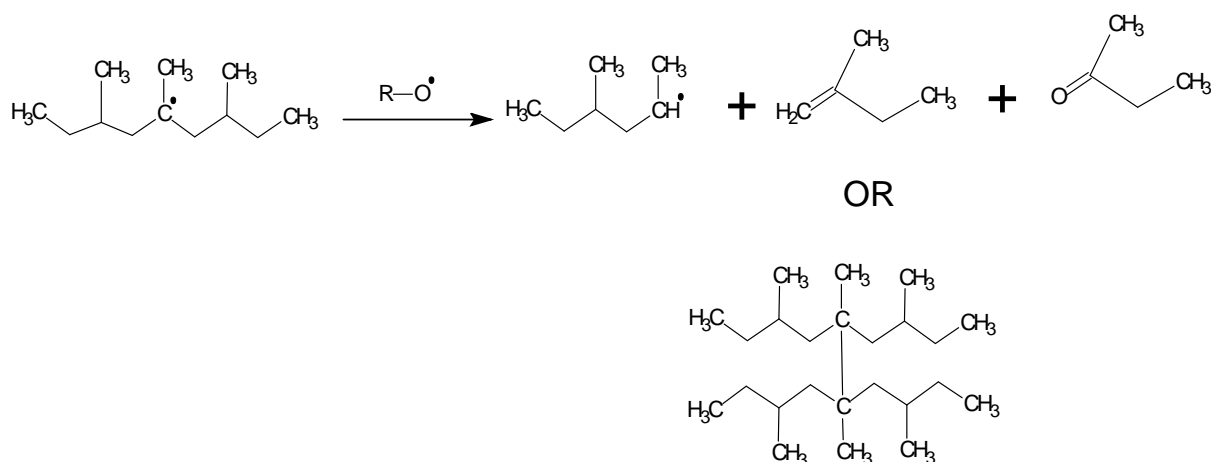
Thermal decomposition of the peroxide to form radicals



Formation of the new polymer radicals via peroxide attack



-scission and formation of new polyolefin structures and possibility of cross-linking<sup>5</sup>



Scheme 1: Vis-breaking of polypropylene sequence by an organic peroxide

The bulk vis-broken IPC samples were analysed using SEC, DSC, CRYSTAF, HT-HPLC and FT-IR. The IPC samples were prepared as model copolymers in laboratory scale with sample IPC-1 was the non-degraded reference copolymer, while samples IPC-2 and -3 were vis-broken samples with increasing melt flow rates (MFR). There was a significant decrease in the molar masses of the samples upon addition of the peroxide. The results from the DSC, CRYSTAF and HT-HPLC did not reveal any major changes in the molecular compositions of the vis-broken IPC since the major phase present in the samples was found to be iPP homopolymer. CRYSTAF results showed a slight increase in the amount of solubles of the bulk material with higher MFR values. The minor components were masked by the iPP phase, hence, they could not be detected due to their low concentrations. On the other hand, FT-IR showed a clear effect of the peroxide on the vis-broken samples with the presence of carbonyl groups (C=O) in the region of 1500 – 1800  $\text{cm}^{-1}$ . The intensity of the C=O absorption bands was found to increase with high amounts of the peroxide added during the vis-breaking process. The major limitation of FT-IR technique was that it provided only average chemical composition, as such the details about which phase (amorphous, semi-crystalline or highly crystalline) of the IPC material had been affected by action of an organic peroxide was not established. The bulk samples were fractionated by preparative TREF to obtain comprehensive information on the chemical composition of the IPC



after degradation. The three IPC samples were separated according to their crystallinities by TREF technique.

Figure 6.1 presents the fractionation results from TREF and the analyses of the TREF fractions using multiple analytical techniques. Upon fractionation with preparative TREF, the minor components including the segmented EP copolymers were isolated and collected, see Fig 6.1(A). The iPP phase formed the major component of the vis-broken samples being about ~70 % of the total samples which was collected at 130 °C. The rubber phase that is responsible for impact properties of IPC constituted about ~20 % of the bulk material. The co-crystallization or co-elution existed in the segmented EP copolymers due to different lengths of ethylene and propylene sequences. As such, further analyses on the TREF fractions were essential to obtain comprehensive microstructural properties of the IPC materials upon the effect of the organic peroxide.

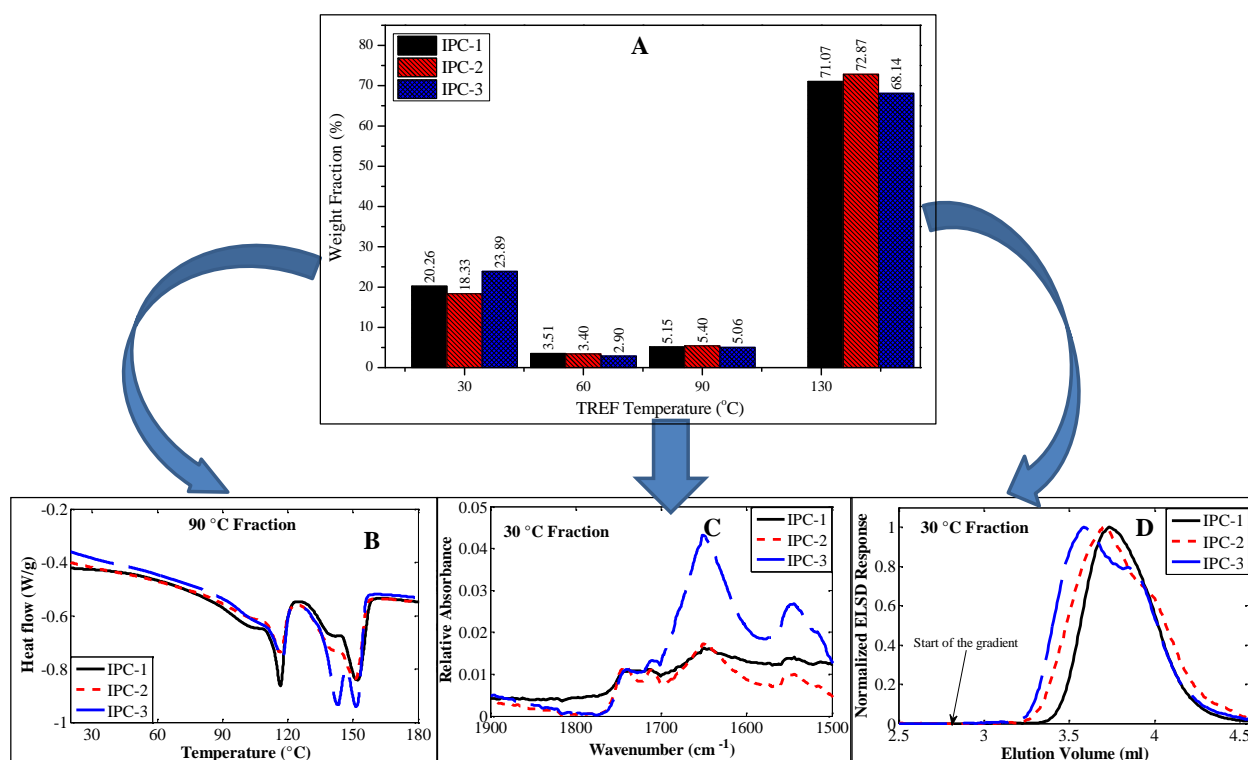


Figure 6.1: prep-TREF fractionation (A) results of vis-broken IPC samples and analyses of the TREF fractions using DSC (B), FT-IR (C) and HT-HPLC (D).

The results from the DSC, CRYSTAF and HPLC confirmed that the 130 °C fractions consist mainly of the iPP phase. These last eluting TREF materials were mainly due to highly crystalline material of high molar mass iPP with melting temperatures occurring at 160 °C. The 90 °C

TREF fractions were found to contain segmented EP copolymers having complex molecular compositions as indicated by multiple melting peaks from the DSC analyses, see Fig. 6.1(B). The DSC peaks were assigned to ethylene-rich copolymers at  $\sim 120$  °C, propylene-rich copolymers at  $\sim 140$  °C and low molar mass iPP with low isotacticity at  $\sim 150$  °C. The melting peaks at  $140 - 150$  °C were more pronounced with an increase in amount of peroxide during the degradation process. FT-IR analyses revealed that the  $30$  °C TREF fractions contain the highest amount of products of the degradation process as indicated by the carbonyl spectral region. Figure 6.1(C) shows that the number of the carbonyl products increases with the amount of the peroxide added to the IPC samples. Absorption peaks at  $1750\text{ cm}^{-1}$  and  $1650\text{ cm}^{-1}$  were due to the presence of C=O stretches from the conjugated aldehydes and ketones, respectively, whereas peaks at  $1550\text{ cm}^{-1}$  had resulted from C=C stretching. The concentration of the carbonyl products decreases with increase in TREF elution temperature. The  $130$  °C TREF fractions had no detectable amounts of carbonyl products.

HT-HPLC gave more insight into the effect of the peroxide on the chemical composition changes of the IPC samples since detailed information on the molecular structures of the samples can be obtained from the technique. The  $30$  °C TREF fractions contained only the random EP copolymer since all the samples eluted after the start of the gradient with TCB. It was found that the elution volumes of the samples on the graphitic stationary phase shift to lower values as depicted in Fig. 6.1(D). The HPLC chromatograms indicated that these fractions do not contain any PP components as these would appear at elution volumes of  $3$  mL or lower, compare to elution patterns of the  $60$ ,  $90$  and  $130$  °C TREF fractions. The  $60$  and  $90$  °C TREF fractions have three distinct chemical compositions namely low molar mass iPP at  $1.3$  mL, segmented EP copolymers between  $3 - 4.5$  mL and ethylene-rich copolymer between  $5 - 6.5$  mL. The results are similar to DSC analyses since they showed that these two set of fractions have complex molecular compositions. In comparison to the DSC and CRYSTAF techniques, HT-HPLC was able to characterize both amorphous and crystalline fractions of the vis-broken IPC samples.

In conclusion, upon vis-breaking the amount of the  $30$  °C TREF fractions increases indicating that additional soluble material is produced through chain scission. The present study has proved that an effective multidimensional analytical approach is necessary to explore the compositional heterogeneities of the vis-broken IPC materials. A better understanding of the vis-breaking process was attained through the current study.

## 6.2 References

1. M. Swart, A. J. van Reenen. *Journal of Applied Polymer Science* **2015**, *132*, 41783.
2. E. de Goede, P. E. Mallon, K. Rode, H. Pasch. *Macromolecular Materials and Engineering* **2011**, *296*, 1018-1027.
3. H. Pasch, E. de Goede, P. Mallon. *Macromolecular Symposia* **2012**, *312*, 174-190.
4. E. de Goede, P. E. Mallon, H. Pasch. *Macromolecular Materials and Engineering* **2012**, *297*, 26-38.
5. P. R. Dluzneski. *Rubber Chemistry and Technology* **2001**, *74*, 451.
6. G. Moad, I. J. Dagley, J. Habsuda, C. J. Garvey, G. Li, L. Nichols, G. P. Simon, M. R. Nobile. *Polymer Degradation and Stability* **2015**, *117*, 97-108.

# Exploring the Compositional Heterogeneity of Vis-broken Impact Polypropylene Copolymers by Advanced Fractionation Methods

Mohau Justice Phiri<sup>1</sup>, Harald Pasch<sup>1\*</sup>

<sup>1</sup> Stellenbosch University, Department of Chemistry and Polymer Science, 7602 Matieland, South Africa

\* Corresponding author: [hpasch@sun.ac.za](mailto:hpasch@sun.ac.za)

## Abstract

Vis-breaking or rheology control is an important technical process to improve the processability of impact polypropylene copolymers (IPC). In the vis-breaking process the molar mass and its dispersity are reduced, the crystallinity changes and polar carbonyl functionalities are introduced due to the reaction of the polymer with peroxide. Although the fundamental principles of vis-breaking are well understood, not much research has been devoted to the investigation of the molecular changes brought about by the vis-breaking process. In the present study, the effect of vis-breaking on the molecular properties of IPC is elucidated using advanced fractionation methods. After the analysis of the bulk sample properties, the samples are fractionated using preparative TREF and the fractions are analysed by FTIR, DSC, CRYSTAF and HT-HPLC techniques. For the first time, an effective multidimensional analytical approach is established to study compositional heterogeneities in vis-broken IPC materials.

**Keywords:** Impact polypropylene copolymers, vis-breaking process, preparative TREF, FTIR, high-temperature HPLC

## 1. Introduction

Impact polypropylene copolymers (IPC) have been used extensively for many applications in the automotive and electrical appliances industries<sup>[1-4]</sup> since these materials have superior properties over traditional polypropylene (PP) materials due their multiphase morphology where ethylene-propylene rubber particles are incorporated in an isotactic polypropylene (i-PP) matrix<sup>[1, 5-10]</sup>. As such, IPC materials have increased impact strengths and tensile-fracture properties as compared to i-PP. Hence, they can be used also for low temperature applications<sup>[11, 12]</sup>. One very feasible approach for increasing the melt flow rate of IPC is the so called 'vis-breaking' or controlled rheology process. Numerous studies have shown that the vis-breaking process can be applied to IPC to decrease the average molar mass and to reduce the molar mass dispersity. Longer polymer chains are broken down to shorter chains with the help of peroxides<sup>[13-16]</sup>. The vis-broken IPC materials have higher melt flow rates, hence e.g. filling of the narrow cavity molds in injection molding applications is facilitated<sup>[13]</sup>.

The complex molecular characteristics of IPC have been investigated in many studies<sup>[17-20]</sup>. However, the effect of the peroxide in the vis-breaking process makes these materials even more complex in terms of molar mass distribution (MMD) and chemical composition distribution (CCD)<sup>[11, 16]</sup>. The need to understand how the peroxide affects the microstructure of these complex copolymers is critical in

determining the final applicability and properties of the vis-broken materials. Several studies have been conducted using high temperature size exclusion chromatography (HT-SEC) to prove that the vis-broken IPCs exhibit reduced molar masses and MMDs<sup>[11, 13, 14, 16, 21]</sup>. Swart and van Reenen<sup>[11]</sup> studied vis-broken IPC bulk materials and their TREF fractions using <sup>13</sup>C NMR and SEC coupled to FTIR spectroscopy. Based on the <sup>13</sup>C NMR analysis of the TREF fractions they showed that the vis-breaking process affects mainly copolymers with long ethylene sequences. DSC analyses have revealed multiple endotherms due to presence of carbonyl-containing products that formed during the degradation process<sup>[16]</sup>. Similar results were observed with CRYSTAF analysis of vis-broken IPCs<sup>[13, 16]</sup>. However, as shown in our previous work<sup>[22]</sup>, crystallisation-based techniques are not sufficient to provide comprehensive CCD information on these complex materials since these techniques cannot address the compositional heterogeneity of the amorphous part. Recently, comprehensive solvent-gradient high temperature HPLC which can analyse both the crystalline and amorphous materials has been used to separate and characterise complex IPCs<sup>[19, 23-30]</sup>.

As has been pointed out by different authors, the effect of vis-breaking on the molecular characteristics and the microstructure of IPC is still largely unexplored<sup>[11, 31]</sup>. In particular, advanced fractionation techniques such as HT-HPLC have never been used to characterise the vis-breaking process. In this study, IPC materials were vis-broken to

varying melt flow rates by action of an organic peroxide. Then, a comprehensive analytical approach was adopted to determine the microstructure of the vis-broken materials. Firstly, the bulk materials were fractionated according to crystallisability using preparative TREF. Subsequently, the microstructure of the TREF fractions as compared to the bulk samples was explored using advanced fractionation methods including HT-HPLC and HT-SEC and combined with information from DSC, CRYSTAF and FTIR spectroscopy. The multidimensional analytical approach proposed in this study was found to be very effective in determining the molecular characteristics of vis-broken IPC materials.

## 2. Experimental

### 2.1 Materials

HPLC grade 1,2,4-trichlorobenzene (TCB) was purchased from Sigma-Aldrich and filtered through a 0.2  $\mu\text{m}$  membrane filter before use. Xylene (>99% purity) and 1-decanol (>99% purity) were purchased from Chemical&Laboratory suppliers and Aldrich, respectively, and used as received. The IPC samples were prepared as model copolymers in laboratory scale. The vis-breaking process was carried out in a twin-screw extruder using organic peroxides to produce materials with different melt flow rates (MFRs). The compositional information of the bulk samples is given in Table 1.

Table 1. Details on the composition of the bulk IPC samples

Sample Name	Ethylene content (C <sub>2</sub> ) (mol%)	M <sub>w</sub> <sup>a</sup> by SEC (kg/mol)	M <sub>w</sub> /M <sub>n</sub>	Melt Flow Rate (g/10min)
IPC-1	8.1	338.4	6.53	12
IPC-2	8.4	273.3	5.14	20
IPC-3	8.3	226.3	4.40	48

<sup>a</sup> molar masses are polystyrene equivalents. <sup>b</sup> reference or base material, IPC reactor powder

### 2.2 Temperature Rising Elution Fractionation (TREF)

Preparative TREF was carried out using an instrument developed and built in-house. Approximately 3.0 g of polymer and 2.0 wt% Irganox 1010 (Ciba Specialty Chemicals, Switzerland) were dissolved in 300 mL of xylene at 130 °C in a glass reactor. The reactor was then transferred to a temperature-controlled oil bath and filled with sand (white quartz, Sigma-Aldrich, South Africa), used as a crystallization support. The oil bath and support were both preheated to 130 °C. The oil bath was then cooled at a controlled rate of 1 °C/h in order to facilitate the controlled

crystallization of the polymer. The crystallized mixture was then packed into a stainless steel column which was inserted into a modified gas chromatography oven for the elution step. Xylene (preheated) was used as eluent in order to collect the fractions at predetermined intervals as the temperature of the oven was raised. The fractions were isolated by precipitation in acetone, followed by drying to a constant weight.

### 2.3 Differential Scanning Calorimetry (DSC)

Melting and crystallization behaviours of the samples were measured on a TA Instruments Q100 DSC system, calibrated with indium metal according to standard procedures. A scanning rate of 10 °C/min was applied across the temperature range of 0–200 °C. Data obtained during the second heating cycle were used for all thermal analysis calculations. Measurements were conducted in a nitrogen atmosphere at a purge gas flow rate of 50 mL/min.

### 2.4 Crystallization Analysis Fractionation (CRYSTAF)

CRYSTAF experiments were carried out using a commercial CRYSTAF apparatus Model 200 (Polymer Char, Valencia, Spain). For each sample, approximately 20 mg were dissolved in 35 mL of 1,2,4-trichlorobenzene (TCB). Crystallization was carried out under agitation in stainless steel reactors, equipped with automatic stirring and filtration devices. After dissolution, the temperature was decreased from 100 °C to approximately 30 °C at a rate of 0.1 °C/min. Fractions were taken automatically and the concentration of the solution was determined by an infrared detector, using 3.5  $\mu\text{m}$  as the chosen wavelength.

### 2.5 High Temperature Size Exclusion Chromatography (HT-SEC)

Molar mass measurements for all samples were performed at 150 °C using a PL GPC 220 high temperature chromatograph (Polymer Laboratories, Church Stretton, UK) equipped with a differential refractive index (RI) detector. The column set used consisted of three 300×7.5 mm i.d. PLgel Olexis columns together with a 50×7.5 mm i.d. PLgel Olexis guard column (Polymer Laboratories, Church Stretton, UK). The eluent used was TCB at a flow rate of 1.0 mL/min with 0.0125 wt% 2,6-ditertbutyl-4-methylphenol (BHT) added as a stabilizer. Samples were dissolved at 160 °C in TCB at a concentration of 1 mg/mL for 1- 2 h (depending on the sample type) and 200  $\mu\text{L}$  of each sample was injected. Narrowly distributed polystyrene standards (Polymer Laboratories, Church Stretton, UK) were used for calibration.

## 2.6 High Temperature High Performance Liquid Chromatography (HT-HPLC)

The separations were conducted on a high temperature solvent gradient interaction chromatograph (SGIC) constructed by Polymer Char (Valencia, Spain), comprising of an autosampler, two separate ovens, switching valves and two pumps equipped with vacuum degassers (Agilent, Waldbronn, Germany). One oven was used for the HPLC column, while the second oven is the location of the injector and a switching valve. The autosampler was a separate unit connected to the injector through a heated transfer line. A high-pressure binary gradient pump was used for HPLC in the first dimension.

An evaporative light scattering detector (ELSD, model PL-ELS 1000, Polymer Laboratories, Church Stretton, England) was used with the following parameters: a gas flow rate of 1.5 L/min, a nebuliser temperature of 160 °C, and an evaporator temperature of 270 °C. HT-HPLC was carried out using a Hypercarb column (Hypercarb®, Thermo Scientific, Dreieich, Germany) with the following parameters: 100×4.6 mm i.d., packed with porous graphite particles with a particle diameter of 5µm, a surface area of 120 m<sup>2</sup>/g, and a pore size of 250 Å. The flow rate of the mobile phase was 0.5 mL/min. The column was placed in the column oven maintained at 160 °C. The HPLC separations were accomplished by applying a linear gradient from 1-decanol to TCB. The volume fraction of TCB was linearly increased to 100% within 10 min after the sample injection and then held constant for 25 min. Finally, the initial chromatographic conditions were re-established with 100% 1-decanol. The dwell and void volumes of 1.7 mL and 1.1 mL, respectively, were measured according to the method described by Ginzburg et al. [32]. This reflects that there is an isocratic elution of 1-decanol (1.7 mL) before the gradient hits the column [17, 33]. Samples were injected at a concentration of 1-1.2 mg/mL, with 20 µL of each sample being injected.

## 2.7 Fourier Transform Infrared Spectroscopy (FTIR)

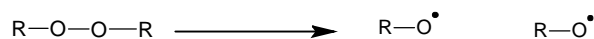
FTIR analyses of the samples were performed on a Thermo Nicolet iS10 Spectrometer (Thermo Scientific, Waltham, MA). Spectra were recorded at a resolution of 8 cm<sup>-1</sup> with 16 scans being recorded for each spectrum. Thermo Scientific OMNIC software (version 8.1) was used for data collection and processing.

## 3. Results and Discussion

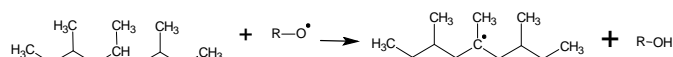
The present study demonstrates the usefulness of various advanced analytical techniques to investigate the correlation between molecular properties and the effect of the organic peroxide in the vis-breaking process. Vis-breaking is

considered to be a very complex process that, upon the action of a peroxide, reduces the molar mass of the sample and introduces oxygen functionalities into the polymer structure. It can schematically be presented as shown in Scheme 1 [34, 35].

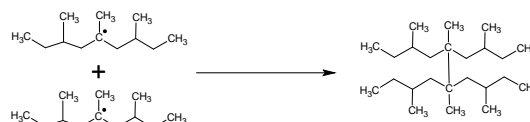
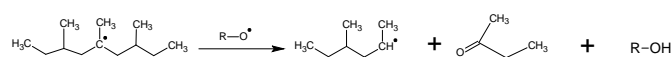
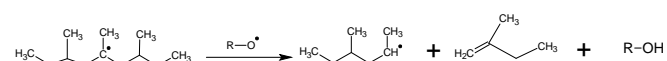
Thermal decomposition of the peroxide to form radicals



Formation of the new polymer radicals via peroxide attack



Formation of the new polyolefin materials [36]



*Scheme 1:* Vis-breaking of an ethylene-propylene copolymer by an organic peroxide

Although vis-breaking is considered to be a mature technical process for impact polypropylene copolymers (IPC), the changes in the molecular structure of the IPC have not been investigated in detail. Most of the investigations so far have been conducted on bulk samples and only standard analytical techniques have been used.

In the present analytical protocol, only the first step is the analysis of the bulk samples (see Table 1) which is then followed by TREF fractionation and the detailed analysis of the TREF fractions. The newly developed high-temperature HPLC technique will provide new insight into the structure of the vis-broken materials being able to provide information on both the amorphous and the crystalline fractions. Sample IPC-1 is the non-degraded reference copolymer, while samples IPC-2, and -3 are vis-broken samples with increasing melt flow rates.

The molar masses of the reference and the vis-broken samples shown in Table 1 are consistent with what has been reported by other authors in that vis-breaking decreases molar mass and molar mass dispersity [11, 13, 16]. From an original value of 326 kg/mol the molar mass decreases to 226 kg/mol for a sample with a MFR of 48. As can be seen in Table 1, the molar mass dispersity decreases with MFR indicating that polymer chain scission occurs statistically. The fact that the molar mass decreases by only 30% indicates that chain

scission takes place not for all polymer chain and the molecular structure will change only gradually. This is confirmed by the DSC and CRYSTAF traces shown in Fig. 1.

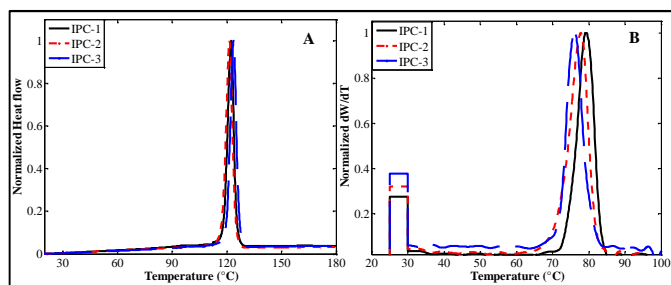


Figure 1. Bulk analysis of the samples by DSC (A) and CRYSTAF (B), DSC curves represent first crystallization.

The DSC and CRYSTAF crystallization curves give a first indication on compositional changes as a result of the visbreaking process. The DSC crystallization curve for the non-degraded IPC-1 shows a relatively broad crystallization range that stretches from about 30 to 130 °C. Slightly narrower crystallization ranges are obtained for the degraded samples IPC-2 and -3, however, there is not much difference seen between the non-degraded and the degraded samples. The CRYSTAF curves in Fig. 1B show that most of the semi-crystalline material crystallizes at a temperature around 80 °C. This material can be assigned to the isotactic polypropylene (iPP) matrix. The rubber phase that is composed of a variety of random ethylene-propylene copolymers does not crystallize but appears at 30 °C as the soluble fraction. While there only a slight shift seen in the peak crystallization temperatures for the crystallizing fractions, the weight percentage of the soluble fraction increases from IPC-1 to IPC-3. IPC-3 is the most degraded sample having the highest MFR and the lowest molar mass. It contains the polymer molecules that underwent chain scission and (probably) functionalization. This is in agreement with the slight shift of the peak crystallization temperatures to lower values from sample IPC-1 to IPC-3.

It is known from previous investigations that the iPP matrix is most susceptible to thermo-oxidative degradation as compared to the EP rubber phase<sup>[12-14]</sup>. It is, therefore, likely that the increase of the soluble fraction as seen in CRYSTAF is due to chain scission of iPP resulting in short (functionalized) polypropylene chains that do not crystallize in CRYSTAF at temperatures above 30 °C. The fact that DSC indicates the gradual decrease of the fractions crystallizing at 30-110 °C (see Fig. 1A for IPC-1) might indicate that not only iPP but also EP copolymer fractions with long propylene sequences are degraded. This assumption, however, must be confirmed by more detailed studies.

As has been shown previously, more molecular information can be obtained by FTIR spectroscopy and HT-HPLC. For IPC bulk analysis, however, HT-HPLC has been shown not to provide much information. This is due to the fact that the majority phase iPP dominates the HPLC behavior. The elution peaks at 1.3 mL are due to low molar mass iPP while the peaks at ~3.0 mL after the start of the solvent gradient are due to high molar mass iPP, see Fig. 2B. More valuable information can be obtained for TREF fractions as will be shown later. In contrast, FTIR shows very clearly that upon vis-breaking the samples are functionalized, see Fig. 2A. The absorptions at ~1630-1770  $\text{cm}^{-1}$  indicate the presence of carbonyl containing functional groups and the peak intensities increase with higher values of MFR. The carbonyl products are assumed to be formed during the vis-breaking process.

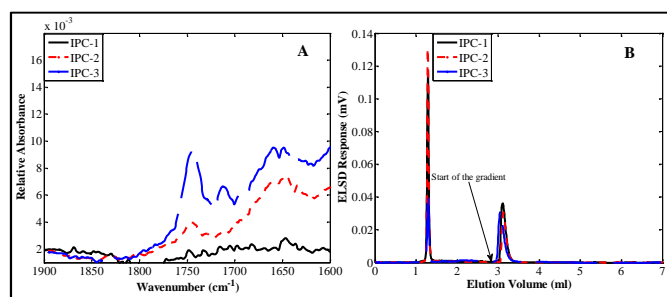


Figure 2. Bulk analysis of the samples by FTIR (A) and HT-HPLC (B).

The major limitation of the FTIR technique is that it provides only average chemical composition and as such the details about which phase (amorphous, semi-crystalline or highly crystalline) of the IPC materials is affected by the action of the peroxide cannot be established. Hence, the fractionation of the bulk samples is very important to obtain comprehensive information on the molecular properties of the reference and the vis-broken IPCs and to elucidate the effect of the peroxide on the different IPC phases.

The IPC samples were fractionated according to their crystallizabilities using preparative TREF. The TREF fractionation results are depicted in Fig. 3 indicating the weight percentage of the collected material as a function of the TREF elution temperature. As has been shown in previous work and confirmed by the CRYSTAF results, the majority phase (iPP) elutes at high temperature (130 °C) reflecting the highly crystallinity of this fraction. The rubber phase that is responsible for the impact properties of IPC constitutes about ~20 wt% of the bulk material. Due to its low crystallinity it elutes at a temperature of 30 °C. In addition to these components, segmented EP copolymer fractions elute between 60 – 90 °C. These components, however, make only about 10 wt% of the total samples. One has to keep in mind that co-crystallization and co-elution of

different components may occur. Hence, detailed analysis of the TREF fractions is essential to obtain comprehensive structural information on the IPC materials that underwent the vis-breaking process.

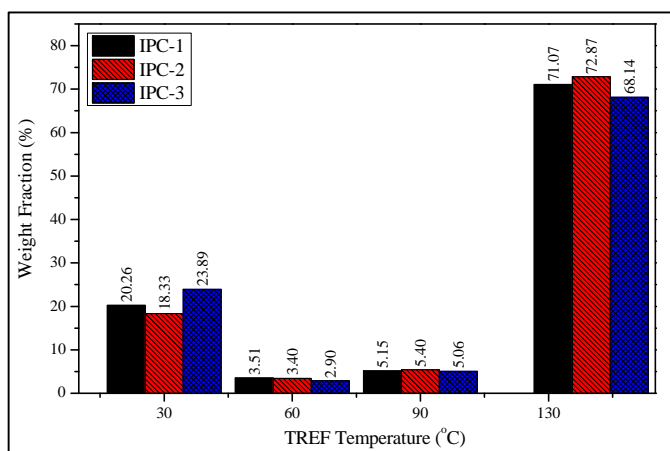


Figure 3. Preparative TREF results for the samples, indicating the weight percentages of each fraction as a function of the elution temperature.

The results of the molar mass analyses of the TREF fractions are depicted in Fig.4. The molar mass results of the 130 °C TREF fractions indicate unimodal molar mass distributions (MMD) for all samples. In contrast to these TREF fractions and the bulk samples, the TREF fractions collected at 30, 60 and 90 °C show bimodal MMDs. The peak maxima of the higher molar mass components shift to lower values indicating that chain scission takes place. The concentration of lower molar mass components increases for the 30, 60 and 90 °C TREF fractions. In order to obtain comprehensive information about the vis-breaking process, chemical composition analyses of the TREF fractions were performed.

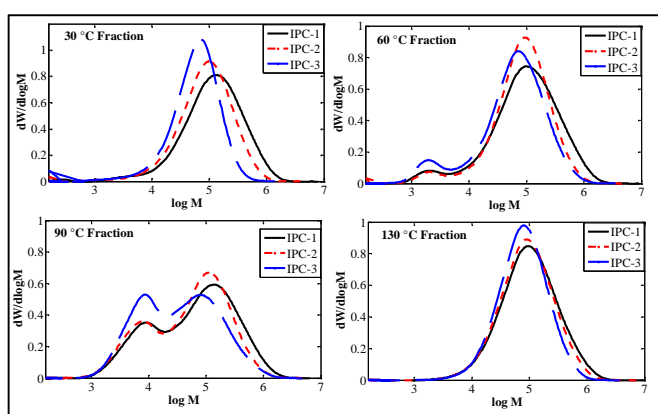


Figure 4. SEC curves for the TREF fractions of the IPC samples.

Assuming that the 30 °C fractions contain components that are amorphous or have a low crystallinity and that the 130 °C fractions contain components that have the highest crystallinity, the samples were investigated by DSC. In agreement with the assumption, the DSC melting curves of

the 30 °C fractions show no melting events thus confirming that these fractions are completely amorphous<sup>[18, 22, 37]</sup>, see Fig. 5. At the same time, the 130 °C fractions exhibit very similar melting peaks at about 160 °C that can be assigned to iPP being the components with the highest crystallinity<sup>[33]</sup>.

The most distinct differences between the samples can be seen for the 60 and 90 °C fractions. These contain EP copolymer molecules with different ethylene and propylene sequence lengths. In addition, these fractions may contain some low molar mass iPP that is co-crystallizing/co-eluting with the copolymers as has been shown previously<sup>[17, 18, 20]</sup>. From the melting pattern it can be assumed that the 90 °C fractions contain larger amounts of copolymers with long propylene sequences that melt at temperatures between 130 and 160 °C. In these fractions the components melting at 120 °C and below are believed to be due to components with longer ethylene sequences. The 60 °C fractions exhibit a very broad spectrum of EP copolymers with different chemical compositions.

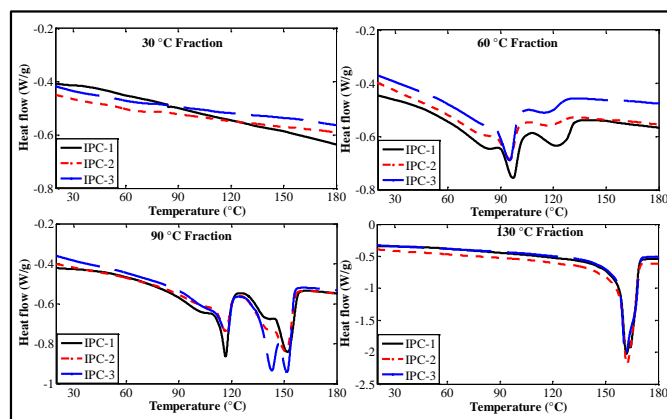


Figure 5. DSC melting curves for the TREF fractions of the IPC samples showing second heating measurements at a scan rate of 10 °C/min.

Fig. 6 shows the crystallization CRYSTAF curves for the TREF fractions of the four IPC samples. These results confirm the DSC findings in that both the 30 and 60 °C TREF fractions contain amorphous EP copolymers and certain amounts of crystallizable material at 30 – 50 °C, respectively. The 130 °C TREF fractions show unimodal crystallization peaks between 65 and 85 °C for all the IPC samples which are characteristic of high molar mass, high isotacticity iPP. The 90 °C TREF fractions exhibit complex crystallization patterns with the non-crystallizing part (probably) being degraded PP that is co-crystallizing/co-eluting in the TREF fractionation. In contrast to DSC, there are no distinct peaks seen for different components as was the case in DSC due to the fact that in CRYSTAF components having different molecular compositions co-crystallize from dilute solution<sup>[38-40]</sup>.



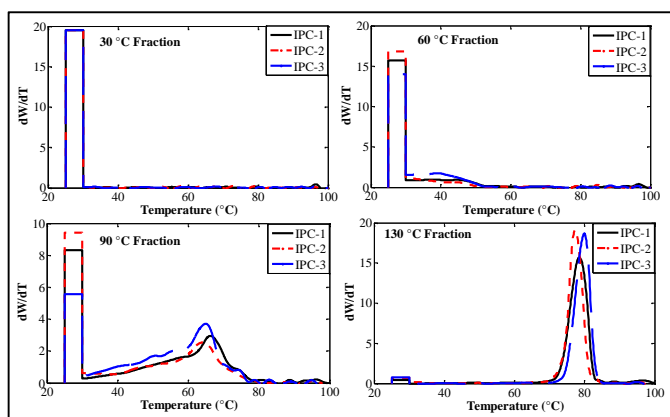


Figure 6. CRYSTAF curves for the TREF fractions of the IPC samples obtained at crystallisation temperatures between 30 – 100 °C.

Considering the fact that upon vis-breaking carbonyl functionalities are formed across the polymer chains, FTIR spectra were obtained for all fractions to see which fractions contain degraded material, see Fig. 7. On a first glance it can be seen that the 130 °C fractions do not contain any carbonyl groups. In agreement with all other results, these fractions contain exclusively high molar mass non-degraded iPP. Very low amounts of carbonyl-containing species are found in the 90 °C fractions. Interestingly, the 90 °C fraction of sample IPC-2 is showing the highest carbonyl intensity but this might be due to the inhomogeneity of the fraction after precipitation that shows when doing ATR instead of transmission FTIR. The spectra of the 60 °C fractions exhibit significantly higher carbonyl intensities. While the non-degraded sample IPC-1 does not show carbonyl groups, these groups develop in the order of increasing MFR which is a measure for degradation. The chemical compositions of these fractions still remain to be explored quantitatively, however, it can be assumed that they contain degraded (carbonyl-functionalized) iPP and a range of degraded and non-degraded EP copolymers.

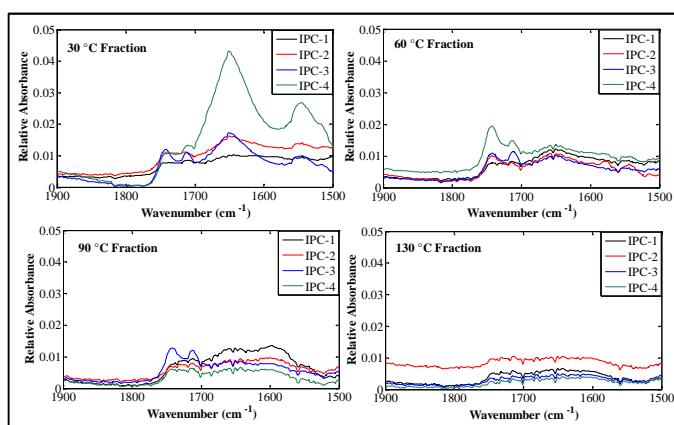


Figure 7 Enlarged parts of the FTIR spectra for the TREF fractions indicating the appearance of carbonyl groups upon vis-breaking.

Finally, the 30 °C TREF fractions exhibit the highest carbonyl group intensities and the absorption peak profiles become increasingly complex. In the most degraded sample IPC-3 distinct absorption peaks at wavenumbers of 1650 and 1550  $\text{cm}^{-1}$  are seen. Absorption peak at 1650  $\text{cm}^{-1}$  is due to the presence of C=O stretches from the conjugated aldehydes, whereas peak at 1550  $\text{cm}^{-1}$  has resulted from C=C stretching. Tentatively it is assumed that the 30 °C TREF fractions contain mostly degraded and non-degraded EP rubber components. These fractions can also contain amorphous (degraded and non-degraded) PP but based on previous experience it is expected that the concentration of these components is rather low.

Although FTIR can reveal changes in molecular composition brought about by the degradation process, detailed information on specific components cannot be obtained since FTIR provides the average composition of the fractions. A new highly selective solvent-gradient chromatographic separation method, HT-HPLC, is able to separate the fractions according to chemical composition irrespective of their crystallinity. As has been shown in previous studies, the present HPLC method separates according to the ethylene-to-propylene ratio in the order of low to high ethylene contents [17, 18, 20, 22].

The HPLC results for all TREF fractions are presented in Fig. 8. As expected, the 30 °C TREF fractions contain only random EP copolymers since all the samples elute between 3.2 – 4.5 mL. The chromatograms indicate that these fractions do not contain any PP components as these would appear at elution volumes of 3 mL or lower, compare to elution patterns of the 130 °C TREF fractions. The 130 °C TREF fractions elute as two distinct elution peaks at 1.3 and 3.0 mL, respectively. These have been shown previously to belong to low molar mass and high molar mass iPP, respectively. For both fractions there are no distinct changes due to the fact that vis-breaking took place. This is rather unexpected for the 30 °C TREF fractions since these fractions show the highest amounts of carbonyl functionalities that indicate significant degradation. A possible explanation for this behaviour is that separation in HPLC occurs mainly with regard to hydrophobicity and long ethylene sequences and not according to the number of polar groups. In future investigations, similar samples shall be fractionated according to polarity based on interaction with these polar groups.

The 60 and 90 °C TREF fractions exhibit three distinct elution peaks, namely at 1.3 mL for low molar mass PP, at 3 – 4.5 mL for propylene-rich EP copolymers and at 5 – 6.5 mL for ethylene-rich EP copolymers. The results are similar to DSC analyses since they show that these two sets of fractions have complex molecular compositions.

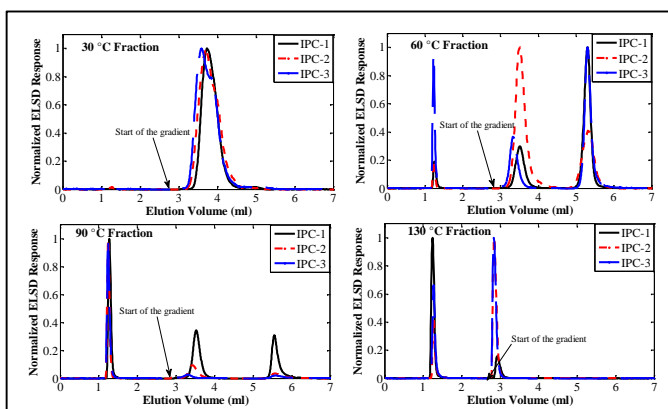


Figure 8. HT-HPLC chromatograms for the TREF fractions of the IPC samples, solvent gradient elution (1-decanol to TCB) after an initial isocratic step.

The effect of peroxide on the molecular composition of the TREF fractions can be seen even more clearly when comparing the enlarged parts of the chromatograms as illustrated in Fig. 8. The results for all TREF fractions indicate that the maxima of the elution peaks shift to lower elution volumes with increasing degrees of degradation (increasing MFR values). Most pronounced are these effects for the 30 and 60 °C fractions.

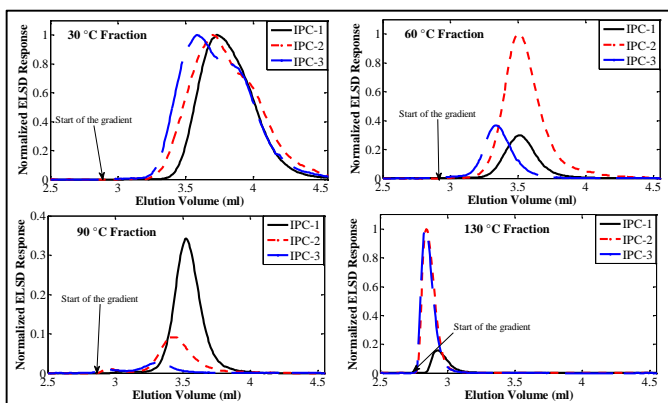


Figure 9. Enlarged parts of the HT-HPLC chromatograms (see Fig. 8) of the TREF fractions.

There are a number of explanations for these observations. First of all, the molar masses of the samples decrease upon vis-breaking. In addition to reducing the total molar masses, the numbers and the lengths of (crystallisable) ethylene sequences will be reduced and, accordingly, elution in HPLC shifts to lower volumes. Secondly, carbonyl groups are introduced in the polymer structure that will increase the polarity of the polymer chains. Although HPLC separation is mainly driven by the number and length of the ethylene sequences an extra effect of the carbonyl groups may be encountered that causes a shift to lower elution volumes (less

interaction). Finally, the presence of carbonyl groups changes the molecular conformation and longer ethylene sequences cannot properly align to the surface of the stationary phase. Again, interactions with the stationary phase will be weaker and elution volume will decrease.

#### 4. Conclusions

The present investigations have shown that the vis-breaking process does not only decrease the molar mass by chain scission resulting in lower viscosity and better processability. The vis-breaking process brings about significant changes in the molecular composition of the material. These changes, however, do only affect a certain fraction of the material. The TREF results indicate that upon vis-breaking the percentage of semi-crystalline iPP decreases only gradually from about 72 to 68 wt%. This proves that most of the iPP matrix remains intact.

Upon vis-breaking the amount of soluble material (30 °C TREF fractions) increases which indicates that additional soluble material is produced through chain scission. This material is amorphous and has a distinctively different molecular composition compared to the original soluble material. As can be seen from the FTIR spectra of the fractions, the 30 °C TREF fractions contain the highest concentration of carbonyl and vinyl functionalities. The shift of the HPLC elution peaks towards lower elution volumes could indicate that the degraded material has a higher propylene content compared to the non-degraded material. This would prove that degradation does not take place uniformly over all polymer chains but preferentially for iPP molecules. It is interesting to note that the 60 and 90 °C TREF fractions even after the vis-breaking process do not show significant intensities of the carbonyl peaks. This indicates that the segmented EP copolymer fractions are less susceptible to degradation.

In conclusion, the combination of preparative TREF with various advanced analysis and fractionation methods has proved to be an effective approach to understand the vis-breaking process better and to shed light on the molecular composition of the vis-broken IPC materials.

Acknowledgements: The authors thank SASOL, South Africa, and Lummus Novolen Technology GmbH, Germany, for the financial support of this work. The IPC samples provided by Novolen Technology GmbH are gratefully acknowledged.

- [1] C. Kock, M. Gahleitner, A. Schausberger, E. Ingolic, *J. Appl. Polym. Sci.* **2012**, *128*, 1484.
- [2] H. Pasch, M. I. Malik, T. Macko, *Adv. Polym. Sci.* **2013**, *251*, 77.
- [3] R. A. García, B. Coto, M. T. Expósito, I. Suarez, A. Fernández-Fernández, S. Caveda, *Macromol. Res.* **2011**, *19*, 778.
- [4] M. Gahleitner, C. Tranninger, P. Doshev, *J. Appl. Polym. Sci.* **2013**, *130*, 3028.
- [5] V. Agarwal, T. B. Van Erp, L. Balzano, M. Gahleitner, M. Parkinson, L. E. Govaert, V. Litvinov, A. P. M. Kentgens, *Polymer* **2014**, *55*, 896.
- [6] C. Grein, M. Gahleitner, K. Bernreitner, *Express Polym. Lett.* **2012**, *6*, 688.
- [7] F. M. Mirabella Jr, *Polymer* **1993**, *34*, 1729.
- [8] R. Zacur, G. Goizueta, N. Capiati, *Polym. Eng. Sci.* **2000**, *40*, 1921.
- [9] R. Zacur, G. Goizueta, N. Capiati, *Polym. Eng. Sci.* **1999**, *39*, 921.
- [10] C. Kock, N. Aust, C. Grein, M. Gahleitner, *J. Appl. Polym. Sci.* **2013**, *130*, 287.
- [11] M. Swart, A. J. van Reenen, *J. Appl. Polym. Sci.* **2015**, *132*, 41783.
- [12] E. de Goede, P. Mallon, H. Pasch, *Macromol. Mater. Eng.* **2010**, *295*, 366.
- [13] E. de Goede, P. E. Mallon, H. Pasch, *Macromol. Mater. Eng.* **2012**, *297*, 26.
- [14] E. de Goede, P. E. Mallon, K. Rode, H. Pasch, *Macromol. Mater. Eng.* **2011**, *296*, 1018.
- [15] S. de Goede, R. Brüll, H. Pasch, N. Marshall, *E-Polymers* **2004**, *1*.
- [16] H. Pasch, E. de Goede, P. Mallon, *Macromol. Symp.* **2012**, *312*, 174.
- [17] S. Cheruthazhekatt, G. W. Harding, H. Pasch, *J. Chromatogr. A* **2013**, *1286*, 69.
- [18] S. Cheruthazhekatt, T. F. J. Pijpers, G. W. Harding, V. B. F. Mathot, H. Pasch, *Macromolecules* **2012**, *45*, 5866.
- [19] T. Macko, A. Ginzburg, K. Remerie, R. Brüll, *Macromol. Chem. Phys.* **2012**, *213*, 937.
- [20] S. Cheruthazhekatt, T. F. J. Pijpers, G. W. Harding, V. B. F. Mathot, H. Pasch, *Macromolecules* **2012**, *45*, 2025.
- [21] M. Ahmadi, M. Nekoomanesh, H. Arabi, *Macromol. Theor. Simul.* **2009**, *18*, 195.
- [22] M. J. Phiri, S. Cheruthazhekatt, A. Dimeska, H. Pasch, *J. Polym. Sci. Part A: Polym. Chem.* **2015**, *53*, 863.
- [23] R. Chitta, T. Macko, R. Brüll, C. Boisson, E. Cossoul, O. Boyron, *Macromol. Chem. Phys.* **2015**, *216*, 721.
- [24] T. Macko, R. Brüll, R. G. Alamo, F. J. Stadler, S. Losio, *Anal. Bioanal. Chem.* **2011**, *399*, 1547.
- [25] T. Macko, R. Brüll, Y. Wang, B. Coto, I. Suarez, *J. Appl. Polym. Sci.* **2011**, *122*, 3211.
- [26] H. Pasch, A. Albrecht, R. Brüll, T. Macko, W. Hiller, *Macromol. Symp.* **2009**, *282*, 71.
- [27] A. Albrecht, L. C. Heinz, D. Lilge, H. Pasch, *Macromol. Symp.* **2007**, *257*, 46.
- [28] S. Cheruthazhekatt, H. Pasch, *Polymer* **2015**, *64*, 1.
- [29] H. Pasch, *Polym. Adv. Technol.* **2015**, *26*, 771.
- [30] H. Pasch, M. I. Malik, "Advanced Separation Techniques for Polyolefins", Springer, New York, 2014.
- [31] C. Silvestre, S. Cimmino, R. Triolo, *J. Polym. Sci. Part B: Polym. Phys.* **2003**, *41*, 493.
- [32] A. Ginzburg, T. Macko, V. Dolle, R. Brüll, *Eur. Polym. J.* **2011**, *47*, 319.
- [33] M. J. Phiri, A. Dimeska, H. Pasch, *Macromol. Chem. Phys.* **2015**, *216*, 1619.
- [34] M. J. Scoriah, S. Zhu, A. Psarreas, N. T. McManus, R. Dhib, C. Tzoganakis, A. Penlidis, *Polym. Eng. Sci.* **2009**, *49*, 1760.
- [35] G. Moad, I. J. Dagley, J. Habsuda, C. J. Garvey, G. Li, L. Nichols, G. P. Simon, M. R. Nobile, *Polym. Degrad. Stabil.* **2015**, *117*, 97.
- [36] P. R. Dluznieski, *Rubber Chem. Technol.* **2001**, *74*, 451.
- [37] S. Cheruthazhekatt, T. F. J. Pijpers, V. B. F. Mathot, H. Pasch, *Anal. Bioanal. Chem.* **2013**, *405*, 8995.
- [38] H. Pasch, R. Brüll, U. Wahner, B. Monrabal, *Macromol. Mater. Eng.* **2000**, *279*, 46.
- [39] B. Monrabal, *Adv. Polym. Sci.* **2013**, *257*, 203.
- [40] B. Monrabal, *J. Appl. Polym. Sci.* **1994**, *52*, 491.

## Chapter 7: Conclusions and Recommendations

---

### 7 CONCLUSIONS AND RECOMMENDATIONS

*This chapter outlines the conclusions of the three different parts of the present study. Only the main points are highlighted and presented in the present dissertation. A general conclusion for the overall study is also given. Recommendations for future work are proposed so that additional information can be obtained.*

#### 7.1 Conclusions

Ethylene-propylene rubber (EPR) forms an integral part of complex impact polypropylene copolymer (IPC) formulations. The molecular composition of the EPR affects the impact properties of the IPC materials. In the first part of the current study, investigations on the molecular structures of EPR copolymers synthesized by a Ziegler-Natta catalysts system were carried out. This was followed by exploring the molecular compositions of the metallocene-based EPR copolymers to evaluate the effect of the catalyst type. Finally, the effect of an organic peroxide on the molecular structures of the IPC materials was evaluated. To enhance the processing properties, IPCs are frequently treated with peroxides to increase their melt flow rates. These vis-broken IPC materials have very complex compositions due to the effect of the peroxide used during the degradation process. The understanding of the microstructural properties for both vis-broken IPC and EPR copolymers is essential for the correlation of the molecular structure of IPC with the final application of these materials. The present thesis was dedicated to the fractionation and characterization of vis-broken IPCs and EPR copolymers. The findings of this research can be summarized as follows.

In the first part of the study, bulk analyses of the EPR copolymers prepared with a Ziegler-Natta catalyst system revealed that the major components present in these copolymers are random ethylene-propylene (EP) copolymers. The fractionation experiments using TREF showed that the EPRs contain minor components, one of them being highly crystalline material that was collected at a TREF elution temperature of 130 °C. The results from DSC analyses confirmed the 130 °C TREF fractions to be highly crystalline components of both PE and iPP homopolymers as indicated by the two melting peaks at ~120 °C and ~160 °C, respectively. The 30 °C TREF fractions could not be characterized by CRYSTAF and DSC since these fractions contain random EP copolymers which are completely amorphous. In contrast to the crystallization-based techniques, HT-HPLC was able to analyse both the amorphous and crystalline fractions of the

materials and separations were found to depend on the ethylene contents of the samples. The 60 and 90 °C TREF fractions were determined to contain segmented EP copolymers having different ethylene and propylene sequences. HT-HPLC further confirmed that the 130 °C TREF fractions contain both PE and iPP materials as observed by the elution peaks at ~6 mL for PE homopolymer. HT-HPLC was coupled to FT-IR spectroscopy to obtain the exact chemical compositions of the separated components. The FT-IR spectra linked to the latest eluting HPLC fractions confirmed the presence of crystalline ethylene sequences. These results proved that the late eluting material in HPLC is mainly PE homopolymer.

The second part of the present study dealt with the analyses of metallocene-based EPR copolymers with high comonomer contents. The bulk analyses as performed by SEC, DSC and HPLC showed that the copolymers have narrow molar mass and chemical composition distributions as expected for samples prepared by a metallocene catalyst system. However, using preparative TREF it was found that there was a significant amount of crystallizing material that eluted at 130 °C. As confirmed by DSC, CRYSTAF and HT-HPLC analyses, the 130 °C TREF fractions were found to contain mainly iPP homopolymer. It was rather unexpected for EPR copolymers with such high ethylene contents to have traces of iPP material. The 30 and 60 °C TREF fractions were found to contain random EP copolymers. Crystallization-based techniques such as DSC and CRYSTAF were not able to fractionate and characterize these amorphous fractions. In contrast, HT-HPLC showed that the 30, 60 and 90 °C fractions contain mainly random EP copolymers while the 130 °C fractions contain iPP homopolymer. These results suggested that even metallocene-based EPRs exhibit significant chemical composition heterogeneities. Conclusive information on the heterogeneity in chemical composition of the TREF fractions was obtained by the <sup>13</sup>C NMR analyses. The comonomer contents and monomer sequence distributions were determined for all TREF fractions. The 130 °C TREF fractions showed mainly three distinct NMR peaks due to carbon atoms of the propylene repeating units confirming iPP but the 30 and 60 °C TREF fractions indicated a variety of EP sequences. The NMR analyses further proved that there is a remarkably high chemical heterogeneity among the TREF fractions and thus the bulk EPR samples.

In the last part of the study, vis-broken IPC materials were analysed by various analytical techniques to determine the effect of the peroxide on the molecular compositions of the IPC samples. HT-SEC analyses for the bulk samples showed that there is a decrease in the molar masses of the IPC samples upon addition of the peroxide during the degradation process. FT-IR analyses showed the presence of degradation products, indicated by carbonyl groups, in the

spectral region of 1500 – 1800  $\text{cm}^{-1}$ . However, the bulk analyses done by DSC, CRYSTAF and HT-HPLC showed no observable changes in the bulk chemical compositions of the samples. The bulk analysis results were confirmed by preparative TREF experiments which indicated that ~70 % of the IPC consists of non-degraded iPP with random EP copolymers making up to ~20 % of the overall material and small amounts of the segmented EP copolymers were also detected. The 60 and 90 °C TREF fractions were found to contain segmented EP copolymers having complex molecular compositions. The complex nature of these fractions was proved by the presence of several DSC and CRYSTAF crystallization peaks detected that are due to different crystallizable components present in the fractions. FT-IR analyses showed that the 30 °C TREF fractions have the highest concentration of carbonyl products. The number of the carbonyl products was found to increase as the amount of the peroxide used during the degradation was also increased. In addition, HT-HPLC analyses proved that the 30 °C TREF fractions are the most degraded materials since there was a significant shift in elution peaks to lower volumes with addition of the peroxide. The results from the HT-HPLC analyses indicated that copolymers with longer ethylene sequences were largely affected by the action of the peroxide.

The overall results of the present study demonstrated that multidimensional analytical approaches are essential for understanding the molecular heterogeneity of complex polyolefin systems. These analytical approaches provided more insights on the microstructural properties of vis-broken IPC and EPR copolymers.

## **7.2 Future work**

Detailed characterization is necessary to obtain comprehensive information on the final properties and applications of the investigated materials. The current study should be extended to include mechanical and morphological studies of the vis-broken IPC and EPR copolymers.

The TREF fractions collected for the vis-broken IPC samples showed that the fractions exhibit complex chemical compositions that are also partially due to co-crystallization and co-elution of components having similar crystallizable components. The complex compositions of the fractions can be decreased by increasing the number of the TREF fractions to be collected and to use narrower temperature intervals. The suggested temperatures for the collection of the TREF fractions are as follows, 30, 60, 80, 90, 110, 120 and 130 °C.

In the last part of the present study, FT-IR analyses showed that the vis-broken IPC samples contain large numbers of carbonyl groups due to the action of the peroxide during the degradation process. A HT-HPLC separation based on the polarity of the degraded samples would give additional information on the molecular complexity of the vis-broken samples.